

NASA CR-166,412

NASA CONTRACTOR REPORT 166412

NASA-CR-166412
19830002832

SENSITIVITY ANALYSIS OF HELICOPTER IMC DECELERATING
STEEP APPROACH AND LANDING PERFORMANCE TO
NAVIGATION SYSTEM PARAMETERS

Meheub S. Karmali
Anil V. Phatak

LIBRARY COPY

NOV 1 1982

LANGLEY RESEARCH CENTER
LIBRARY, NASA
HAMPTON, VIRGINIA

CONTRACT NAS2-10670
April 1982



NF02365

NASA

1 2 3 4 5 6 7 8 9 10 11 12 13 14 15 16 17 18 19 20 21 22 23 24 25 26 27 28 29 30 31 32 33 34 35 36 37 38 39 40 41 42 43 44 45 46 47 48 49 50 51 52 53 54 55 56 57 58 59 60 61 62 63 64 65 66 67 68 69 70 71 72 73 74 75 76 77 78 79 80 81 82 83 84 85 86 87 88 89 90 91 92 93 94 95 96 97 98 99 100

NASA CONTRACTOR REPORT 166412

SENSITIVITY ANALYSIS OF HELICOPTER IMC DECELERATING
STEEP APPROACH AND LANDING PERFORMANCE TO
NAVIGATION SYSTEM PARAMETERS

Meheub S. Karmali
Anil V. Phatak

Prepared for
Ames Research Center
under Contract NAS2-10670

NASA

National Aeronautics and
Space Administration

Ames Research Center
Moffett Field, California 94035

N83-11102 #

1
2
3
4
5
6
7
8
9
10
11
12
13
14
15
16
17
18
19
20
21
22
23
24
25
26
27
28
29
30
31
32
33
34
35
36
37
38
39
40
41
42
43
44
45
46
47
48
49
50
51
52
53
54
55
56
57
58
59
60
61
62
63
64
65
66
67
68
69
70
71
72
73
74
75
76
77
78
79
80
81
82
83
84
85
86
87
88
89
90
91
92
93
94
95
96
97
98
99
100

PREFACE

This effort was performed under Contract No. NAS2-10670 from the NASA Ames Research Center and was funded in part by MIPR No. 79-10010 from the U.S. Army Avionics Research and Development Activity, Fort Monmouth, NJ. Dr. John Bull and Mr. Lewis Peach of NASA Ames were the NASA Technical monitors and Mr. Paul S. Demko was the Army technical monitor for this project.

The project manager at AMA, Inc. was Dr. Anil V. Phatak and project engineer was Mr. Meheub S. Karmali.

1
2
3
4
5
6
7
8
9
10
11
12
13
14
15
16
17
18
19
20
21
22
23
24
25
26
27
28
29
30
31
32
33
34
35
36
37
38
39
40
41
42
43
44
45
46
47
48
49
50
51
52
53
54
55
56
57
58
59
60
61
62
63
64
65
66
67
68
69
70
71
72
73
74
75
76
77
78
79
80
81
82
83
84
85
86
87
88
89
90
91
92
93
94
95
96
97
98
99
100

ABSTRACT

This report presents the results of a study to investigate, by means of a computer simulation, the performance sensitivity of helicopter IMC DSAL operations as a function of navigation system parameters. A mathematical model representing generically a navigation system is formulated. The scenario simulated consists of a straight in helicopter approach to landing along a 6° glideslope. The deceleration magnitude chosen is .03g. The navigation model parameters are varied and the statistics of the total system errors (TSE) computed. These statistics are used to determine the critical navigation system parameters that affect the performance of the closed-loop navigation, guidance and control systems of a UH1H helicopter.

1
2
3
4
5
6
7
8
9
10
11
12
13
14
15
16
17
18
19
20
21
22
23
24
25
26
27
28
29
30
31
32
33
34
35
36
37
38
39
40
41
42
43
44
45
46
47
48
49
50
51
52
53
54
55
56
57
58
59
60
61
62
63
64
65
66
67
68
69
70
71
72
73
74
75
76
77
78
79
80
81
82
83
84
85
86
87
88
89
90
91
92
93
94
95
96
97
98
99
100

TABLE OF CONTENTS

INTRODUCTION	1
Background and Objectives	1
Technical Approach	3
HELICOPTER DSAL SYSTEM	5
DSAL Guidance Profile	5
Navigation System	7
SIMULATION AND ANALYSIS.	11
System Performance Measures.	11
Case Descriptions of Navigation System Parameters.	13
System Performance Using Perfect Range/Range Rate and The Nominal Navigation System.	15
Sensitivity to On-board Navigation System Parameters	20
Sensitivity to Ground-based Navigation (LGS) System Parameter	42
CONCLUDING REMARKS	55
REFERENCES	57
APPENDIX A	59
APPENDIX B	67

1
2
3
4
5
6
7
8
9
10
11
12
13
14
15
16
17
18
19
20
21
22
23
24
25
26
27
28
29
30
31
32
33
34
35
36
37
38
39
40
41
42
43
44
45
46
47
48
49
50
51
52
53
54
55
56
57
58
59
60
61
62
63
64
65
66
67
68
69
70
71
72
73
74
75
76
77
78
79
80
81
82
83
84
85
86
87
88
89
90
91
92
93
94
95
96
97
98
99
100

LIST OF FIGURES

Figure	Page
1. Block Diagram of the Helicopter DSAL System	2
2. a. Commanded Range Rate Profile	6
b. Altitude Profile	6
3. Navigation System Model	8
4. Ensemble Statistics for DSAL System with Perfect Range/ Range Rate and Nominal Navigation System.	16
a. Mean Localizer TSE	16
b. Mean Glideslope TSE	16
c. Mean Altitude TSE	17
d. Mean Range Rate TSE	17
e. Mean Range NSE	18
f. Standard Deviation Range NSE	18
g. Mean Range Rate NSE	19
h. Standard Deviation Range Rate NSE.	19
5. a. Sensitivity of Decision Altitude TSE to On-board Navigation Parameters	22
b. Sensitivity of Range Rate TSE to On-board Navigation Parameters.	23
c. Sensitivity of Range TSE at Touchdown to On-board Navigation Parameters	24
6. Sensitivity Results as a Function of Sampling Frequency f (Hz).	25
a. Mean Localizer TSE	25
b. Mean Glideslope TSE	25
c. Mean Altitude TSE	26
d. Mean Range Rate TSE	26
e. Mean Range NSE	27
f. Standard Deviation Range NSE	27
g. Mean Range Rate NSE	28
h. Standard Deviation Range Rate NSE	28
7. Sensitivity Results as a Function of Range Measurement Quantization q (ft)	29
a. Mean Localizer TSE	29
b. Mean Glideslope TSE	29
c. Mean Altitude TSE	30
d. Mean Range Rate TSE	30
e. Mean Range NSE	31
f. Standard Deviation Range NSE	31
g. Mean Range Rate NSE	32
h. Standard Deviation Range Rate NSE	32

LIST OF FIGURES (CONT')

Figure	Page
8. Sensitivity Results as a Function of Range Rate Quantization q_r (ft/s)	33
a. Mean Localizer TSE	33
b. Mean Glideslope TSE	33
c. Mean Altitude TSE	34
d. Mean Range Rate TSE	34
e. Mean Range NSE	35
f. Standard Deviation Range NSE	35
g. Mean Range Rate NSE	36
h. Standard Deviation Range Rate NSE	36
9. Sensitivity Results as a Function of Bandwidth of α - β Filter	38
a. Mean Localizer TSE	38
b. Mean Glideslope TSE	38
c. Mean Altitude TSE	39
d. Mean Range Rate TSE	39
e. Mean Range NSE.	40
f. Standard Deviation Range NSE	40
g. Mean Range Rate NSE	41
h. Standard Deviation Range Rate NSE	41
10. a. Sensitivity of Decision Altitude TSE to Ground-Based Navigation System Parameters	43
b. Sensitivity of Range Rate TSE to Ground-Based Navigation System Parameters	43
c. Sensitivity of Range TSE at Touchdown to Ground-Based Navigation System Parameters	44
11. Sensitivity Results as a Function of Range Measurement Noise σ_n (ft).	45
a. Mean Localizer TSE	45
b. Mean Glideslope TSE	45
c. Mean Altitude TSE	46
d. Mean Range Rate TSE	46
e. Mean Range NSE	47
f. Standard Deviation Range NSE	47
g. Mean Range Rate NSE	48
h. Standard Deviation Range Rate NSE	48
12. a. Sensitivity of Decision Altitude TSE to On-board Navigation Parameters (nominal $\sigma_n = 10$ ft)	50
b. Sensitivity of Range Rate TSE to On-board Navigation Parameters (nominal $\sigma_n = 10$ ft)	51
c. Sensitivity of Range TSE at Touchdown to On-board Navigation Parameters (nominal $\sigma_n = 10$ ft)	52

LIST OF FIGURES (CONT')

Figure		Page
A.1.	Autopilot Flight Path Coupler - Collective Axis	60
A.2.	Autopilot Collective Axis	60
A.3.	Autopilot Flight Path Coupler - Pitch Axis	62
A.4.	SAS - Pitch Axis.	63
A.5.	Autopilot Flight Path Coupler (Roll Axis)	64
A.6.	SAS - Roll Axis	64
A.7.	SCAS: Turn Coordination Mode	66
A.8.	SCAS: Heading Hold Mode	66
B.1.	Analog Representation of the α - β Filter	67

1 2 3 4 5 6 7 8 9 10 11 12 13 14 15 16 17 18 19 20 21 22 23 24 25 26 27 28 29 30 31 32 33 34 35 36 37 38 39 40 41 42 43 44 45 46 47 48 49 50 51 52 53 54 55 56 57 58 59 60 61 62 63 64 65 66 67 68 69 70 71 72 73 74 75 76 77 78 79 80 81 82 83 84 85 86 87 88 89 90 91 92 93 94 95 96 97 98 99 100

INTRODUCTION

Background and Objectives

A truly unique characteristic of the helicopter is its ability to perform Decelerating Steep Approach and Landing (DSAL) maneuvers into a confined landing zone. In the past, such maneuvers have been performed only under Visual Meteorological Conditions (VMC). That is, the helicopter pilot could perform a decelerated steep approach to hover only when he could see the target area from a sufficient distance to safely decelerate to a stop. Under Instrument Meteorological Conditions (IMC), the pilot/autopilot must maneuver the aircraft along a desired flight path and deceleration profile so as to arrive at the Decision Height (DH) with a range rate that would permit a visual approach to a hover over the prescribed landing pad.

A block diagram of a typical automatic DSAL system is shown in Figure 1. The overall closed-loop system is relatively complex and consists of three distinct modules for performing the aircraft navigation, guidance and control tasks. The navigation system must process noisy position data (aircraft range, azimuth and elevation) provided by a ground-based landing guidance system (LGS), using an on-board digital processor, to obtain estimates of the aircraft's position and range rate. These estimates are then used by the guidance and control systems to fly the helicopter along a desired position and velocity profile.

The performance of the DSAL system depends upon a number of factors such as (1) commanded flight path and velocity profile, (2) aircraft dynamics, (3) on-board avionics and flight control sophistication, (4) on-board navigation filter characteristics, and (5) accuracy of the aircraft raw position information provided by the ground-based LGS. An investigation of all these five factors was considered beyond the scope of this effort. Instead this study is limited to an analysis of the DSAL system performance with varying on-board and ground-based (LGS) navigation system parameters.

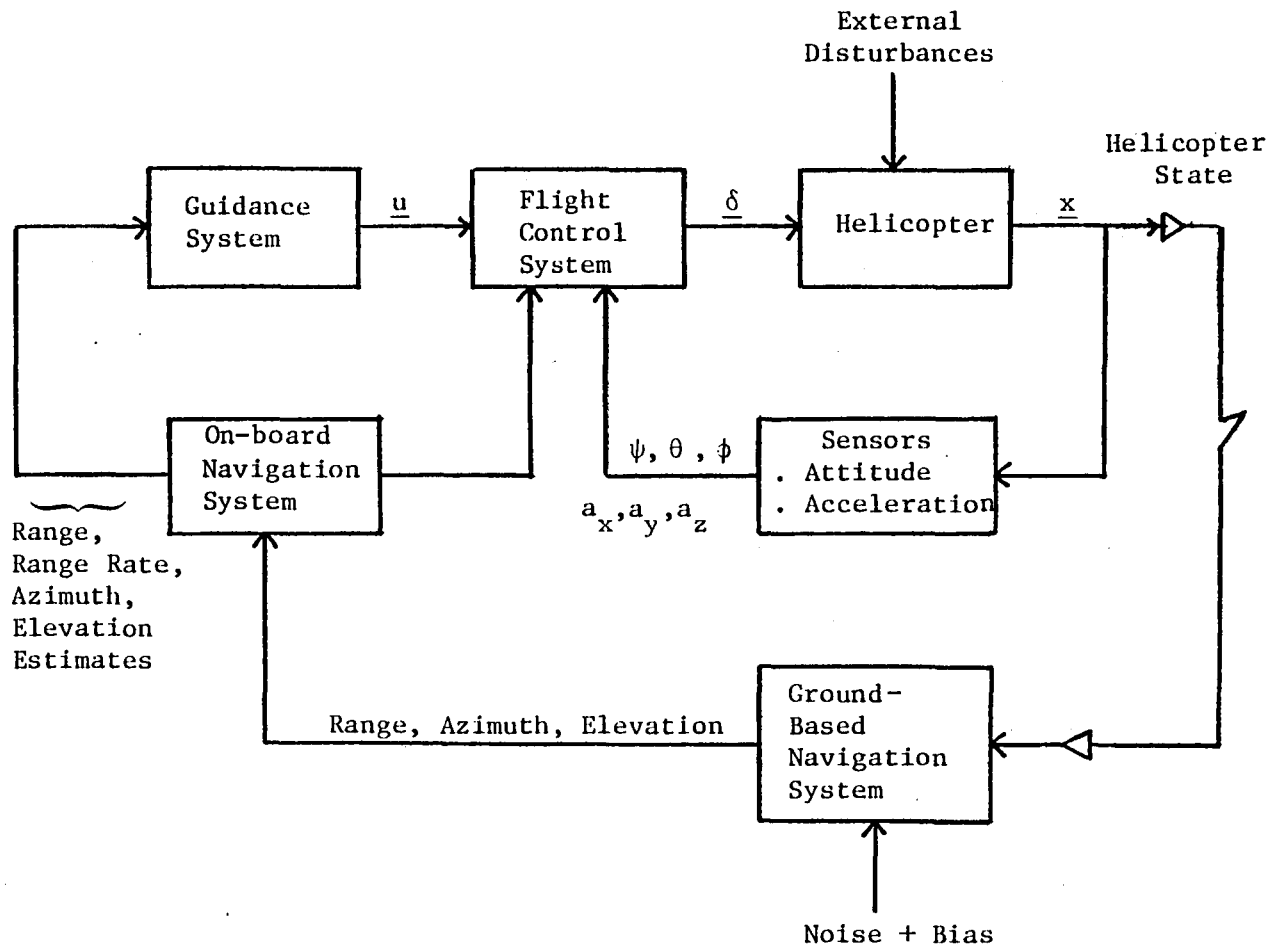


Figure 1. Block Diagram of the Helicopter DSAL System.

The objectives of this effort are basically twofold:

1. Conduct a generic sensitivity analysis of the helicopter DSAL system performance as a function of the on-board and ground-based navigation system parameters; and
2. Investigate flight path and range rate total system errors during helicopter IMC DSAL tasks for various weather minima (DH = 200,150,100,50,0 ft).

Technical Approach

Due to the complexity of the DSAL system, this study uses a computer simulation to meet its goals. Specifically, an off-line computer program was developed to simulate the closed-loop DSAL system described by the functional block diagram of Figure 1. A nonlinear mathematical model is used to represent the UH1H helicopter dynamics [1]. Monte Carlo procedures are used to obtain the ensemble means and standard deviations of several DSAL performance measures. The specific performance measures used in this study are described in the section on Simulation and Analysis. The details of the navigation and guidance laws and of the autopilot and flight control systems are given in the section on the Helicopter DSAL System and Appendix A, respectively. The on-board navigation filters are restricted to the commonly used α - β filter structure [2]. The principal navigation signals affecting the helicopter's DSAL performance are range rate and range from the helipad center. Consequently, the scope of this study is limited to an investigation of helicopter DSAL performance using only range and range rate elements of the navigation system. Aircraft azimuth and elevation signals provided by the ground-based system are assumed to be perfect or without error.



HELICOPTER DSAL SYSTEM

This section describes the specific DSAL guidance profiles and the mathematical models for the on-board (α - β filter) and ground-based (LGS) navigation systems used in the off-line DSAL simulation program.

The IMC DSAL maneuver involves decelerating to zero range rate while tracking the localizer and glideslope. Two deceleration guidance schemes have been investigated by several researchers: (1) Constant Deceleration Profile (CDP) [3] and (2) Constant Attitude Deceleration Profile (CADP) [4]. This study investigated the performance of the navigation systems using CDP guidance and a 6° glideslope trajectory.

DSAL Guidance Profile

Figures 2(a) and 2(b) show the desired range rate and altitude profiles used in the simulation of the straight-in DSAL task. The nominal DSAL maneuver described by these profiles can be segmented into the following four distinct phases: (1) constant altitude (1500 ft) and constant airspeed (60 kts) cruise, (2) glideslope capture at 14271.5 ft followed by constant airspeed (60 kts) glideslope (6° G/S) and localizer tracking, (3) switch to constant range rate (60 kts) glideslope tracking at 8300 ft (4) glideslope tracking to a landing following initiation of a constant 0.03g deceleration maneuver at 5285 ft.

The constant deceleration profile provides a range rate guidance command (\dot{r}_c) as a nonlinear function of range (r) defined by:

$$\dot{r}_c = \sqrt{2ar}$$

where a is the deceleration magnitude. Figure 2(a) shows that after intercepting the deceleration profile the pilot has about 5285 feet to come to a touchdown at zero range rate. This deceleration range remains constant regardless of a glideslope angle at which the pilot approaches the helipad. However, the order in which the glideslope is captured and deceleration initiated depends on the approach altitude, selected glideslope, initial

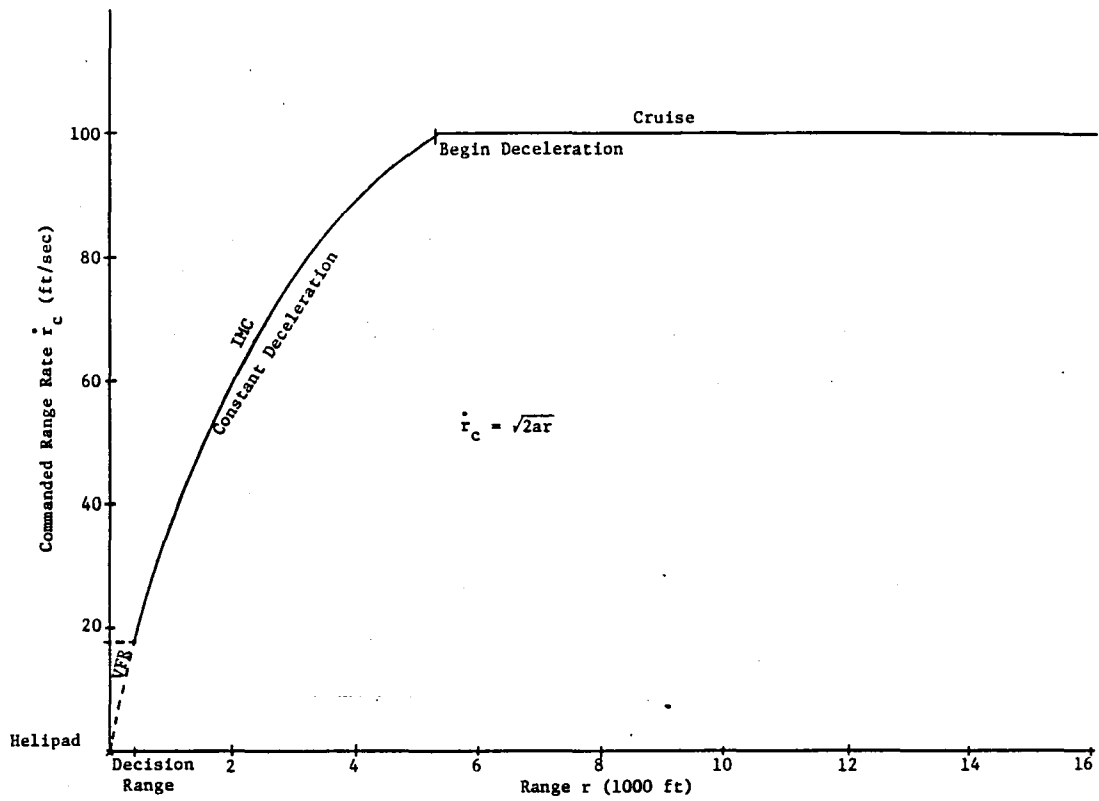


Figure 2(a). Commanded Range Rate Profile

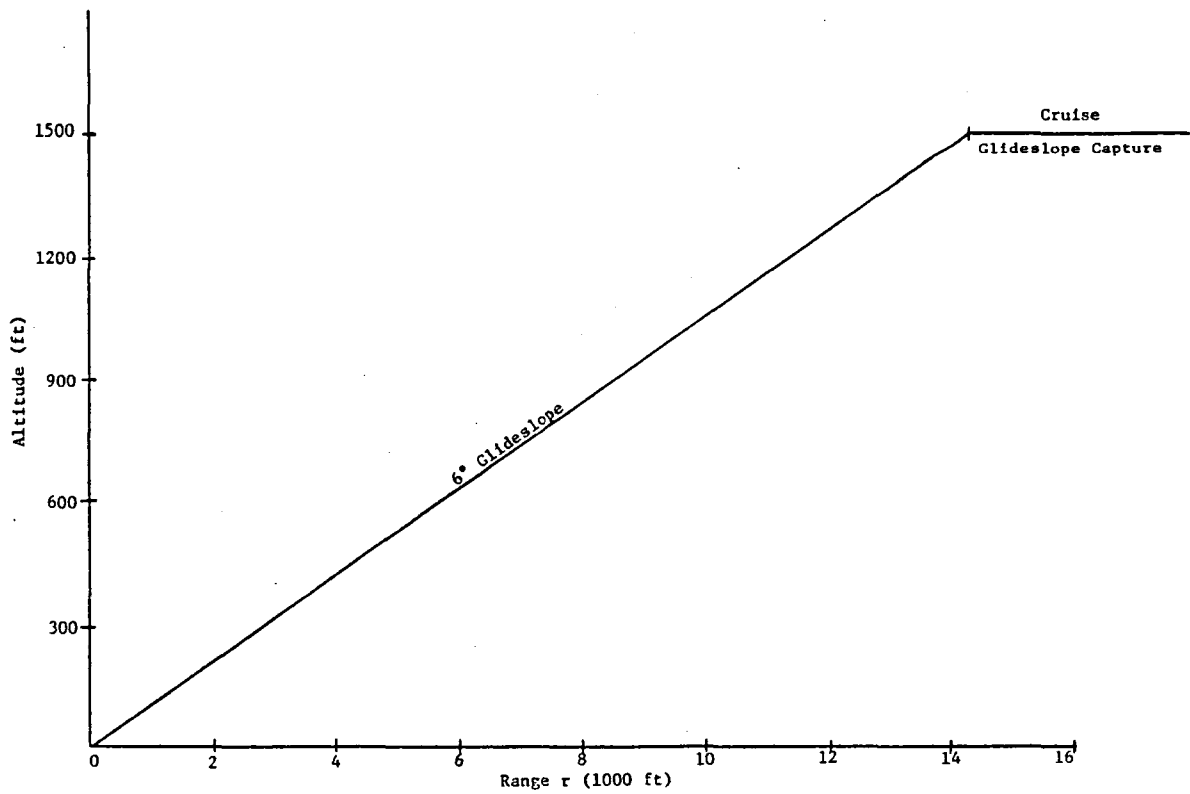


Figure 2(b) Altitude Profile

velocity and deceleration magnitude. In either case, the navigation, guidance and control systems enable the helicopter to fly along the glide-slope, localizer and parabolic velocity profile to come in to touchdown at zero range rate.

Navigation System

The azimuth, elevation, range and range rate signals that drive the helicopter flight control system and autopilot (described in Appendix A) are obtained by on-board digital processing of the raw position signals provided by the ground-based navigation system (LGS). In order to investigate the sensitivity of the helicopter DSAL performance to the navigation system characteristics, a mathematical model representing the acquired raw navigation signals from the ground-based LGS and the on-board processing of these signals is formulated as shown in Figure 3.

The remainder of this section describes the details of the proposed mathematical model of the navigation system. Although, the model is general enough to describe the acquisition and processing of the range, azimuth and elevation signals, it was used only to simulate the range element of the navigation system.

Ground-Based Elements: The ground-based LGS provides noisy measurements of range, azimuth and elevation at regular intervals. The noise in these measurements is modeled as a correlated random process with correlation time constant τ_n seconds and standard deviation σ_n . A constant bias B in the noisy measurement is also included. However, the effect of this bias on the DSAL performance is deterministic and can be removed through calibration. Hence, it's effects are not considered in this study.

Airborne Elements: In the on-board digital system, the raw measurement (y_n) is sampled and quantized. The sampler has a frequency f and the quantization process introduces a truncation (or roundoff) error defined by q units per Least Significant Bit (LSB). q is a function of the full scale capability of the measurement and the word size of the digital processor. This discrete measurement is then filtered by the airborne digital filter as shown in Figure 3.

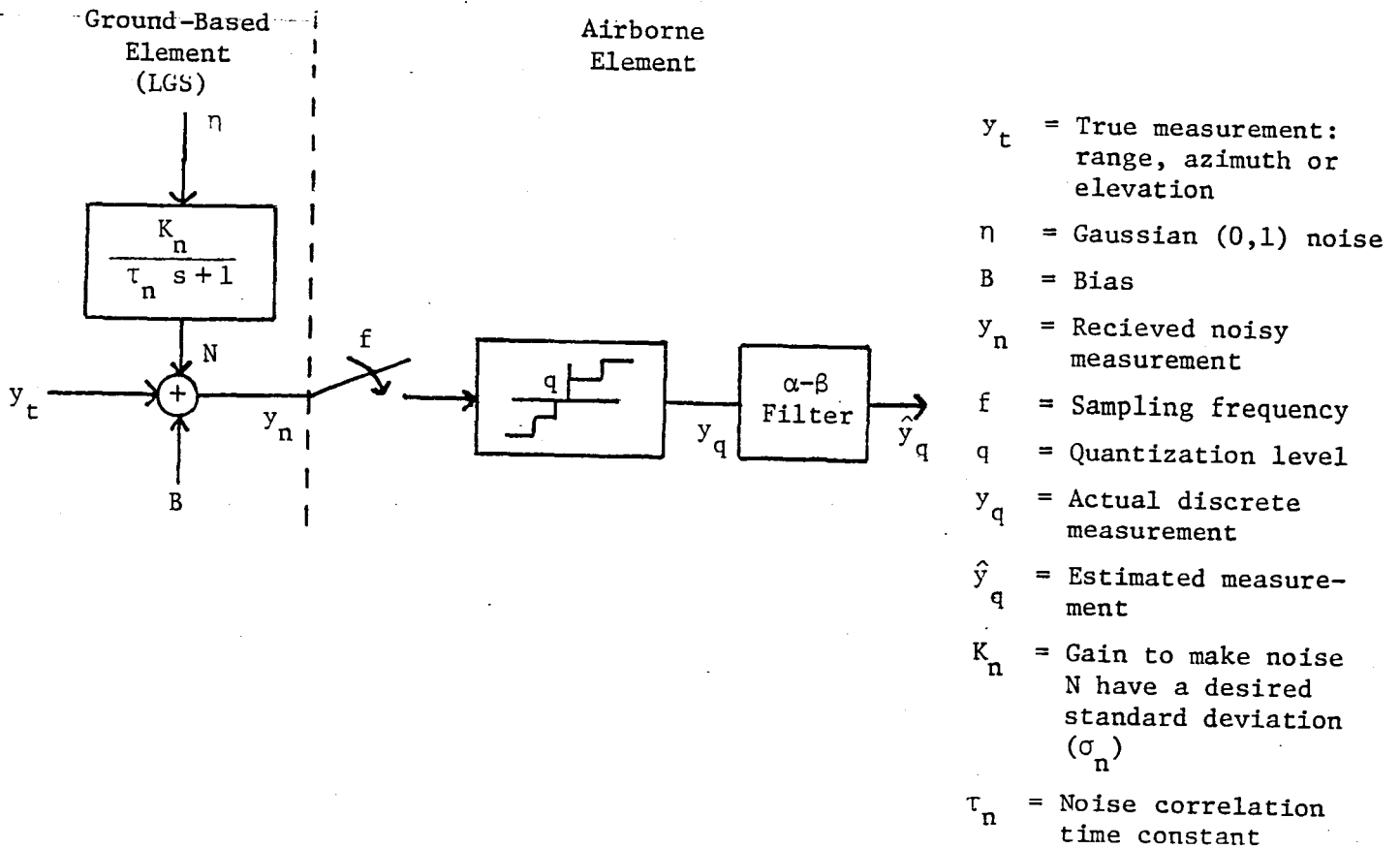


Figure 3. Navigation System Model

The digital filter processes the raw (noisy) range measurements and obtains estimates of the helicopter's current range and range rate. Since the digital filter does not have a floating point processor, the estimated range rate is quantized as well.

The analysis below shows that the quantization of the raw range measurement (y_n) contribute a mean and standard deviation to the discrete time measurements y_q . Considering Figure 3 the raw signal y_n can be written as:

$$y_n = y_t + N + B \tag{1}$$

where N and B are additive colored noise and bias respectively. Further, this raw signal is quantized to give the signal y_q [5]:

$$y_n = y_q + \varepsilon \quad (2)$$

where y_q is the truncated signal and ε is the truncation error.

Consequently, if the quantized signal y_q is measured then the residue r can be written as:

$$\begin{aligned} r &= y_t - y_q \\ &= \varepsilon - (N+B) \end{aligned} \quad (3)$$

Assuming that the truncation errors are random with a uniform density [5], and truncation and noise are independent processes, taking expected values of the above gives:

$$\bar{r} = \frac{q}{2} - B \quad (4)$$

$$\sigma_r^2 = \frac{q^2}{12} + \sigma_n^2 \quad (5)$$

where q is the quantization level of the range,

\bar{r} , σ_r are the mean and standard deviation respectively of the residue r .

Range and Range Rate Filters: A critical part of the airborne navigation subsystem is the digital range/range rate filter. For the purpose of this study, a commonly used α - β filter [2] was simulated. Appendix B describes the α - β filter as implemented in this study. Figure B.1 shows the configuration of this filter. The α - β parameters define the bandwidth (ω_n) and damping (ζ) of the second order filter:

$$\omega_n = \sqrt{\beta} \quad (6)$$

$$\zeta = \frac{\alpha + \beta \Delta T}{2\sqrt{\beta}} \quad (7)$$

where ΔT is the dynamics update rate.

Using the mathematical models for the navigation, guidance and control systems, a simulation was developed to study the sensitivity of the closed loop performance of the UH1H helicopter to the navigation system parameters. The next section presents and discusses the results of this simulation.

SIMULATION AND ANALYSIS

Modules were developed to simulate the navigation, guidance and control system models described above. These modules were combined with an existing program that simulated the nonlinear aerodynamics of the UH1H helicopter. The complete simulation program was then used to study the closed loop behavior of the helicopter DSAL system.

The DSAL simulation begins following localizer capture at a range of 15000 ft. A straight-in approach simulation run consists of the following four phases: (1) cruise at constant altitude of 1500 ft and constant speed of 60 kts, (2) constant speed glideslope capture, (3) constant speed 6° glideslope tracking until initiation of deceleration at 5815 ft range-to-go and (4) constant deceleration (.03 g) to land at the helipad at zero range rate. Initial helicopter cruise altitude is selected to be 1500 ft in order to minimize the effects of glideslope capture transients on the system performance measures at or near touch-down. The simulation run terminates when the helicopter altitude reaches ground level (0 ft). All simulation runs were done on the CDC 7600.

System Performance Measures

In order to evaluate the sensitivity of the overall system to the navigation system parameters, the performance measures shown in Table 1 are used. Definitions (1-4) and (7-9) are measures of the Total System Error (TSE), while definitions (5-6) are measures of the Navigation System Error (NSE).

NOTE:

- (a) Desired azimuth, elevation and altitude are computed in terms of the helicopter's actual range and desired glideslope.
- (b) Desired range rate is computed as a function of the helicopter's actual range.
- (c) Desired altitude at decision range is the altitude the helicopter should be at actual decision range on a desired glideslope path.

Table 1

System Performance Measures

No.	Performance Measure	Definition	Plot Variable
1	Localizer Deviation	Desired Azimuth - Actual Azimuth	LOC ERROR (DEG)
2	Glideslope Deviation	Desired Elevation - Actual Elevation	GS ERROR (DEG)
3	Altitude Error	Desired Altitude - Actual Altitude	ALT ERROR (FT)
4	Range Rate Error	Desired Range Rate - Actual Range Rate	RDOTD - RDOTA (FT/S)
5	Range NSE	Actual Range - Estimated Range	RANGE NSE (FT)
6	Range Rate NSE	Actual Range Rate - Estimated Range Rate	RDOT NSE (FT/S)
7	Altitude Error at Decision Range	(Desired Altitude - Actual Altitude) at Decision Range. Values of 2000, 1500, and 500 ft are chosen corresponding to Decision Heights of 200, 150, 100 and 50 ft, respectively on a 6° approach	DECISION ALTITUDE ERRORS (μ, σ) FT
8	Range Rate Error at Decision Range	(Desired Range Rate - Actual Range Rate) at Decision Range. Decision Range value as defined in 7 above.	RANGE RATE ERRORS (μ, σ) KNOTS
9	Range Error at Touchdown	Desired Range at 0 ft Decision Height - Actual Range at 0 ft Decision Height.	DECISION RANGE ERRORS (μ, σ) FT

Monte Carlo procedures with thirty individual runs are used to compute the ensemble mean and standard deviation of the performance measures defined above. The measurement noise sequences for each run are different. The ensemble statistics of variables (1-6) defined above are plotted as a function of range-to-go. The mean and one standard deviation envelopes ($\mu \pm \sigma$) of variables 7 and 8 are plotted as a function of the decision range.

The remainder of this section is organized in the following four parts:

1. Case descriptions of navigation system parameters.
2. Overall system performance results for the DSAL system with (i) perfect range /range rate information and (ii) with the nominal navigation system.
3. Sensitivity analysis results as a function of on-board navigation system parameters.
4. Sensitivity analysis results as a function of ground-based navigation system parameters.

Case Descriptions of Navigation System Parameters

The navigation system mathematical model described earlier introduced eight parameters that characterize a navigation system. These variables are defined here again for convenience. Nominal values of these parameters for the range system are given in parentheses.

LGS Parameters:

- σ_n = measurement noise: (1 ft)
- τ_n = noise correlation time constant: (0.1 s)
- B = measurement bias: (0 ft)

Airborne System Parameters:

- f = data update frequency = $\frac{1}{\Delta T}$: (16 Hz)
- q = quantization: (1 ft)

q_r = rate quantization: (1 kt \equiv 1.7 ft/s)

ζ = α - β filter damping: (0.707)

ω_n = α - β filter bandwidth: (2 rad/s)

In order to investigate the effects of the navigation system parameters on the overall system performance, a subset of combinations of the eight parameters defined above is selected. The study is conducted by varying some of the parameters defined above about a nominal set. Variations of τ_n , B and ζ are not considered. Any effects due to the changes in τ_n can be minimized by an appropriate selection of the filter bandwidth ω_n . Effects due to the bias B are deterministic and can be corrected for. The filter damping ζ was fixed at .707. Table 2 below shows the combinations of the navigation system parameters investigated in this study.

Table 2. Navigation System Parameters Used in Study

Case	On-board System Parameters				Ground-based System Parameter σ_n (ft)
	f(Hz)	q(ft)	q_r (ft/s)	ω_n (rad/s)	
0 (Nominal)	16.0	1.0	1.7	2.0	1.0
1	4.0	-	-	-	-
2	8.0	-	-	-	-
3	-	10.0	-	-	-
4	-	30.0	-	-	-
5	-	-	8.5	-	-
6	-	-	17.0	-	-
7	-	-	-	0.2	-
8	-	-	-	10.0	-
9	-	-	-	-	10.0
10	-	-	-	-	30.0

Note that entries with a dash (-) mean that the nominal value (case 0) was used for the pertinent parameter.

Cases 1 through 8 are used to investigate the performance sensitivity to on-board navigation system parameters (f, q, q_r, ω_n). Case 9 through 10 show effects of varying the ground-based LGS parameter (σ_n).

The next section compares results of the overall system performance using perfect range/range rate information and the nominal navigation system. These results will then be used as a reference to evaluate the sensitivity of the overall closed-loop system to individual navigation model parameters.

System Performance Using Perfect Range/ Range Rate and the Nominal Navigation System

In order to separate tracking errors caused by the control and navigation systems, the simulation was first run with perfect range and range rate information (i.e., a perfect navigation system is assumed with zero range measurement noise and no on-board quantization or filtering). It was found that when the range rate command as shown in Figure 2(a) is used the helicopter touches down short of the helipad with a non-zero range rate. In order to decrease this touchdown velocity, a 5 ft/s velocity offset was subtracted from the nominal commanded velocity of $\sqrt{1.96r}$. This velocity offset meant that deceleration began at 5815 ft instead of the nominal 5285 ft.

Figures 4(a)-(h) show the ensemble statistics of performance measures (1-6) of Table 1 using (i) perfect range/range rate and (ii) the nominal navigation system parameters (Case 0 in Table 2). Figures 4(a)-(c) show that the localizer, glideslope and altitude deviations are negligible. These errors are large at close range due to the ill-defined nature of these variables at the origin of the reference frame. Figure 4(d) shows that both simulations terminated with the helicopter landing short at a range of 28 ft and moving at about 3 ft/s (1.75 knots). This was regarded as an acceptable touchdown. Since touchdown is defined to occur when the helicopter reaches ground level, compensation must be made in the vertical guidance loop in addition to the range rate loop to ensure that the simulation terminates with the helicopter at zero range and

PERFECT AND NOMINAL SYSTEMS
PERFECT SYS , ---- NOMINAL SYS

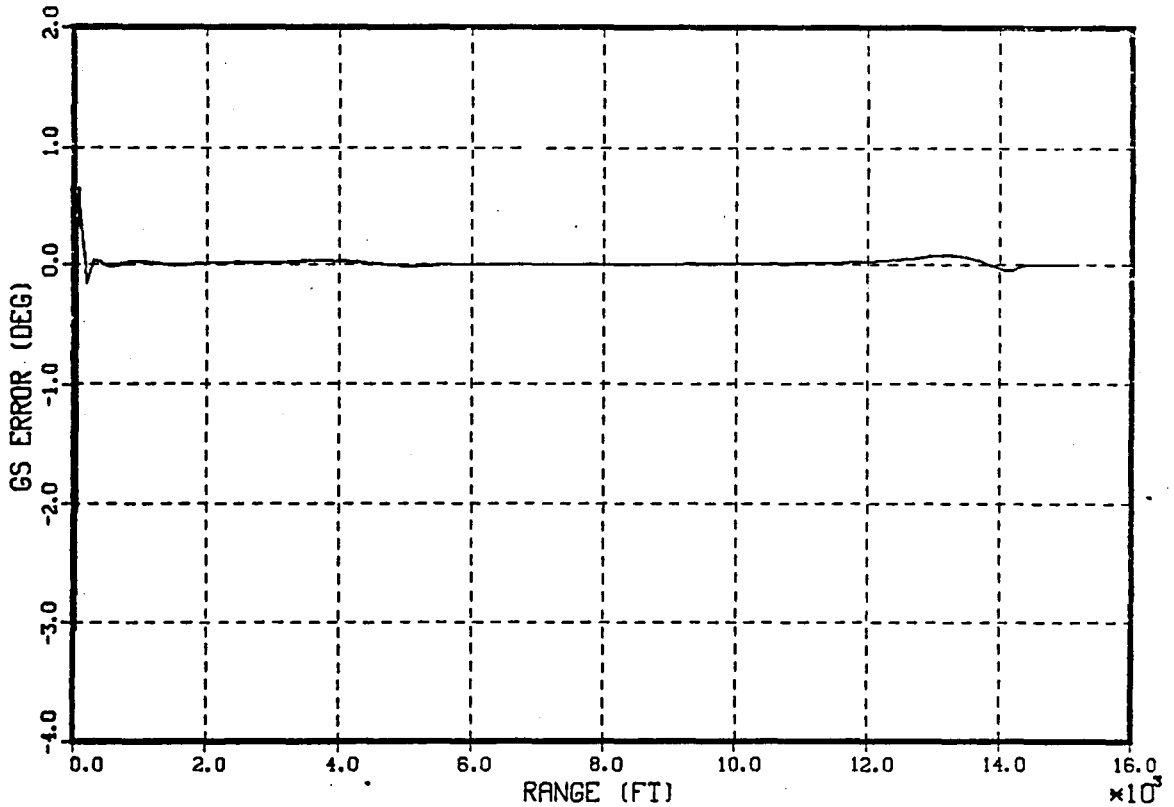
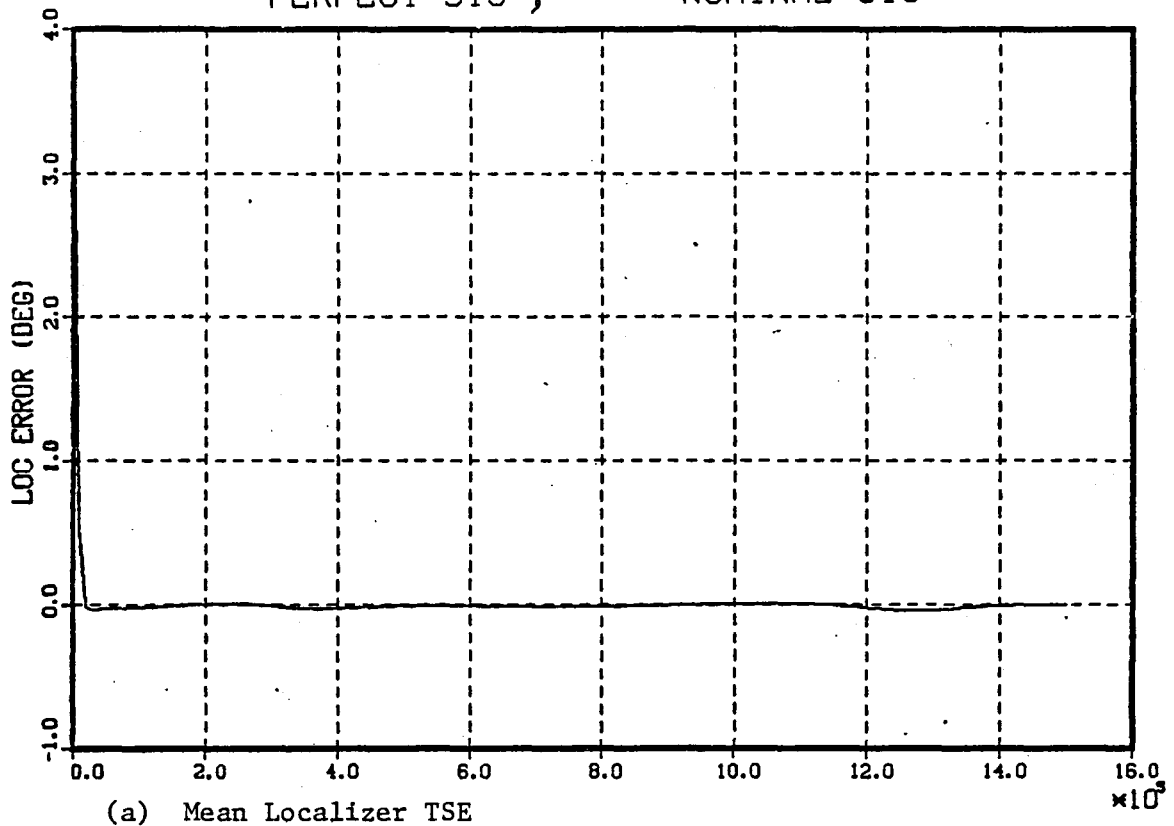
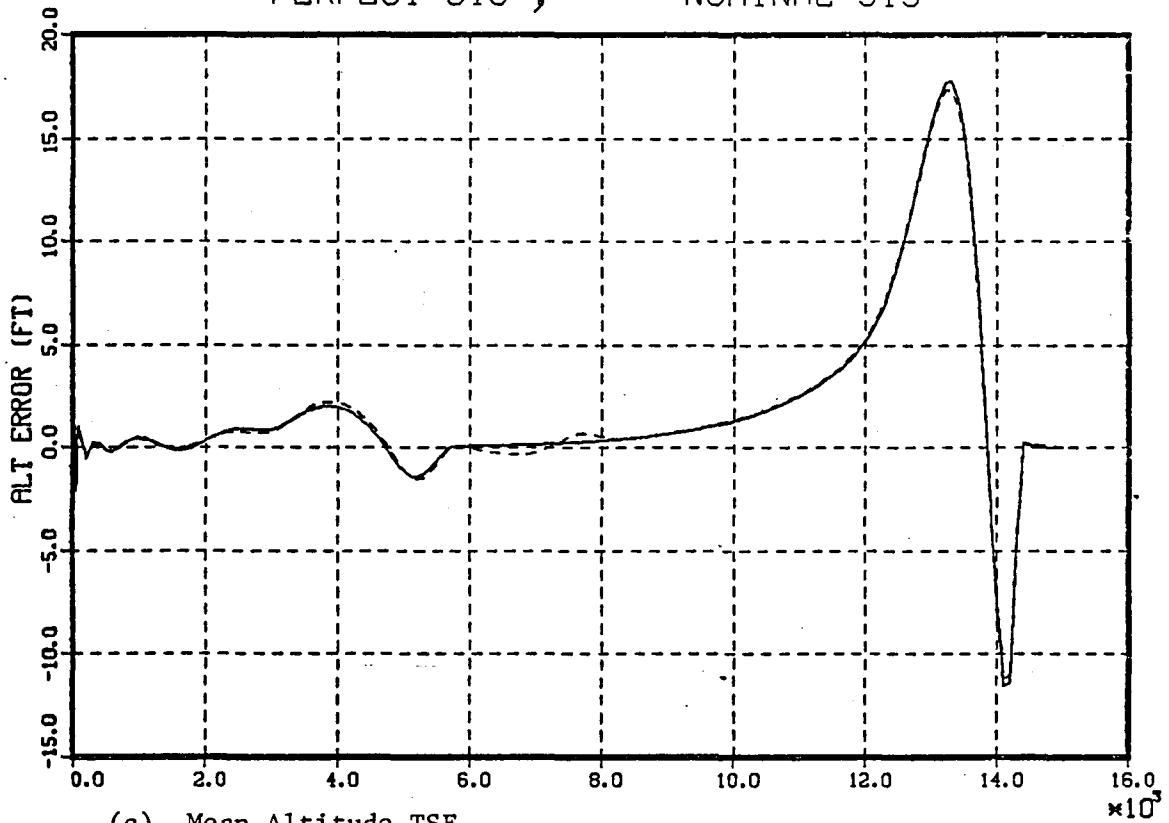
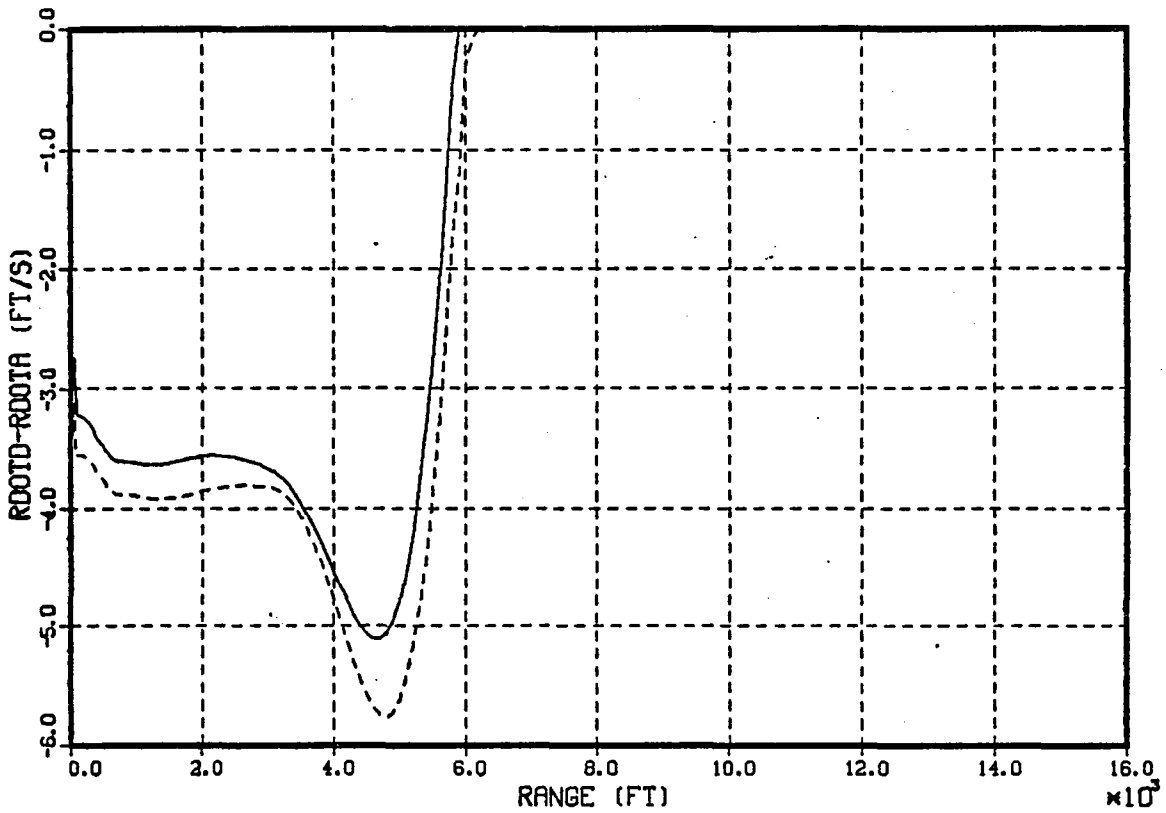


Figure 4. Ensemble Statistics for DSAL System with Perfect Range/
Range Rate and Nominal Navigation System

PERFECT AND NOMINAL SYSTEMS
 PERFECT SYS , ---- NOMINAL SYS



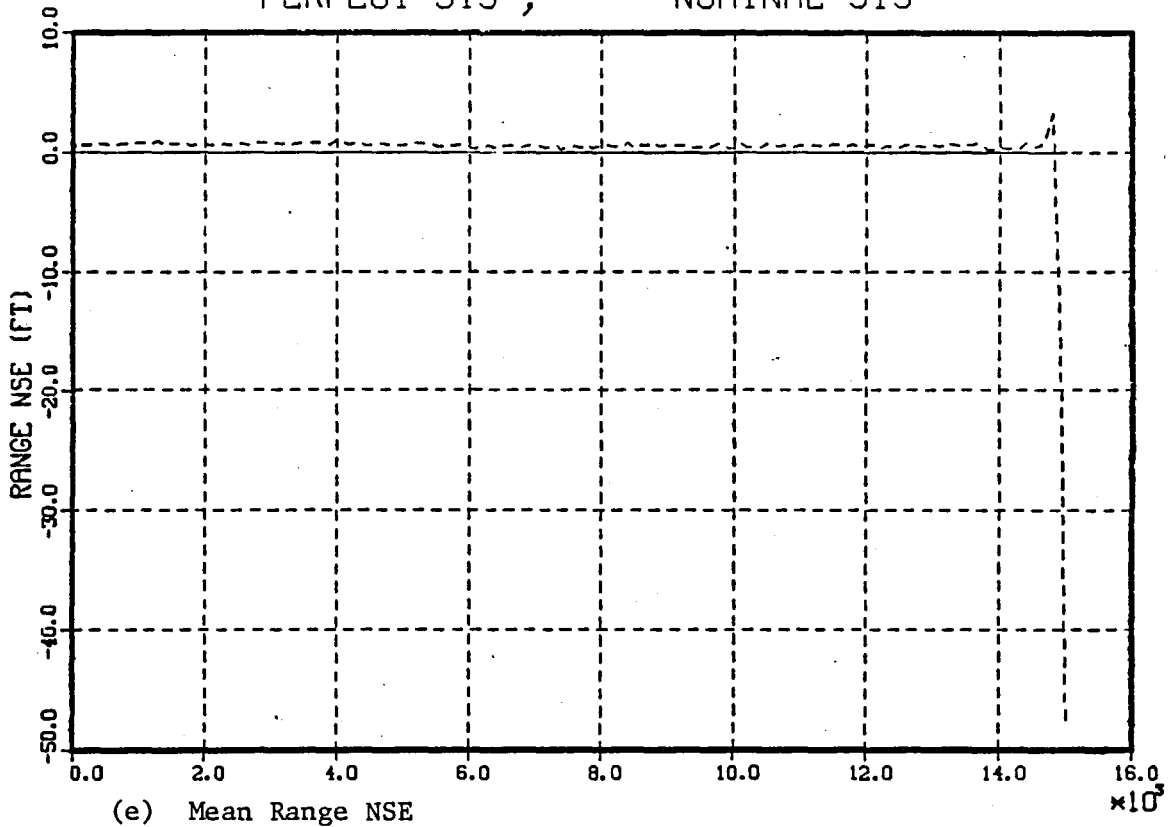
(c) Mean Altitude TSE



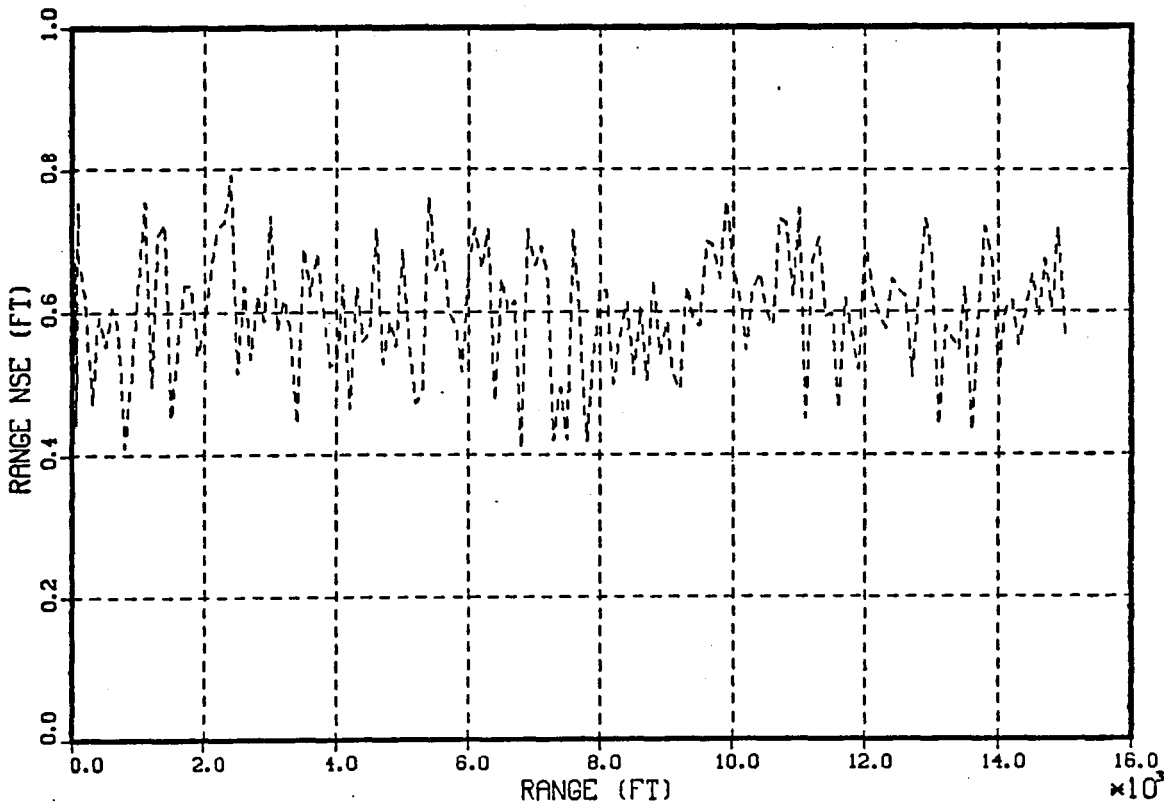
(d) Mean Range Rate TSE

Figure 4. Ensemble Statistics for DSAL System with Perfect Range/
 Range Rate and Nominal Navigation System

PERFECT AND NOMINAL SYSTEMS
PERFECT SYS , ---- NOMINAL SYS



(e) Mean Range NSE



(f) Standard Deviation Range NSE

Figure 4. Ensemble Statistics for DSAL System with Perfect Range/
Range Rate and Nominal Navigation System

PERFECT AND NOMINAL SYSTEMS
 PERFECT SYS , ---- NOMINAL SYS

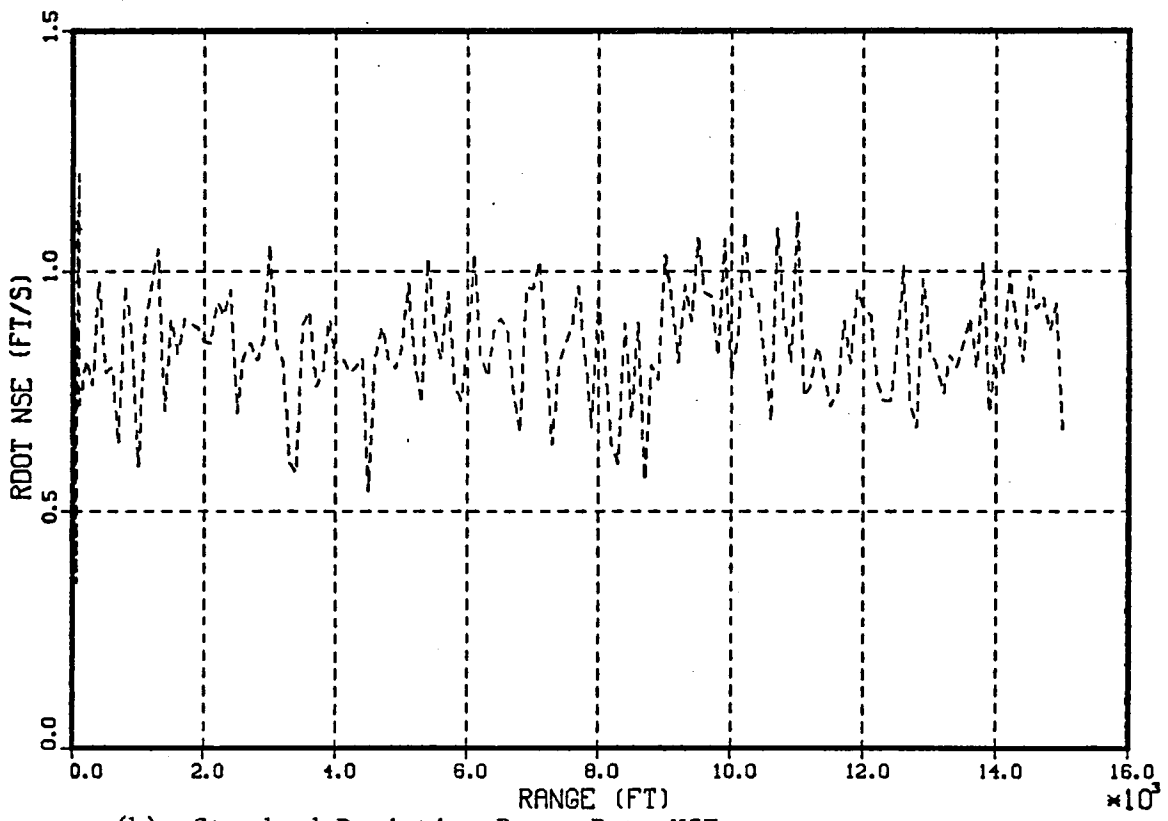
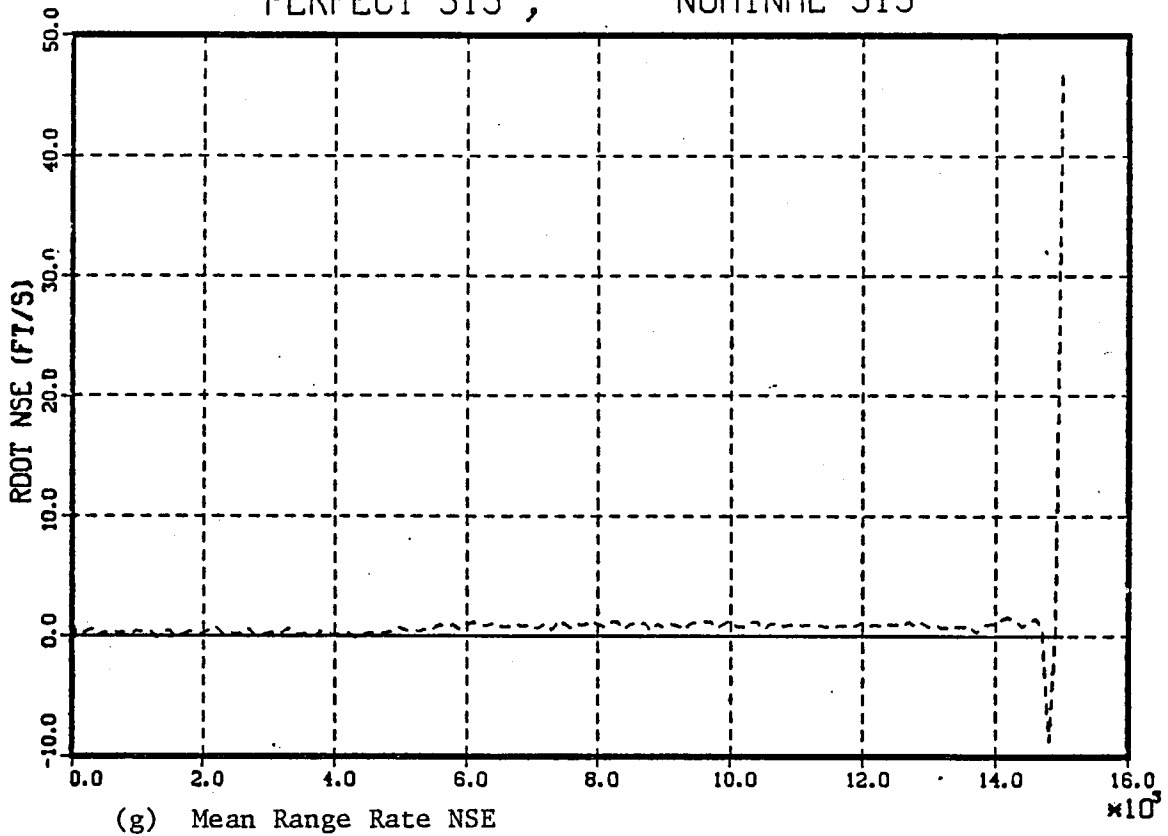


Figure 4. Ensemble Statistics for DSAL System with Perfect Range/
 Range Rate and Nominal Navigation System

range rate. Although compensation for range rate was made, the vertical guidance was not modified. Hence results with the nominal navigation system are used as a baseline to study performance sensitivity to navigation system parameters.

Figure 4(e) shows about .5 ft mean range NSE. This corresponds to the expected mean range NSE due to the range quantization ($q/2$ in Eq. (4)). Similarly, Figure 4(f) shows a mean range rate NSE of 0.85 ft/s due to range rate quantization ($q_r/2$ in Eq. (4)).

The altitude error and range rate error at decision range are not shown since these errors are very small.

Sensitivity to On-board Navigation System Parameters

The on-board receiver and range/range rate filter are characterized by the following four parameters:

- (a) f (Hz) - range measurement sampling frequency.
- (b) q (ft) - range measurement quantization level.
- (c) q_r (ft/s) - quantization level of the estimated range rate.
- (d) ω_n (rad/s) - bandwidth of second order (α - β) range/range rate filter.

The sensitivity of the overall system performance to the above parameters was studied by varying them one at a time while holding all others at the nominal value (see Table 2). The essential results are presented in Figures 5(a)-(c) which show plots of decision altitude, range rate at decision range and of range TSE at touchdown, respectively. The following observations are pertinent:

1. The closed-loop system performance is not very sensitive to range measurement sampling frequency (f) and quantization (q).
2. Increasing the quantization of the estimated range rate causes oscillations in the system as shown by the decision altitude errors (Figure 5(a)). Coarser range rate quantization

increases the magnitude of the mean and standard deviation of the range rate TSE (Figure 5(b)). The standard deviation of the range rate TSE at touchdown is about 7 knots when a range rate quantization of 10 knots (17 ft/s) is used. Consequently, the helicopter flight profile is higher and faster than desired and displays large run-to-run variability during the final 500 ft prior to touchdown.

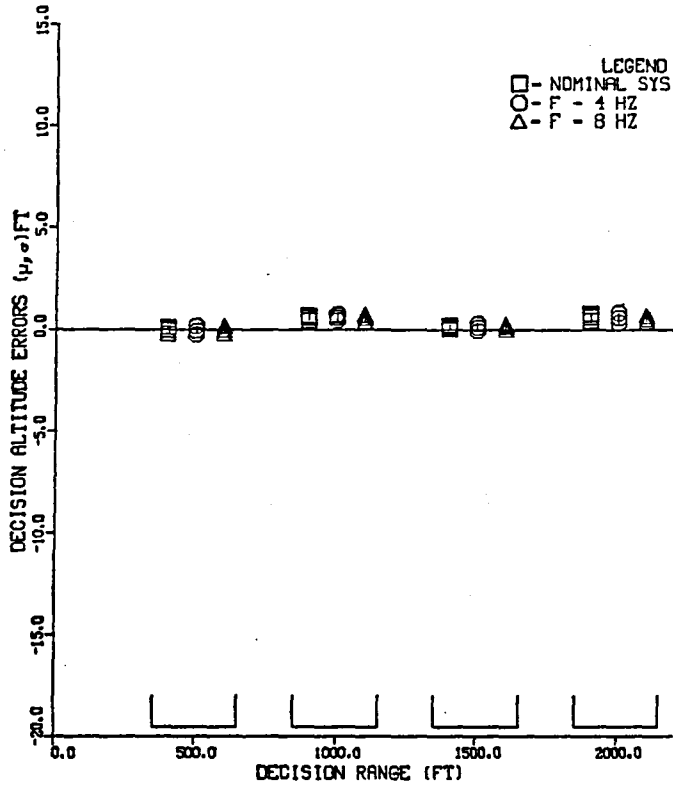
3. Decreasing the bandwidth of the range/range rate filter to .2 rad/s causes oscillations in the system as shown by Figures 5(a),(b). These oscillations are more evident in the ensemble statistics of the TSE as a function of range-to-go (Figures 9(c),(d)).

Figures 6(a)-(h) show the ensemble statistics as the range sampling frequency (f) is varied. These figures confirm that the DSAL performance is not very sensitive to f .

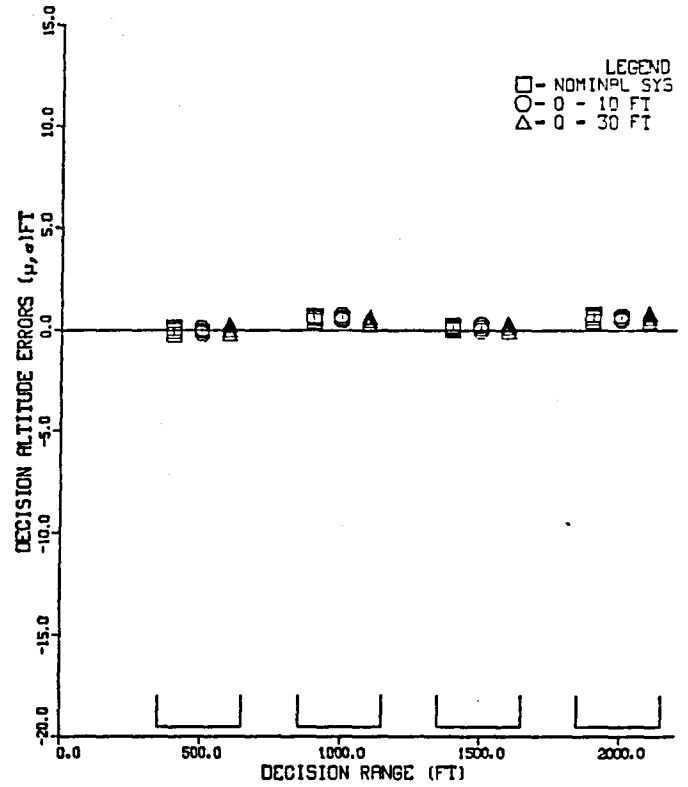
Figures 5(a),(b) show that the altitude and range rate TSE are insensitive to range quantization (q). However, these plots convey no information at ranges less than 500 ft. Figures 7(a)-(h) show the performance sensitivity to range quantization (q). Figure 7(d) shows that the range rate TSE increases as the helicopter comes in to touchdown. Note that the performance of the nominal system (solid line in figures) is to be used as a basis for comparison. Figure 7(c) shows that the effects on altitude TSE as q is increased are not noticeable. Figure 7(e) shows that the range quantization causes a bias in the range NSE as shown by equation (4). It is this bias in estimated range that causes a corresponding error in the range rate TSE.

The oscillations in the helicopter flight profile due to range rate quantization are evident in Figures 8(a)-(h). Once again, note the bias introduced in the range rate NSE (Figure 8(g)) due to the range rate quantization. The figures also show that the mean and standard deviation of range rate NSE decrease drastically around 8000 ft and then increase again. This step change occurs when the pitch axis control system switches to range rate feedback instead of airspeed at about 8300 ft

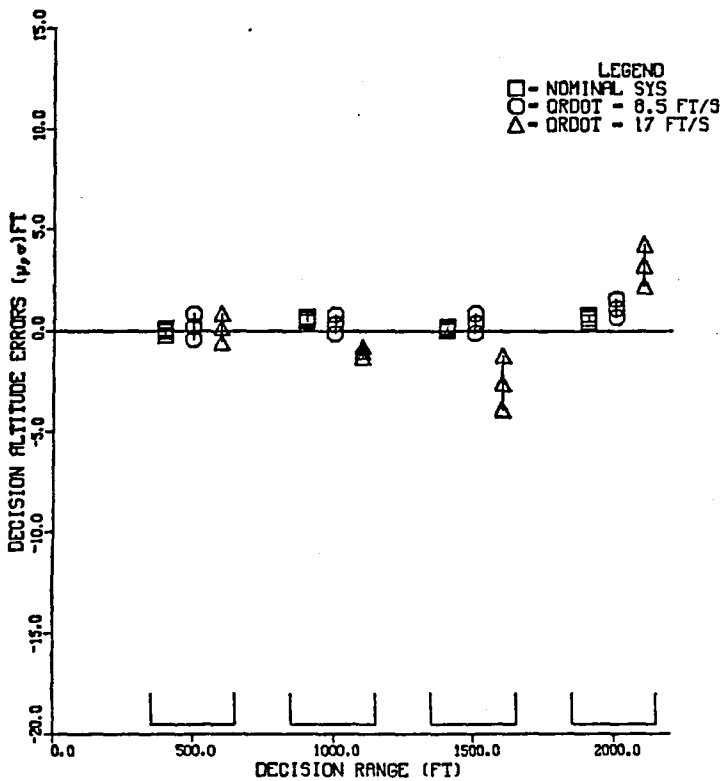
SAMPLING FREQUENCY VARIATION



RANGE QUANTIZATION VARIATION



RANGE RATE QUANTIZATION VARIATION



FILTER BANDWIDTH VARIATION

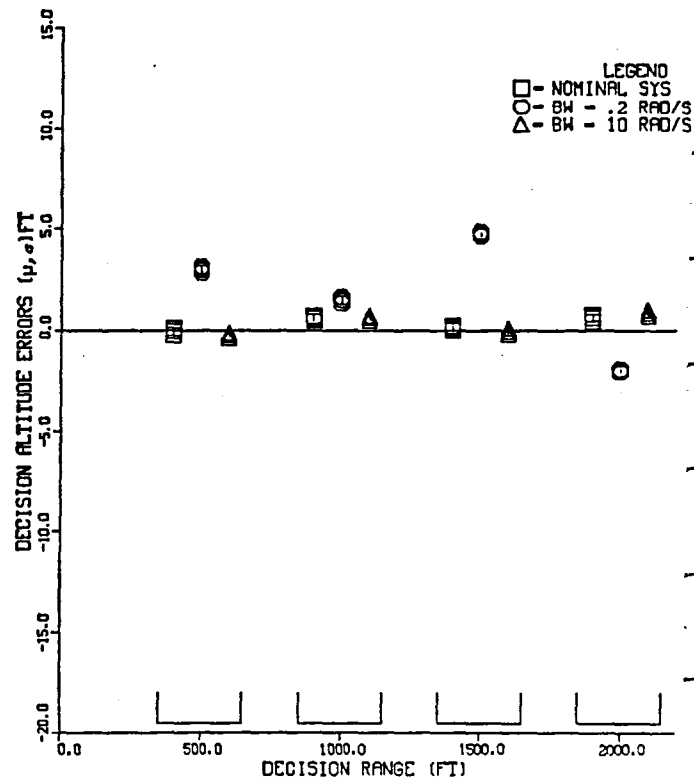
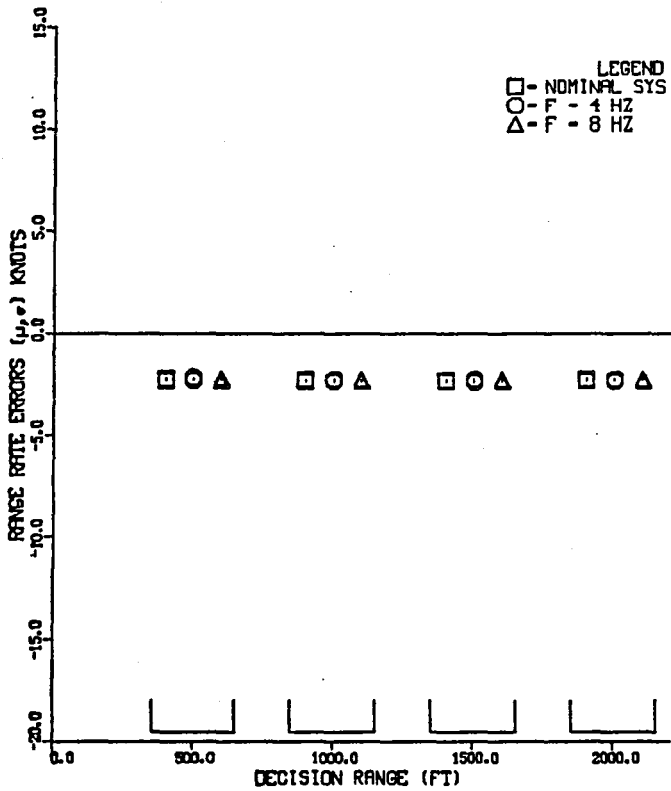
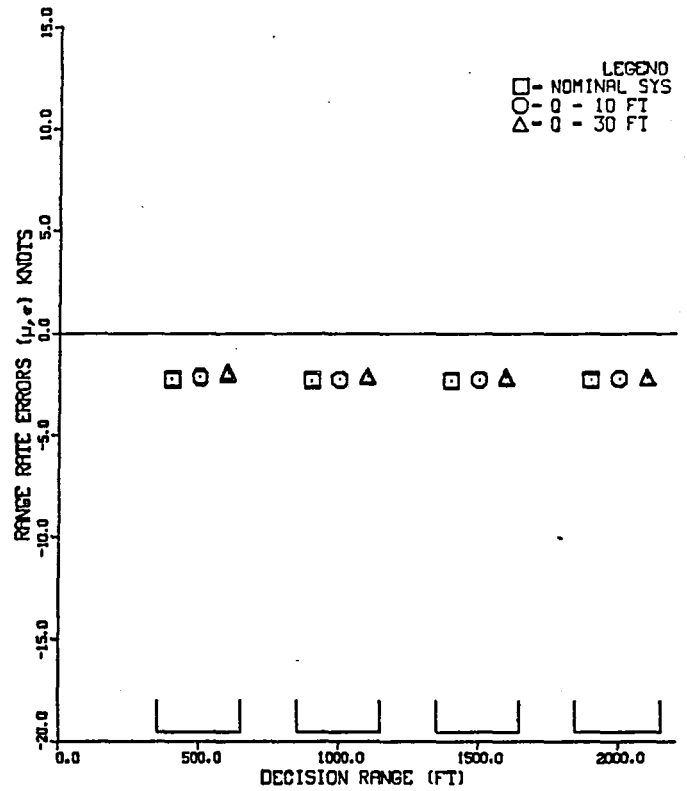


Figure 5(a). Sensitivity of Decision Altitude TSE to On-board Navigation Parameters

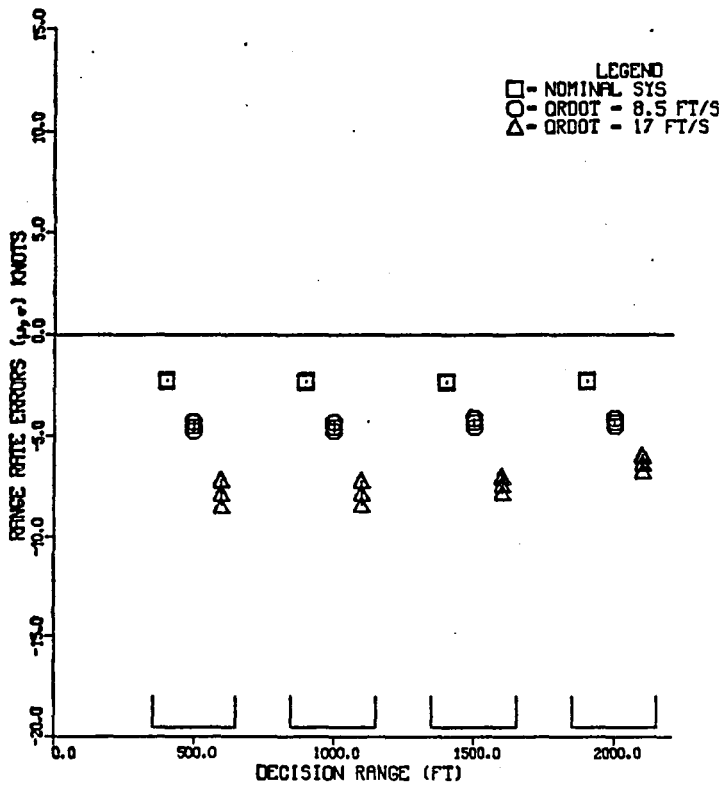
SAMPLING FREQUENCY VARIATION



RANGE QUANTIZATION VARIATION



RANGE RATE QUANTIZATION VARIATION



FILTER BANDWIDTH VARIATION

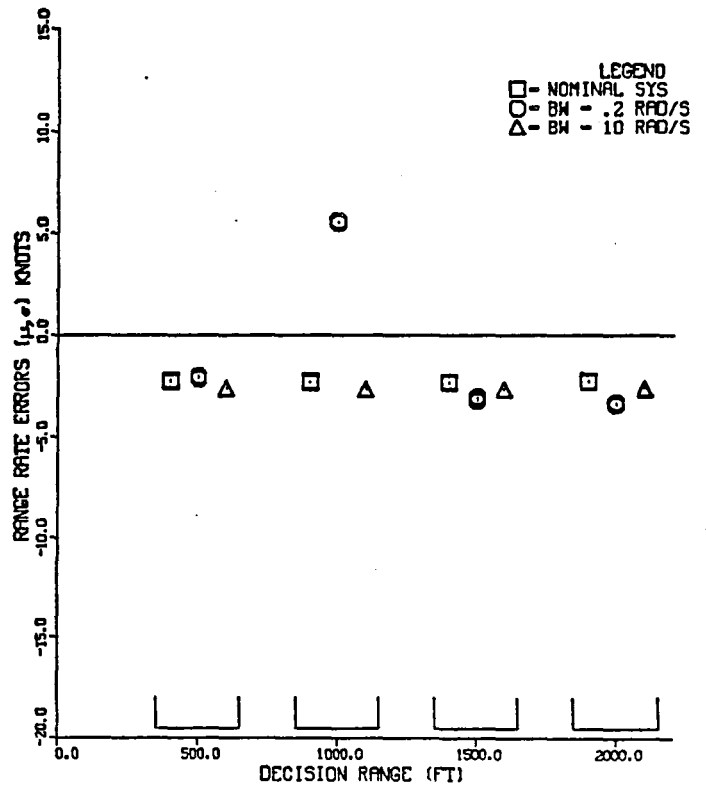


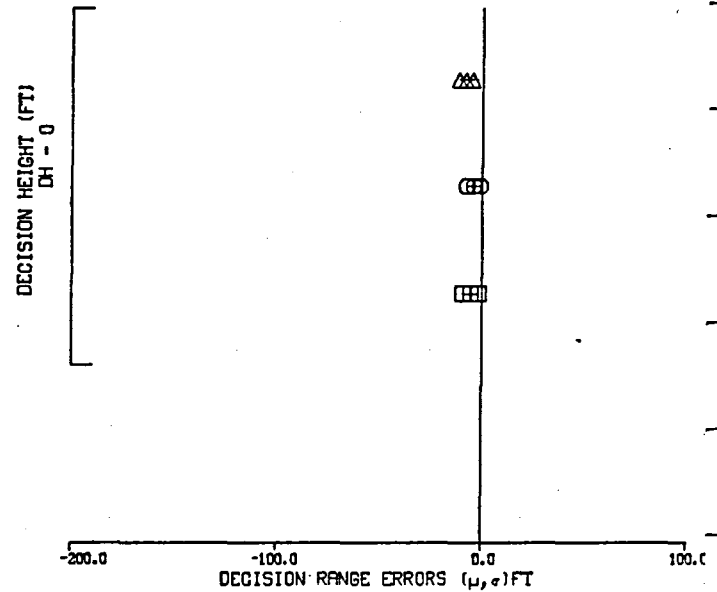
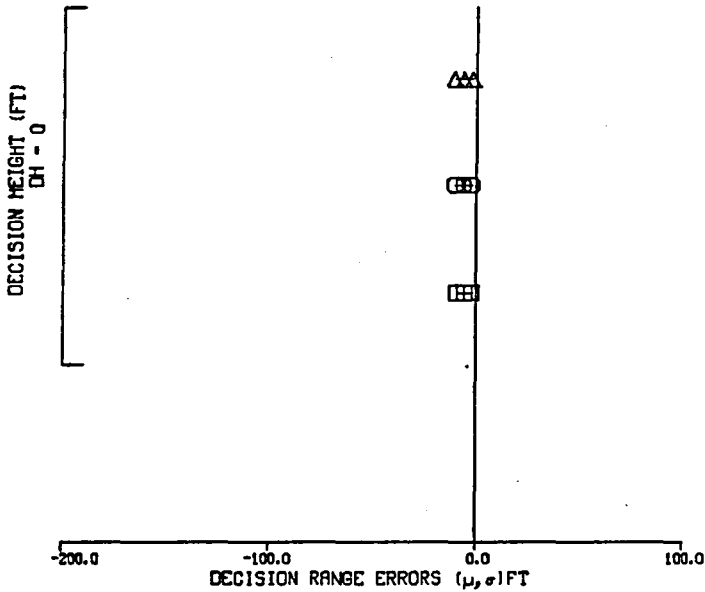
Figure 5(b). Sensitivity of Range Rate TSE to On-board Navigation Parameters

SAMPLING FREQUENCY VARIATION

RANGE QUANTIZATION VARIATION

LEGEND
 □ - NOMINAL SYS
 ○ - F - 4 HZ
 △ - F - 8 HZ

LEGEND
 □ - NOMINAL SYS
 ○ - Q - 10 FT
 △ - Q - 30 FT



RANGE RATE QUANTIZATION VARIATION

FILTER BANDWIDTH VARIATION

LEGEND
 □ - NOMINAL SYS
 ○ - ORDOT = 8.5 FT/S
 △ - ORDOT = 17 FT/S

LEGEND
 □ - NOMINAL SYS
 ○ - BW = .2 RAD/S
 △ - BW = 10 RAD/S

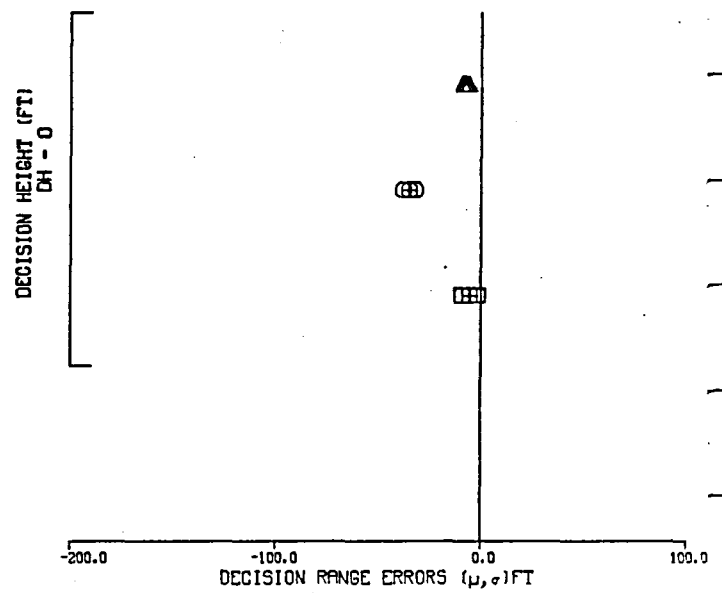
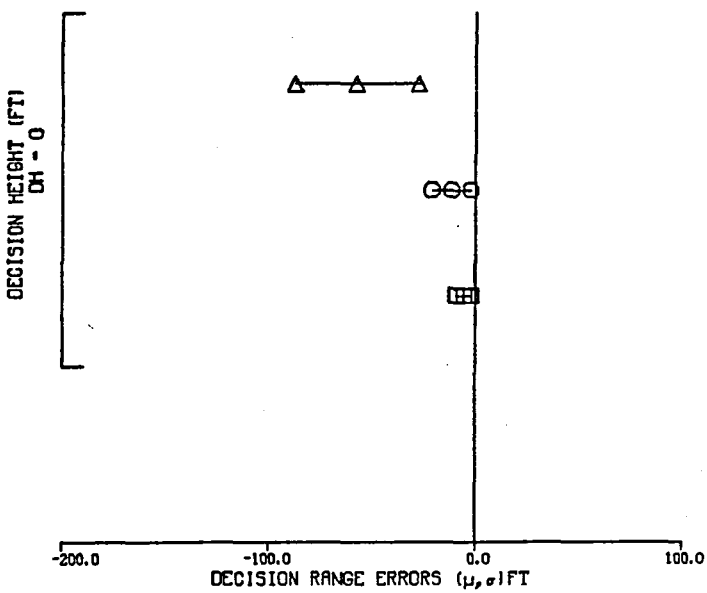


Figure 5(c). Sensitivity of Range TSE at Touchdown to On-board Navigation Parameters

SAMPLING FREQUENCY VARIATION
 NOMINAL SYSTEM , ---- F=4 , F=8 HZ

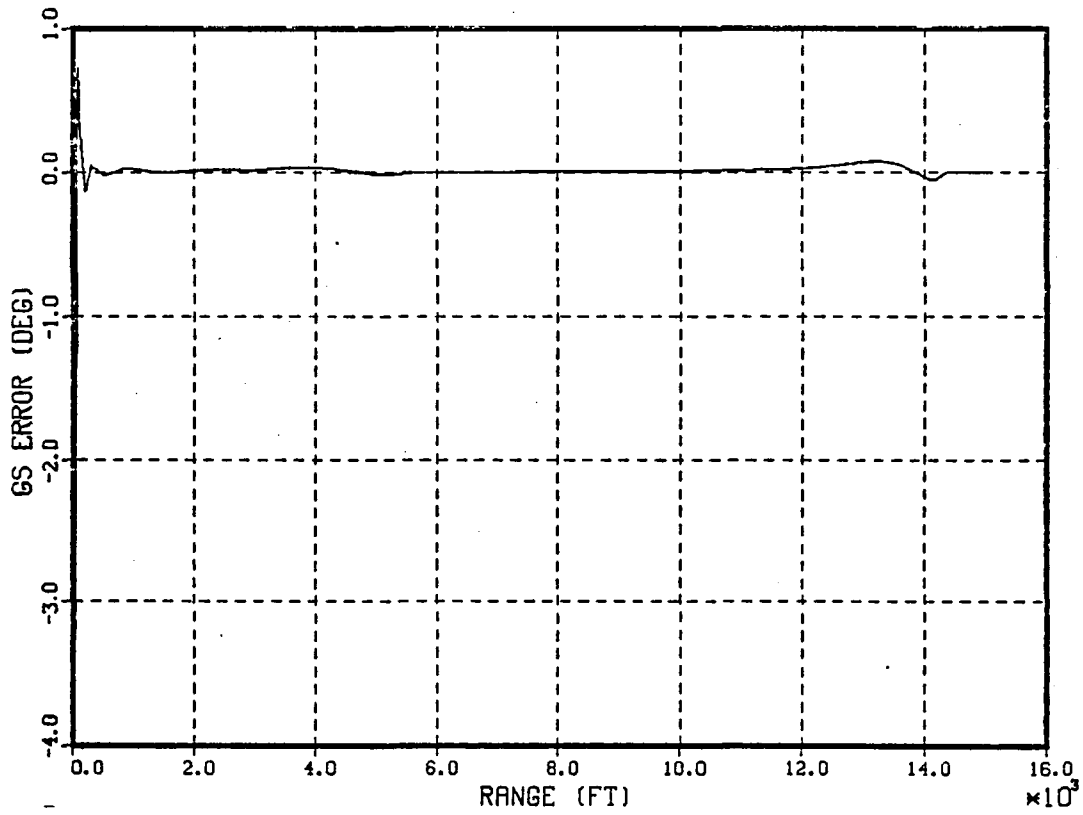
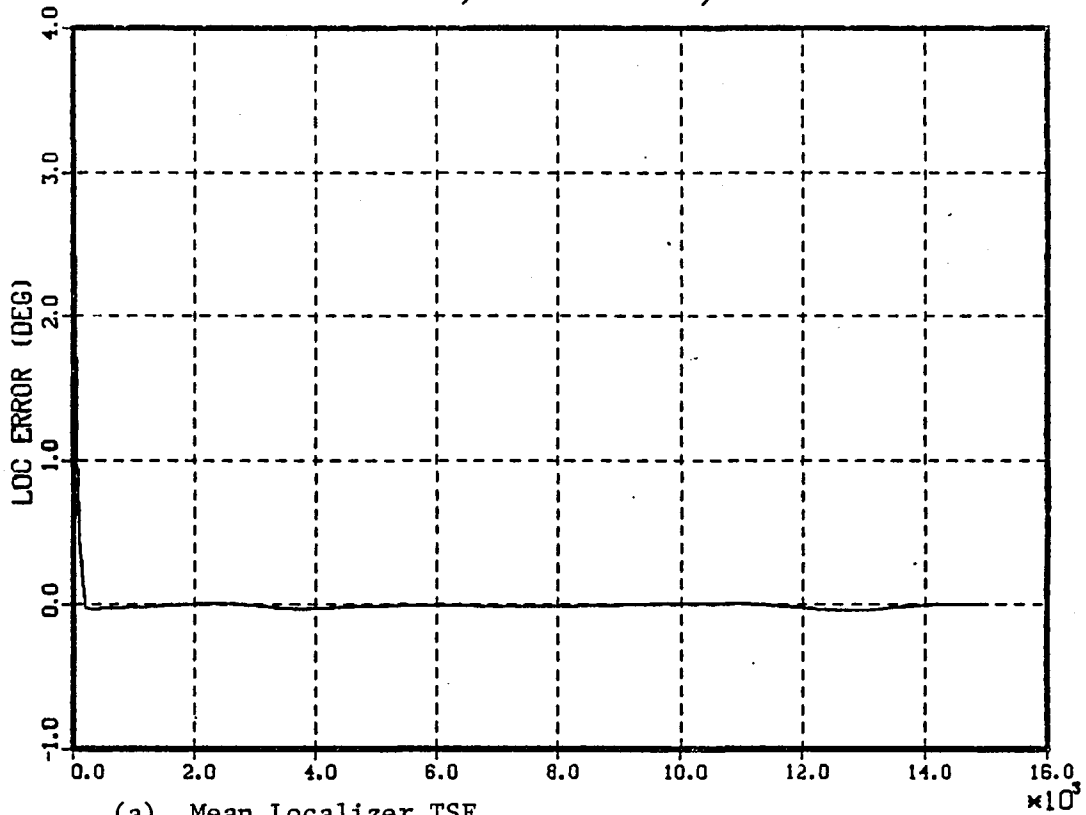
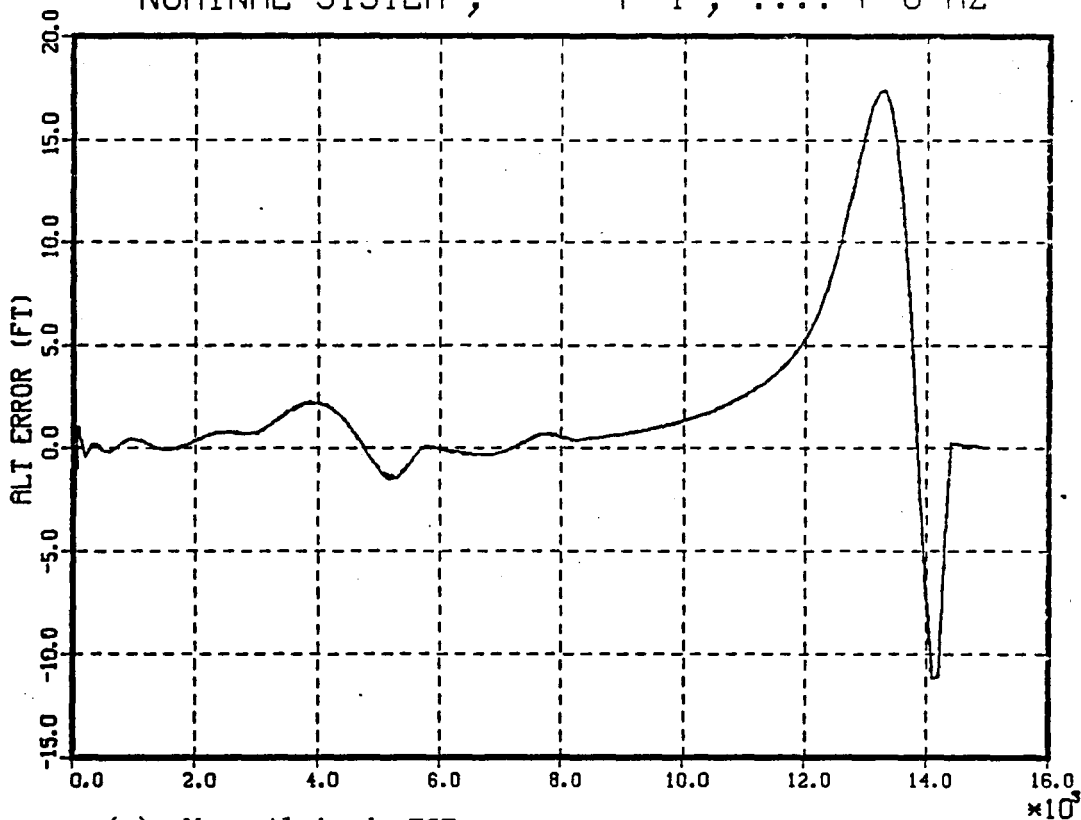
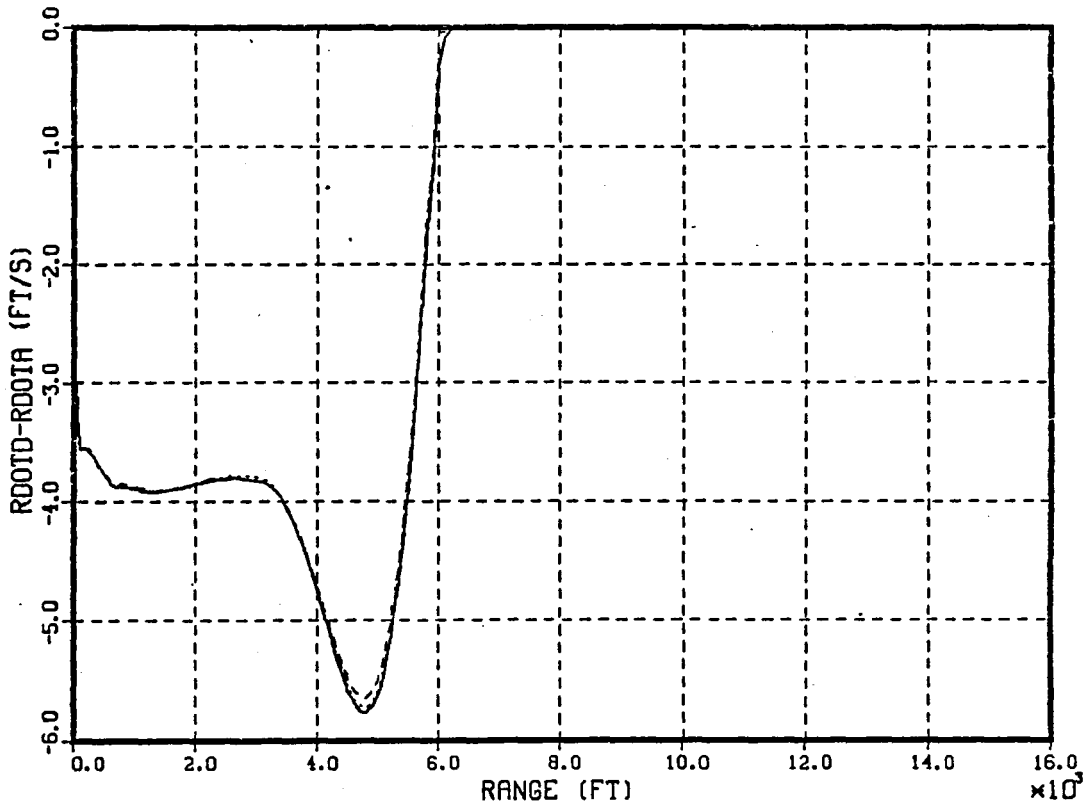


Figure 6. Sensitivity Results as a Function of Sampling Frequency f (Hz)

SAMPLING FREQUENCY VARIATION
 NOMINAL SYSTEM, ---- F=4, F=8 HZ



(c) Mean Altitude TSE



(d) Mean Range Rate TSE

Figure 6. Sensitivity Results as a Function of Sampling Frequency f (Hz)

SAMPLING FREQUENCY VARIATION
 NOMINAL SYSTEM , ---- F=4 , F=8 HZ

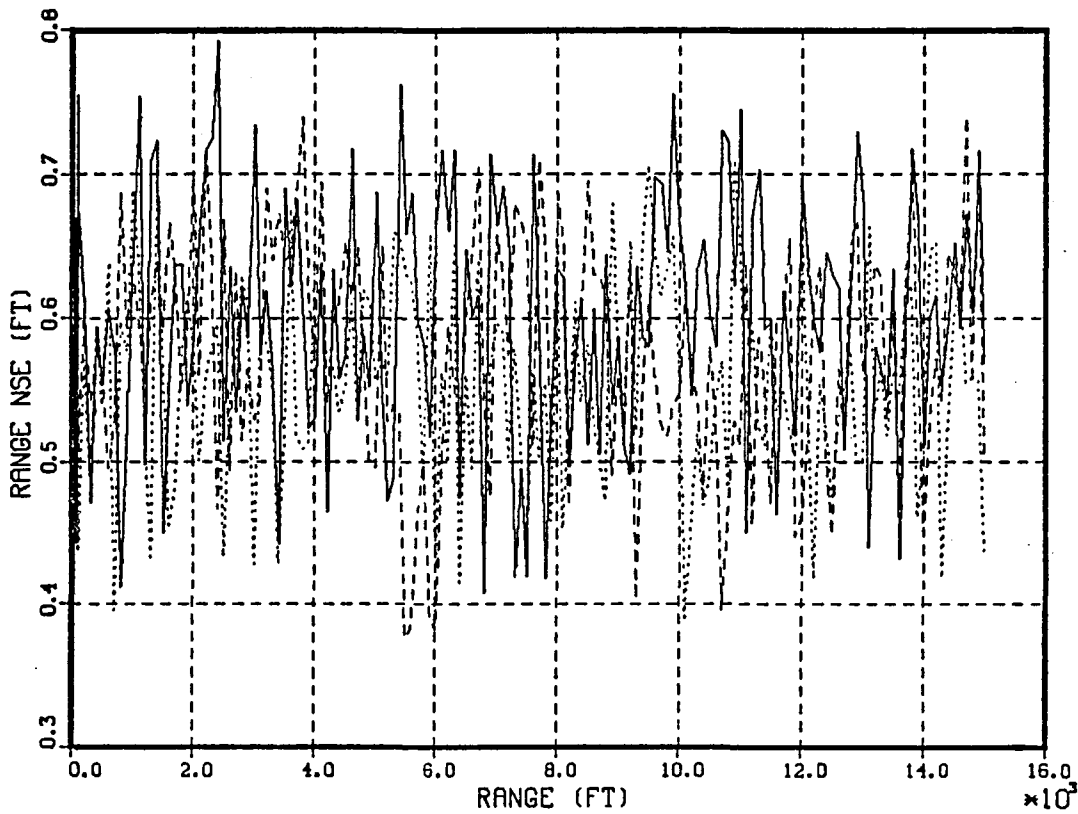
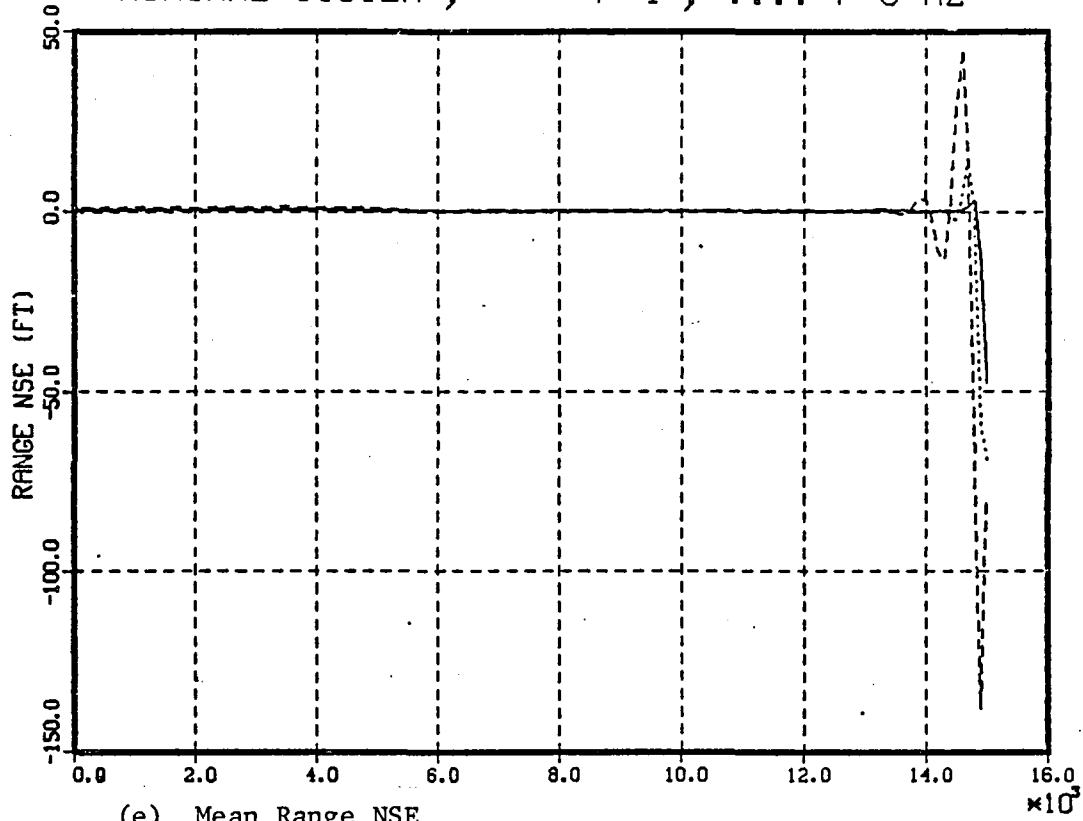


Figure 6. Sensitivity Results as a Function of Sampling Frequency f (Hz)

SAMPLING FREQUENCY VARIATION
 NOMINAL SYSTEM, ---- F=4, F=8 HZ

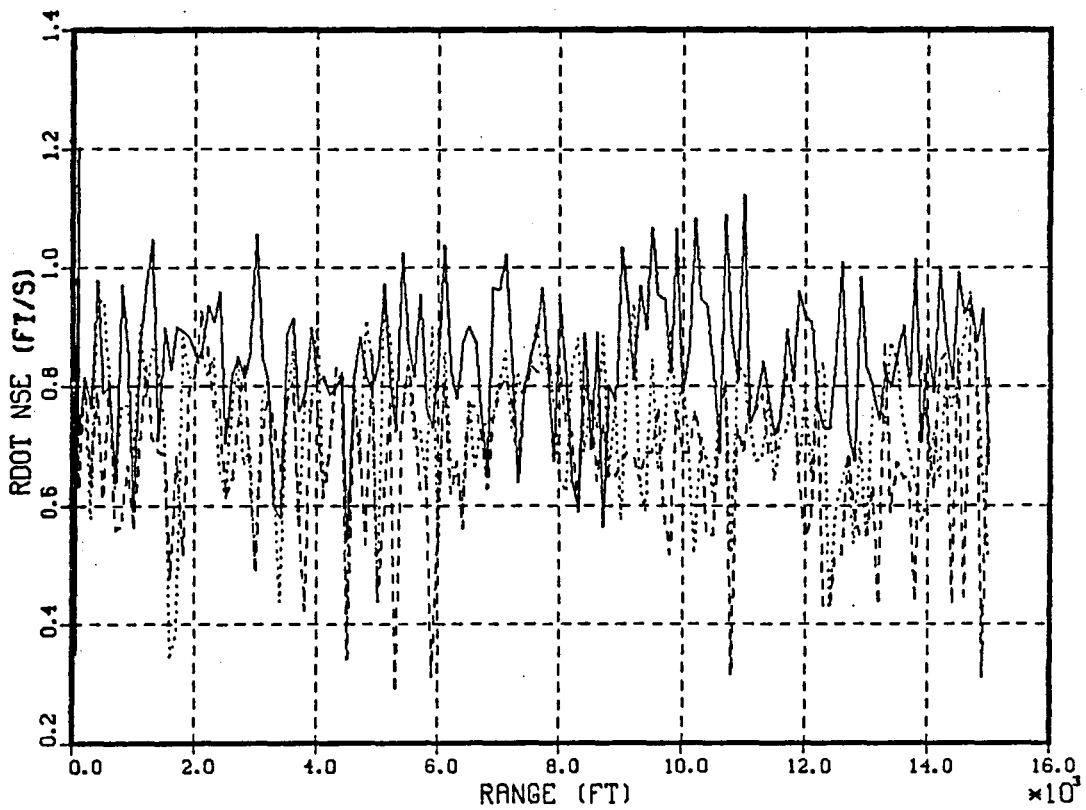
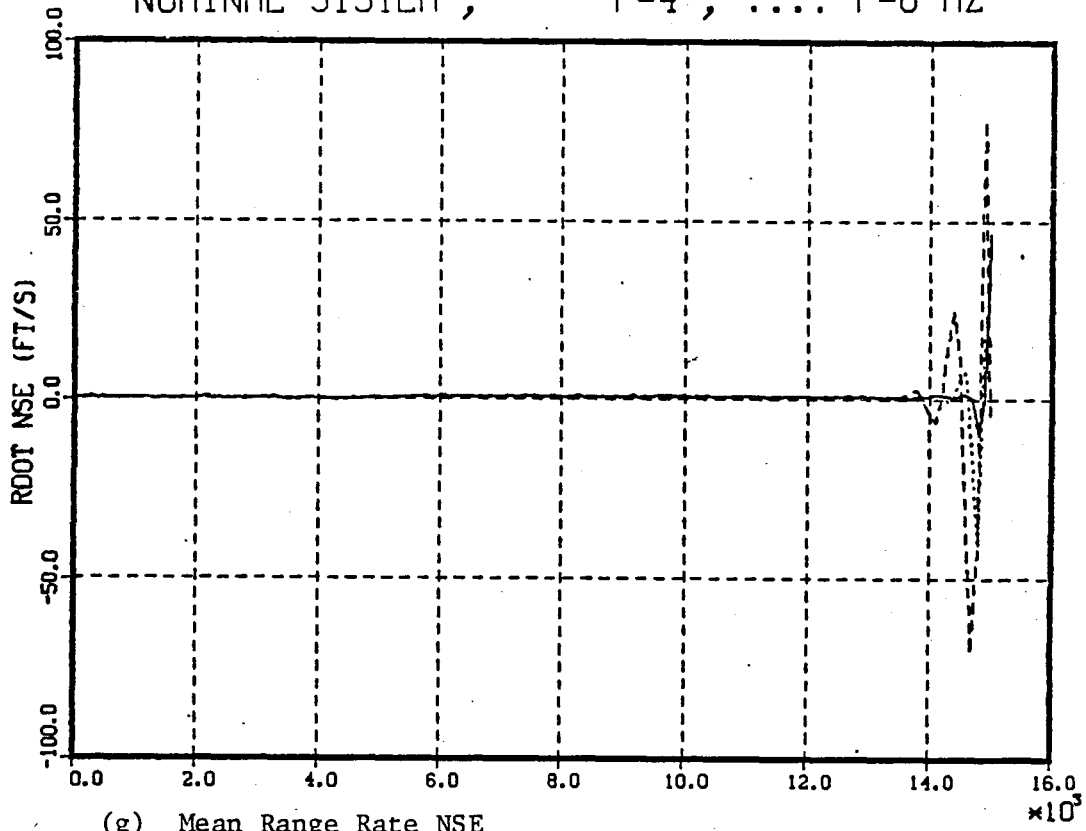


Figure 6. Sensitivity Results as a Function of Sampling Frequency f (Hz)

RANGE QUANTIZATION VARIATION
 NOMINAL SYSTEM , ---- Q=10 , Q=30 FT

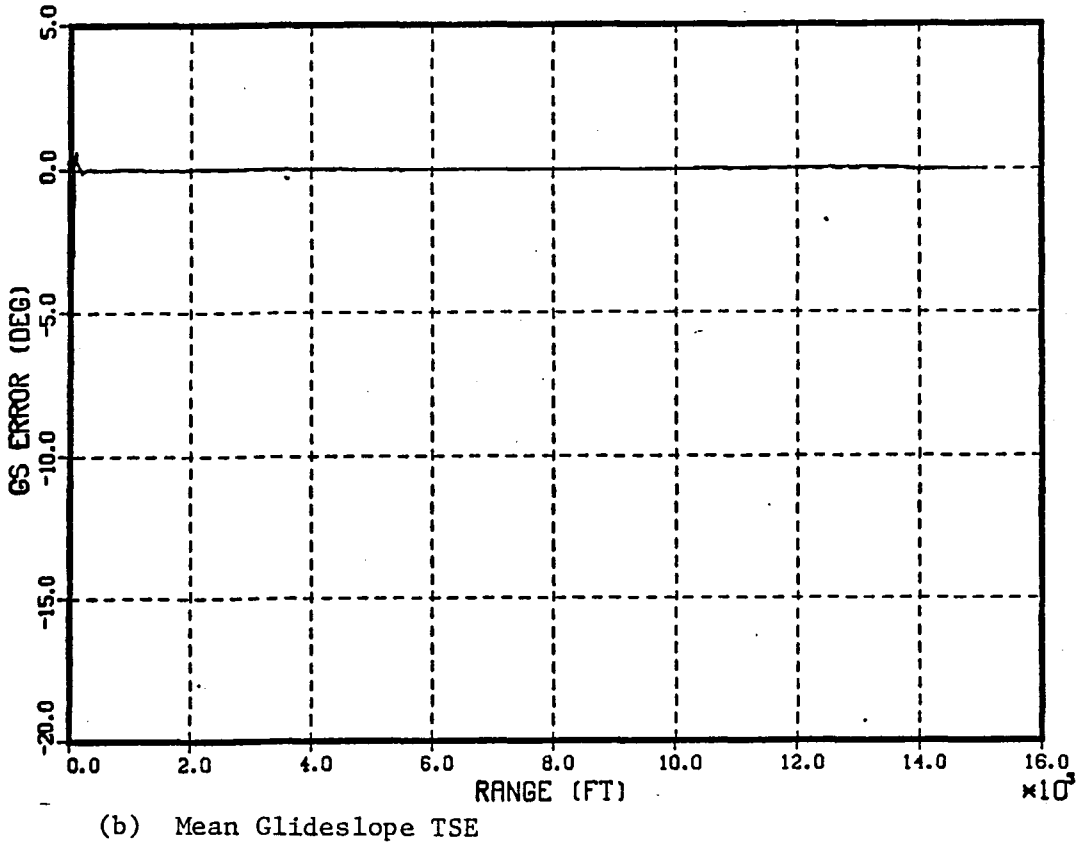
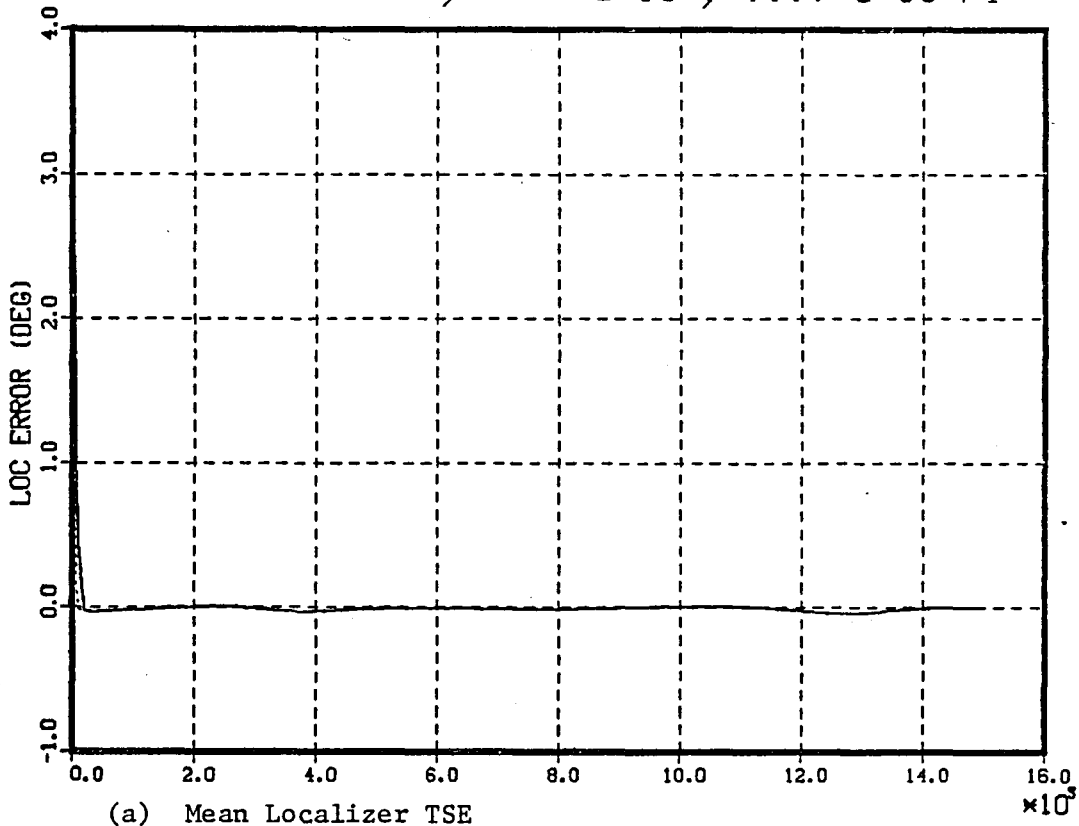


Figure 7. Sensitivity Results as a Function of Range Measurement Quantization q (ft)

RANGE QUANTIZATION VARIATION
 NOMINAL SYSTEM , ---- Q=10 , Q=30 FT

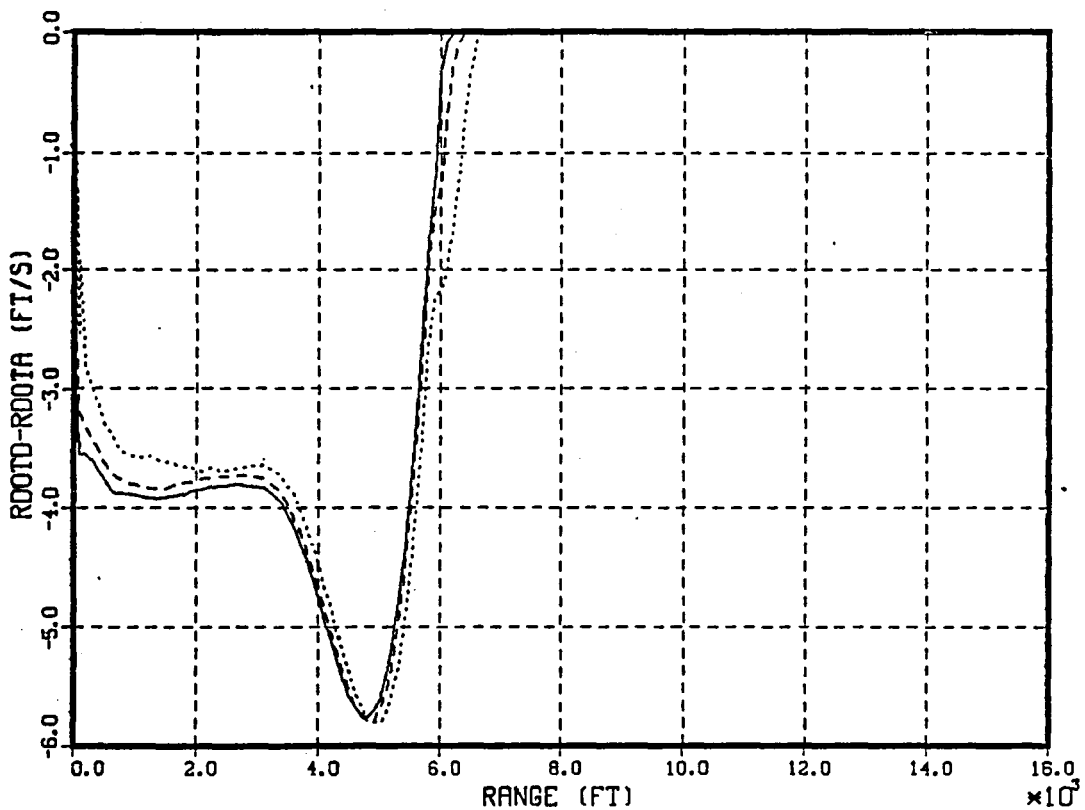
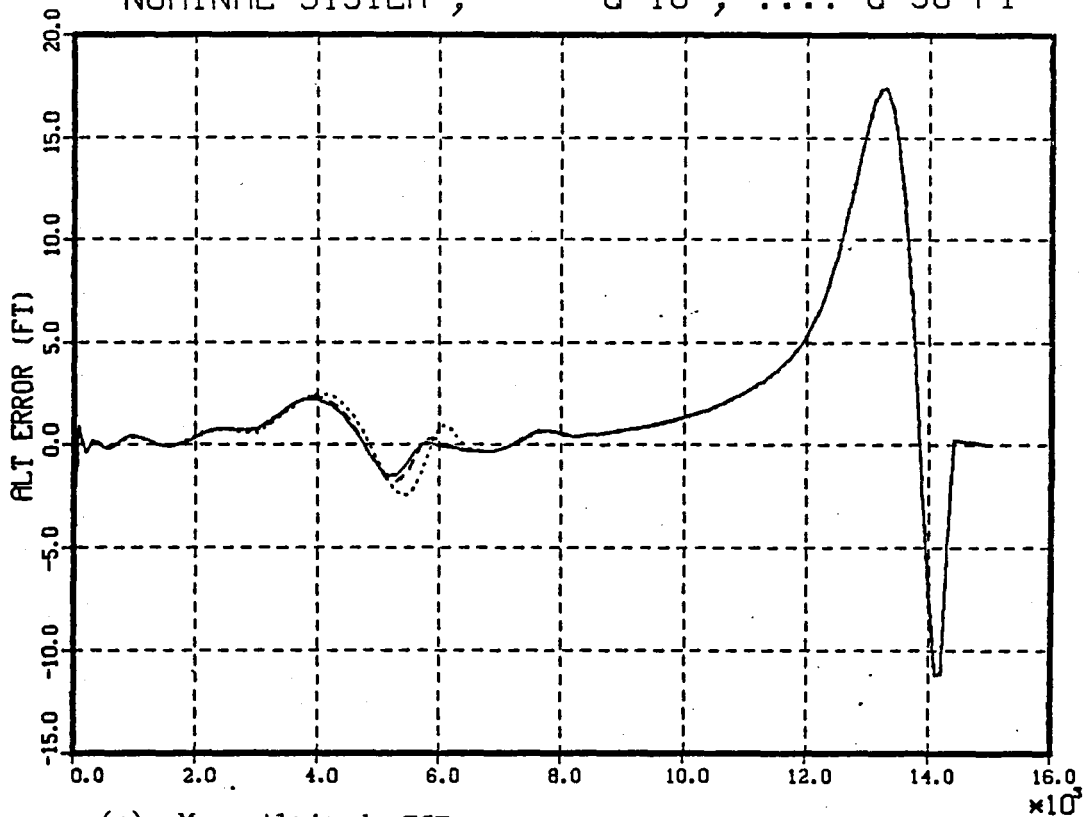


Figure 7. Sensitivity Results as a Function of Range Measurement Quantization q (ft)

RANGE QUANTIZATION VARIATION
 NOMINAL SYSTEM , ---- Q=10 , Q=30 FT

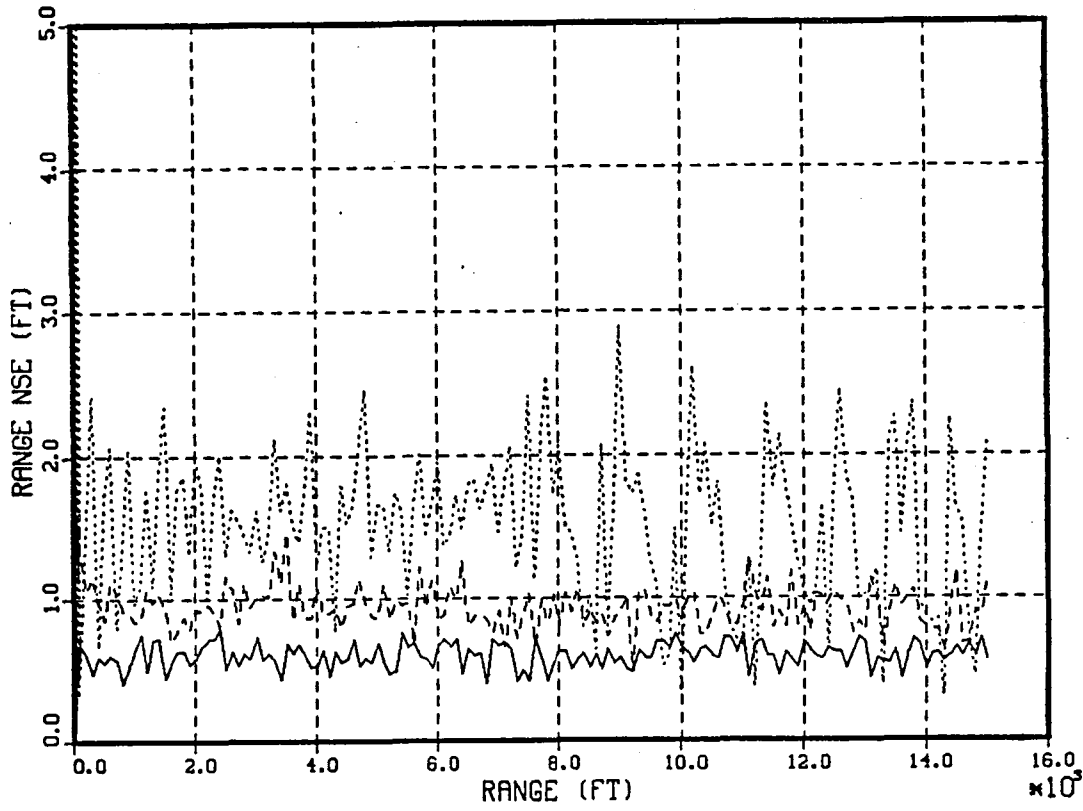
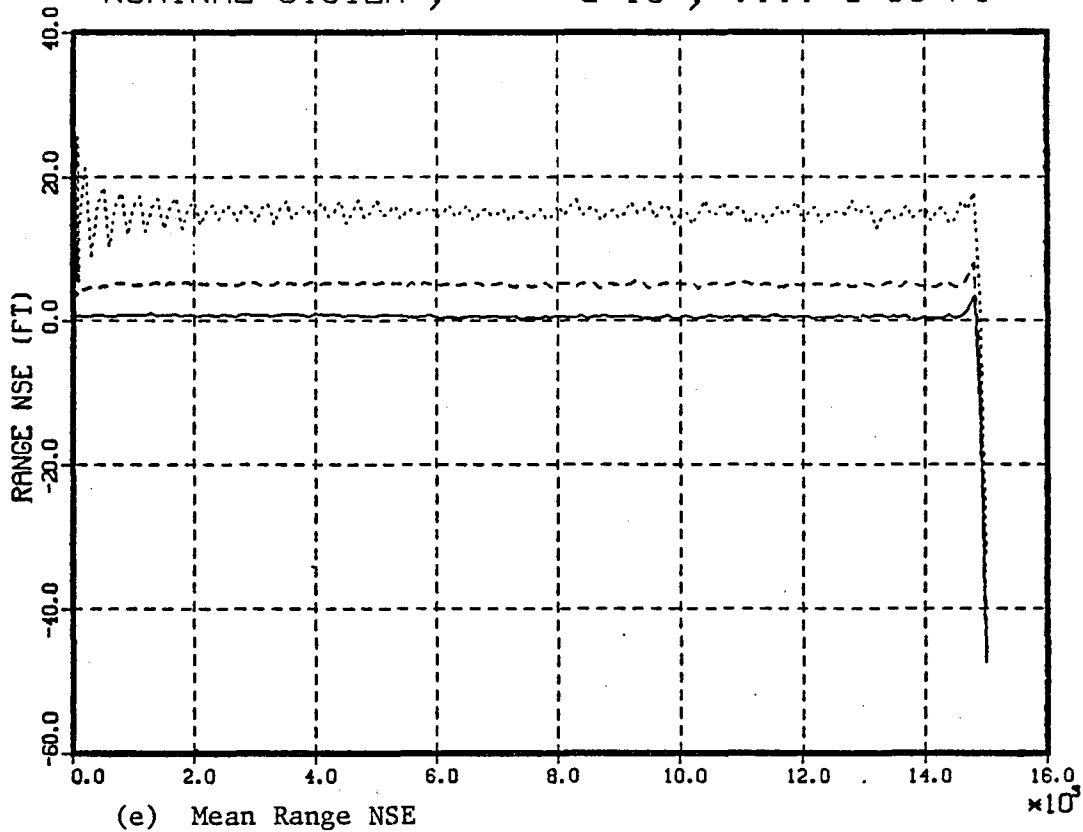


Figure 7. Sensitivity Results as a Function of Range Measurement Quantization q (ft)

RANGE QUANTIZATION VARIATION
 NOMINAL SYSTEM , ---- Q=10 , Q=30 FT

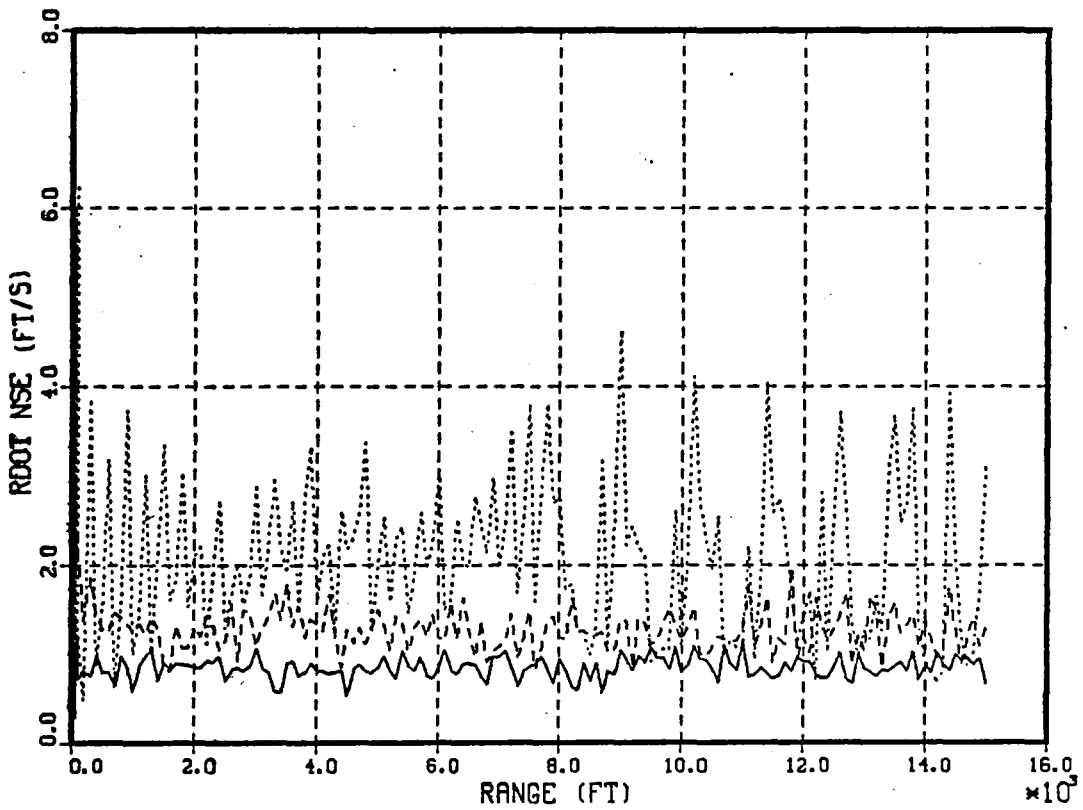
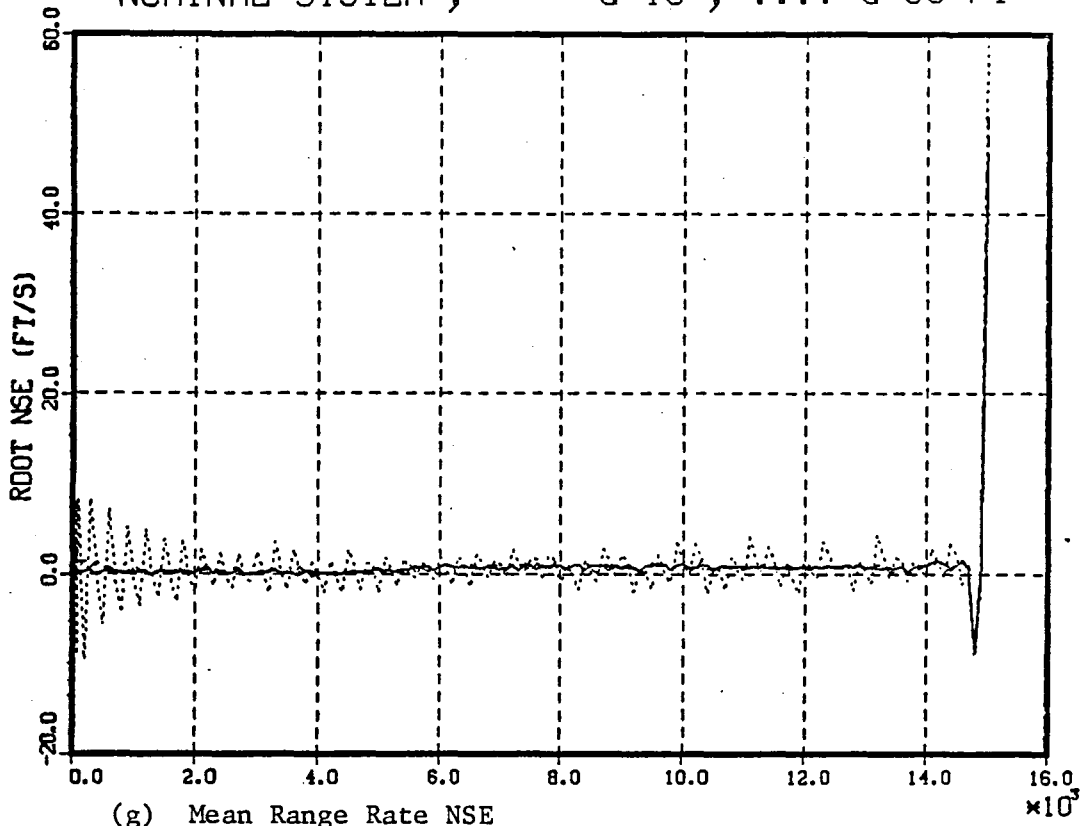
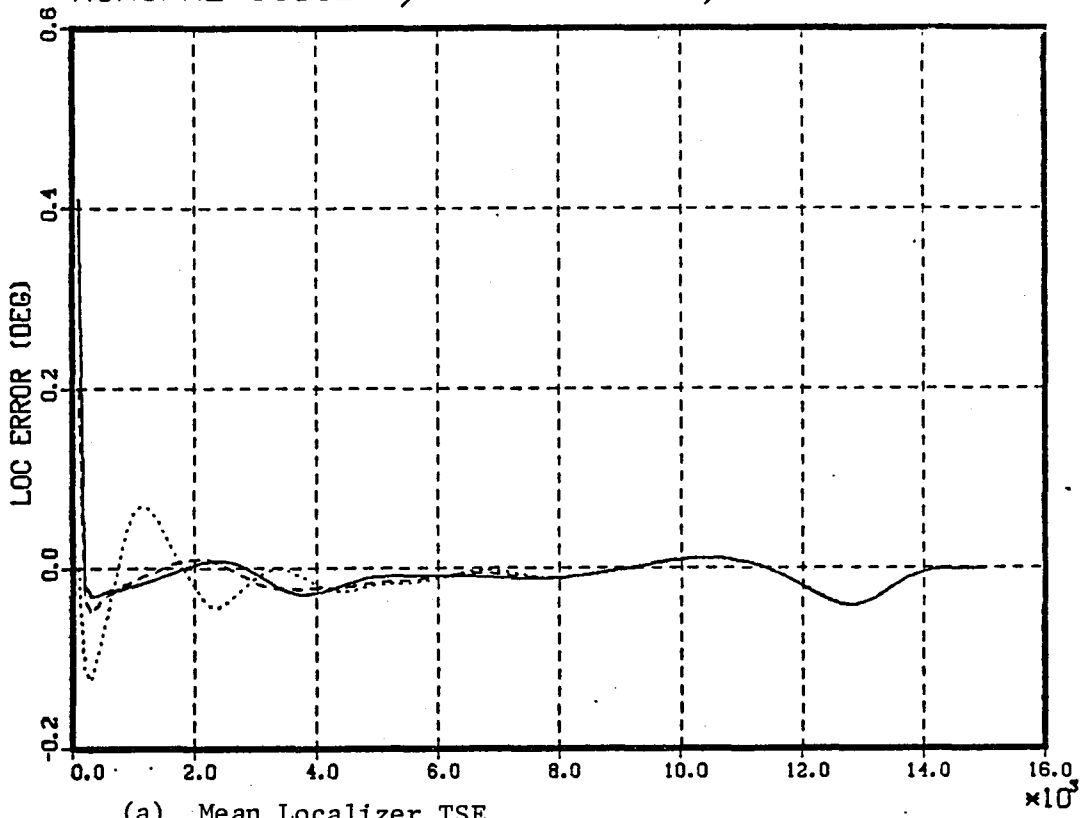
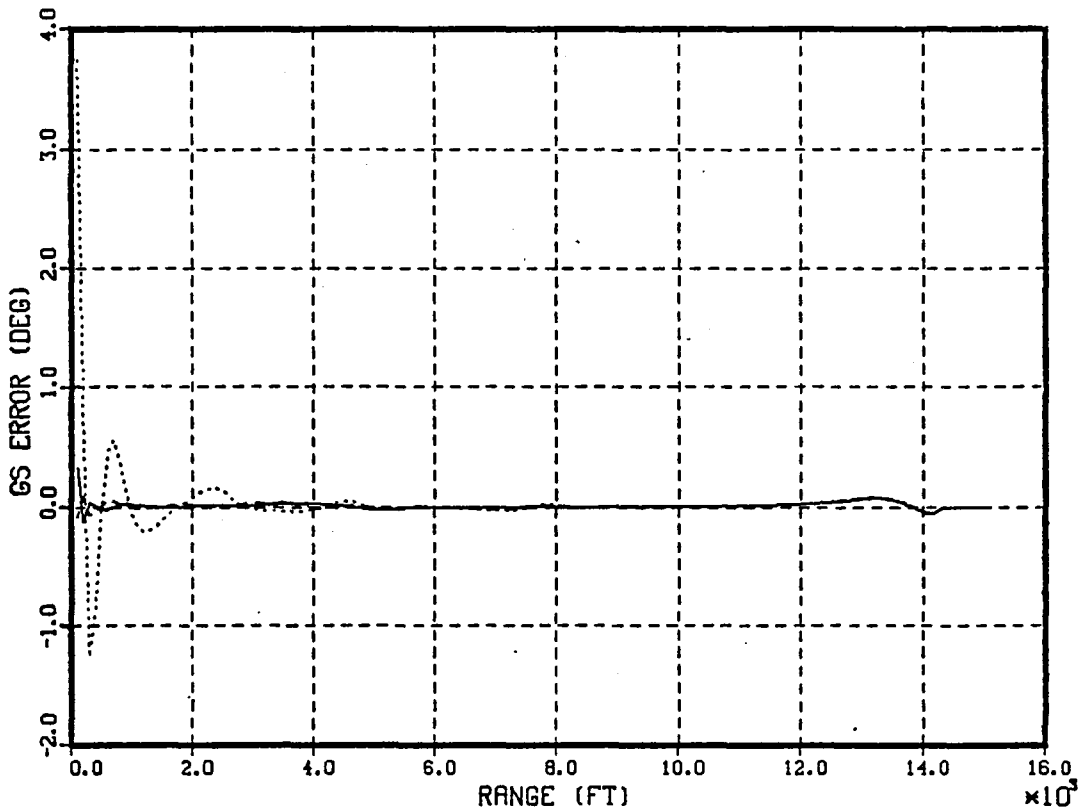


Figure 7. Sensitivity Results as a Function of Range Measurement Quantization q (ft)

RANGE RATE QUANTIZATION VARIATION
 NOMINAL SYSTEM , ---- QR=8.5 , QR=17 FT/S



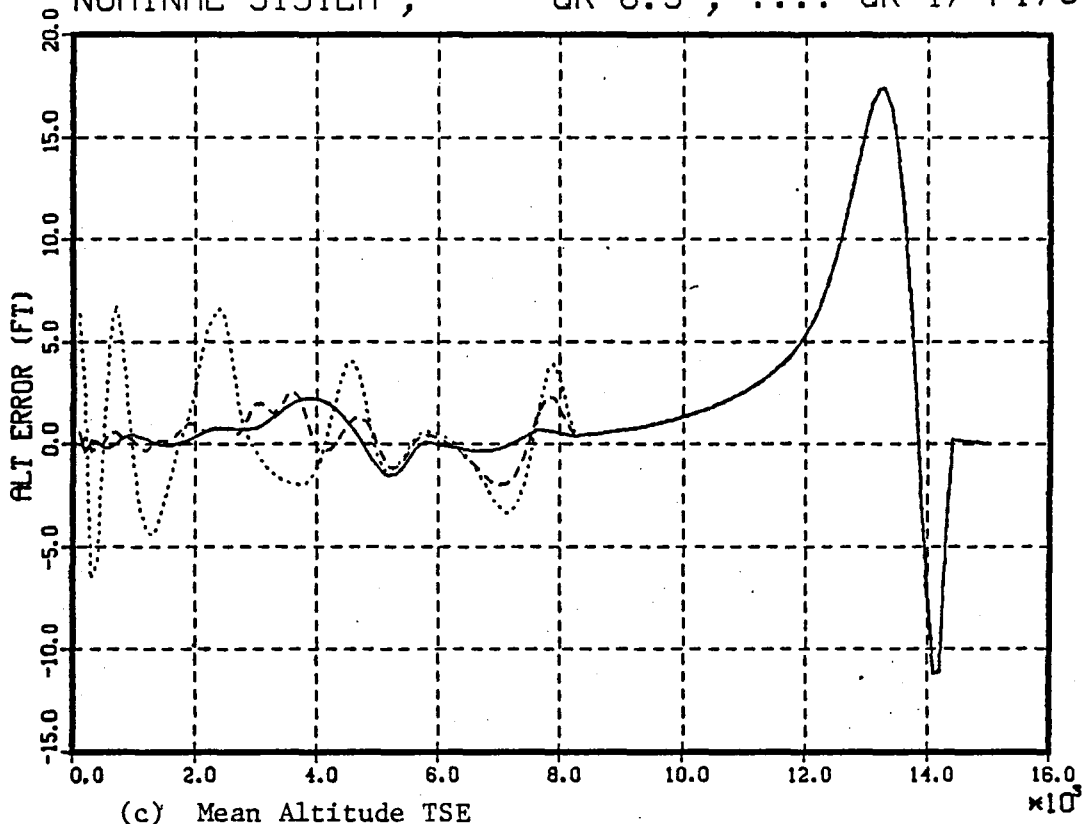
(a) Mean Localizer TSE



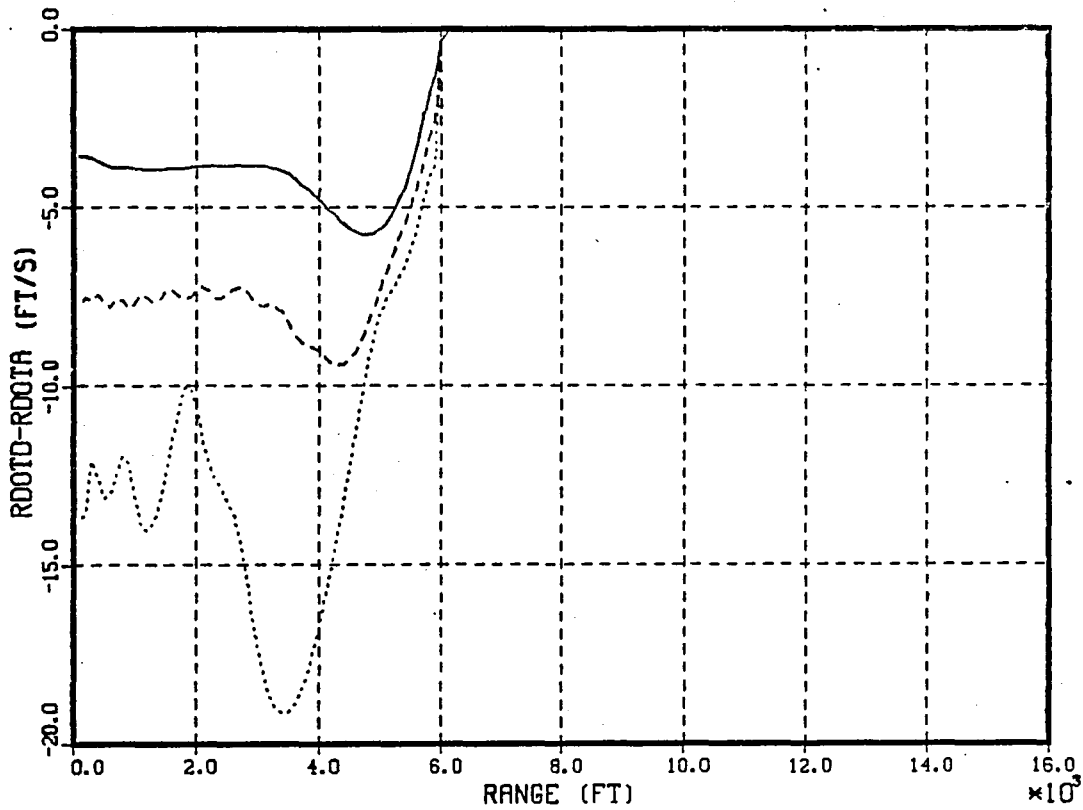
(b) Mean Glideslope TSE

Figure 8. Sensitivity Results as a Function of Range Rate Quantization q_r (ft/s)

RANGE RATE QUANTIZATION VARIATION
 NOMINAL SYSTEM , ---- QR=8.5 , QR=17 FT/S



(c) Mean Altitude TSE



(d) Mean Range Rate TSE

Figure 8. Sensitivity Results as a Function of Range Rate Quantization q_r (ft/s)

RANGE RATE QUANTIZATION VARIATION
 NOMINAL SYSTEM, ---- QR=8.5, QR=17 FT/S

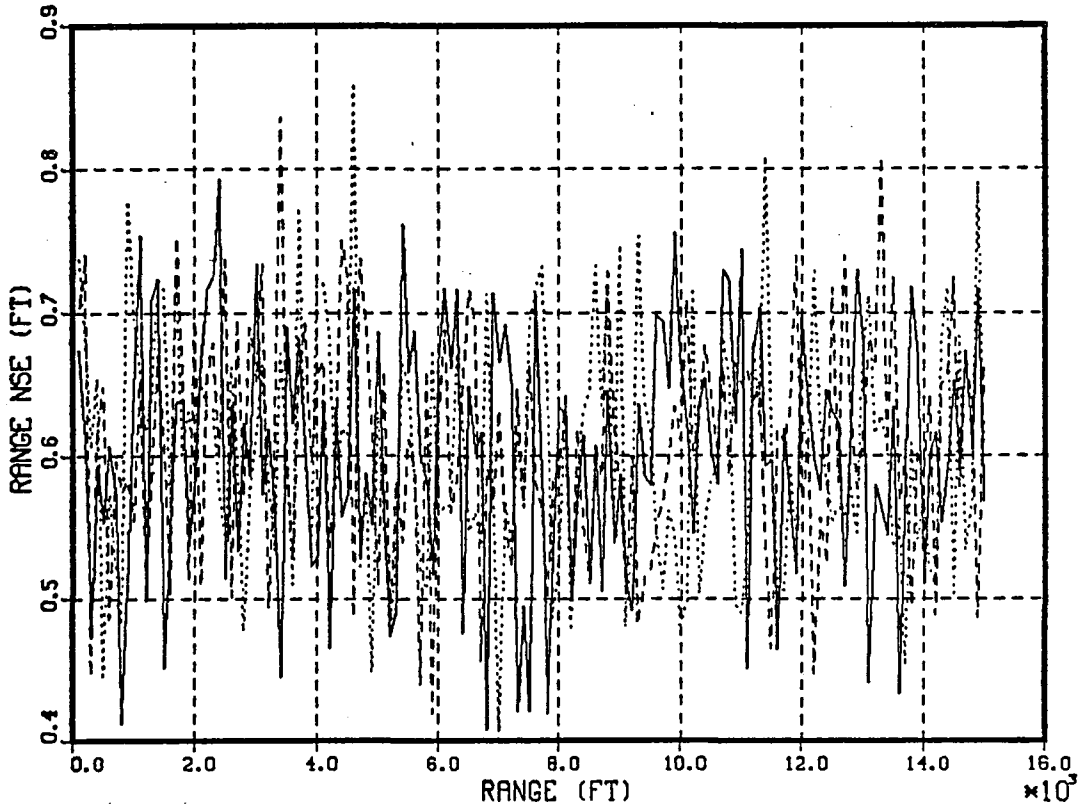
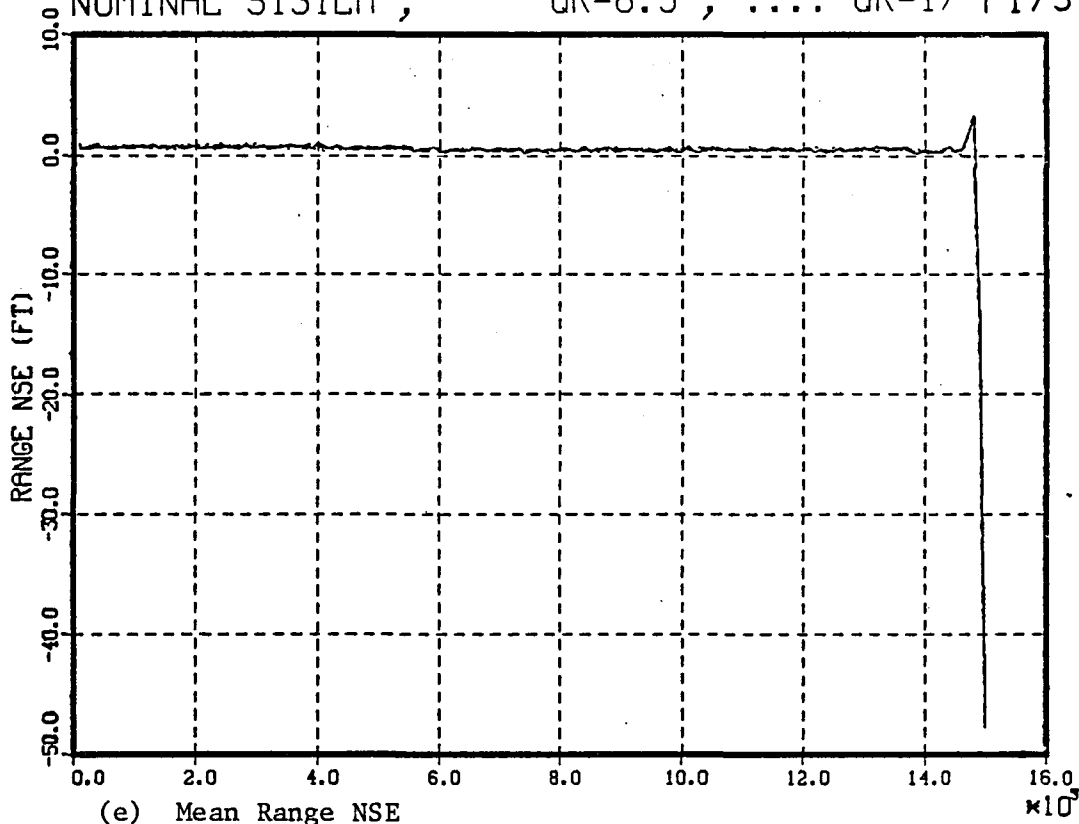


Figure 8. Sensitivity Results as a Function of Range Rate Quantization q_r (ft/s)

RANGE RATE QUANTIZATION VARIATION
 NOMINAL SYSTEM , ---- QR=8.5 , QR=17 FT/S

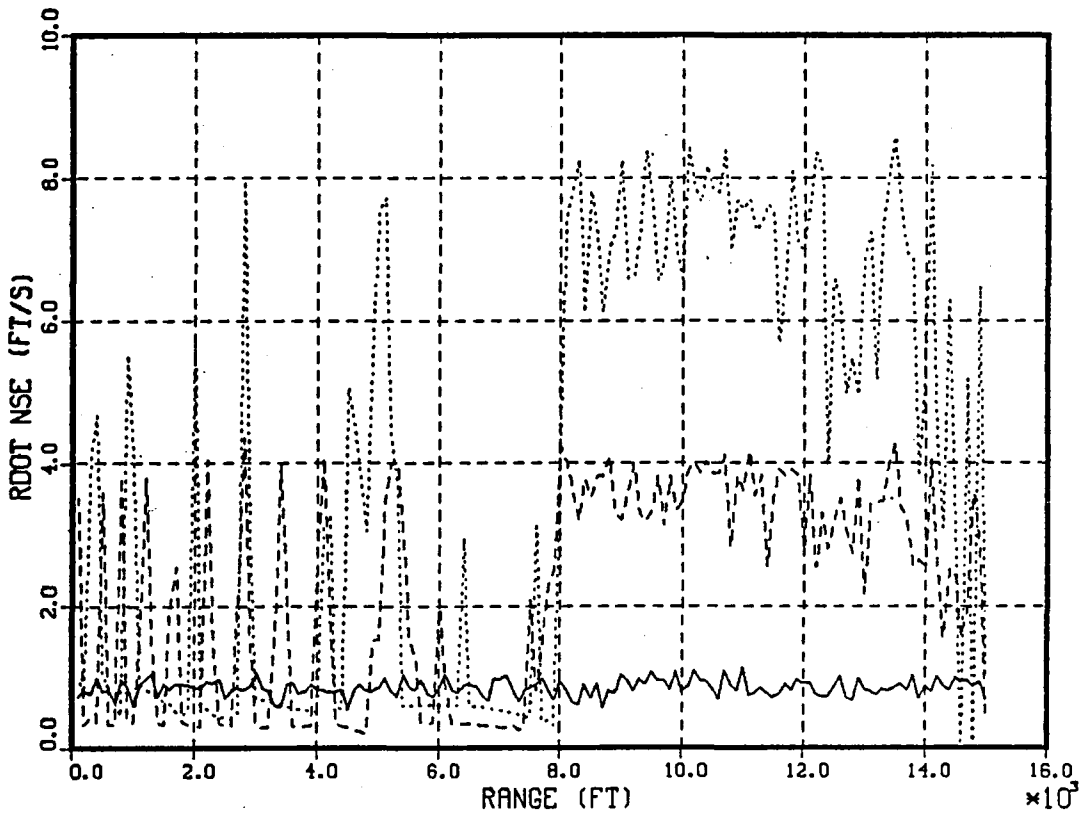
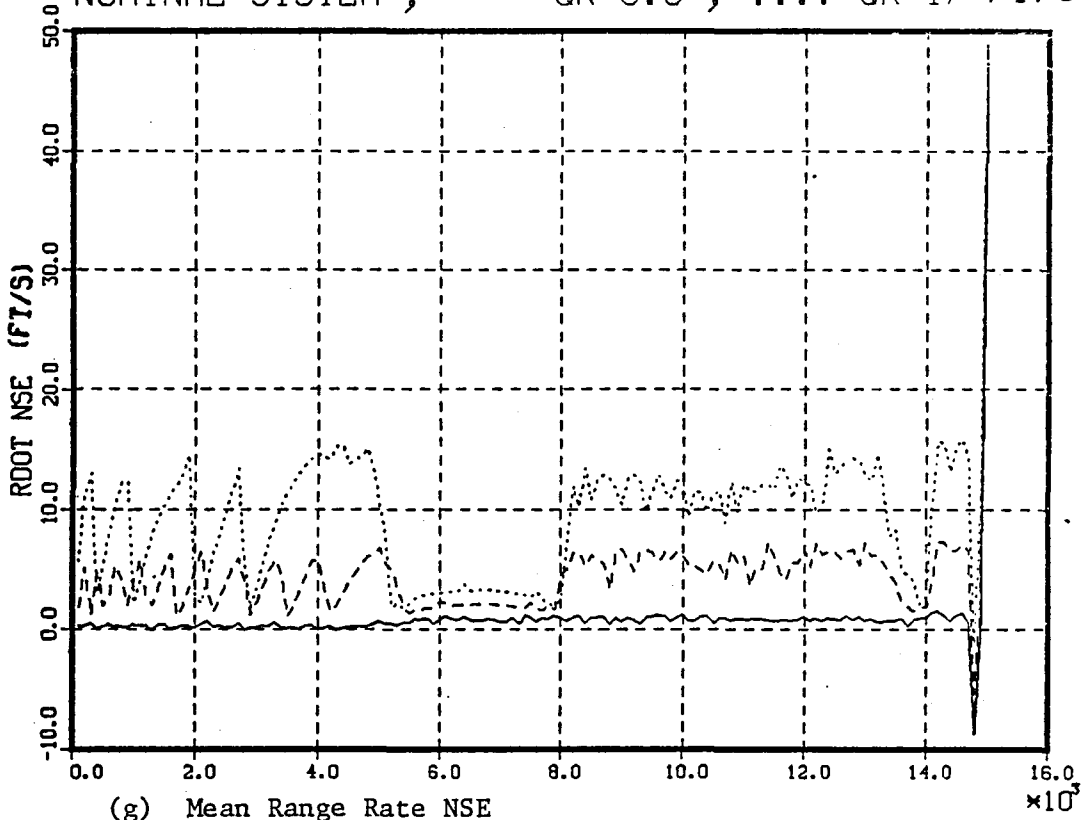


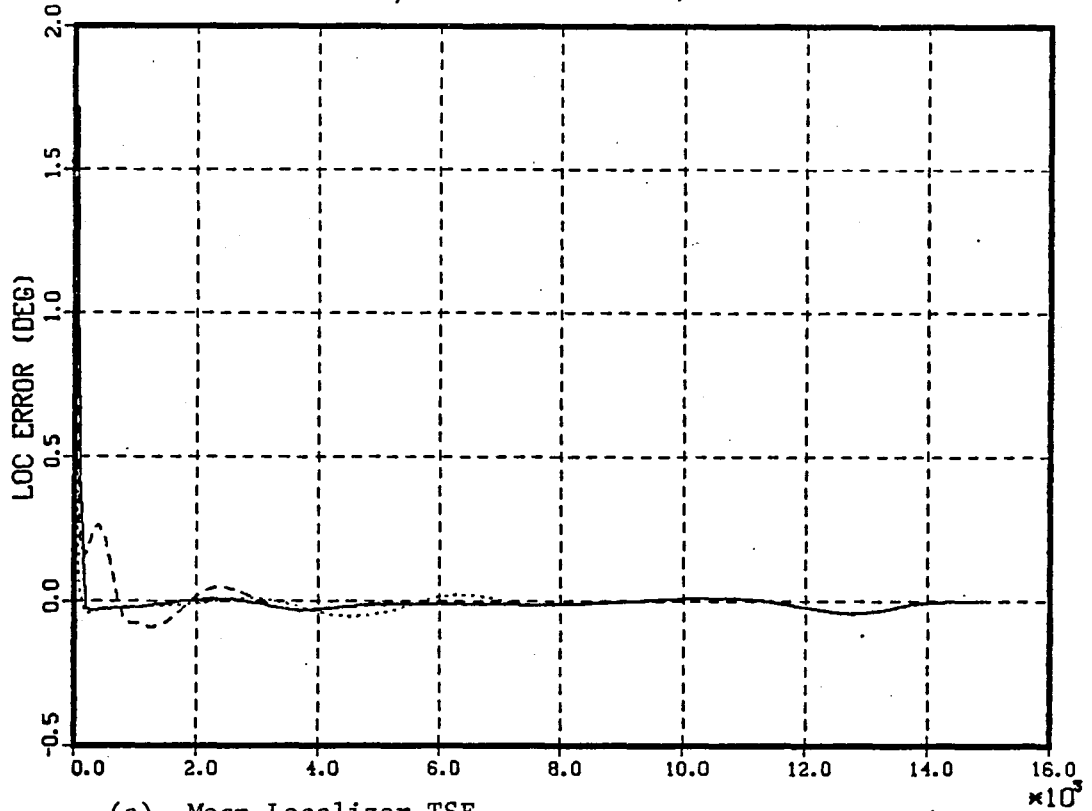
Figure 8. Sensitivity Results as a Function of Range Rate Quantization q_r (ft/s)

range-to-go. Since the aircraft is commanded to maintain a range rate of 101.0 ft/s, the range rate quantization of 8.5 or 17.0 ft/s would cause the estimated range rate to be 93.5 or 85 ft/s, respectively. Consequently, this results in the large range rate NSE for ranges greater than 8300 ft. However, when the range rate is feedback instead of airspeed, the aircraft speeds up and so its actual range rate is slightly greater than 102.0 ft/s. With this speed, quantizations of 8.5 or 17 ft/s result in the estimated range rate being 102.0 ft/s and therefore close to the true range rate. Consequently, the range rate NSE decreases until the aircraft begins decelerating at about 6000 ft.

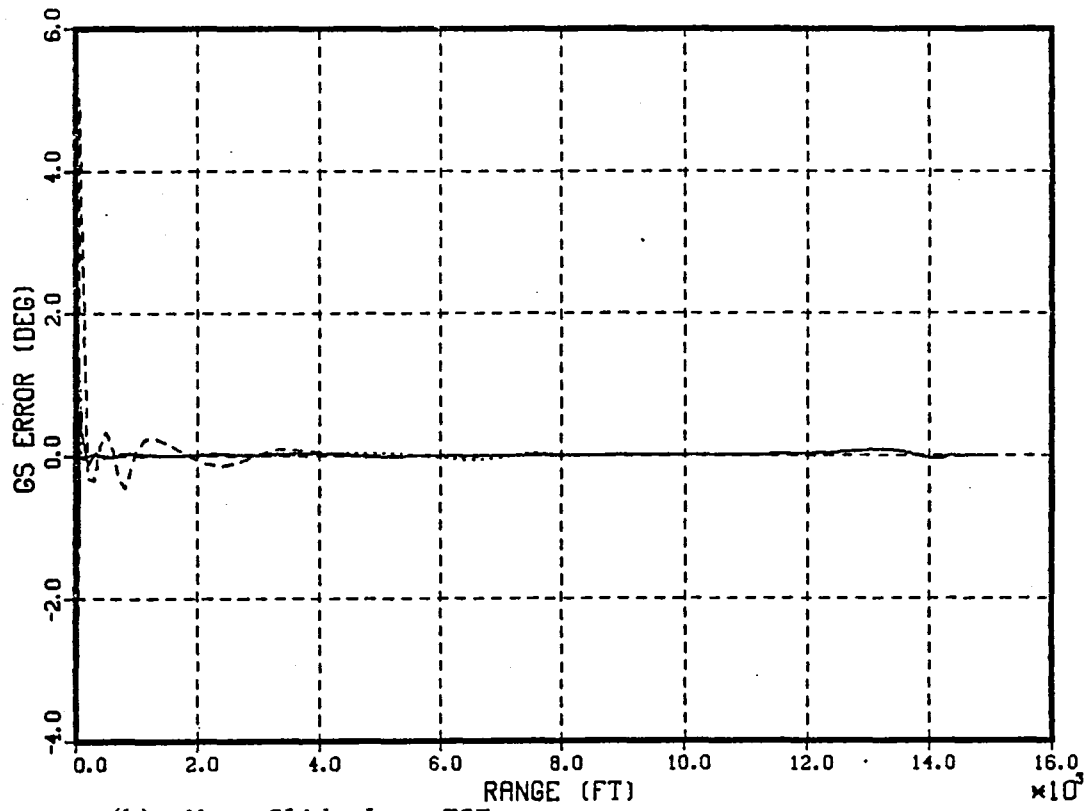
The digital α - β filter has to be designed so that (i) the range measurement noise suppression characteristics are good and (ii) lags introduced in the filtered data are not so severe as to cause system instabilities. Such a design calls for a compromise in the filter bandwidth (ω_n). Sensitivity of the DSAL system to this parameter (ω_n) can be seen in Figures 9(a)-(h). Decreasing the filter bandwidth (ω_n) from 2 rad/s to 0.2 rad/s causes an oscillation in the system as shown by Figures 9(c), (d). The standard deviation of the range NSE decreases as shown by Figures 9(f) as expected because of the lower filter bandwidth. If the bandwidth is increased to 10 rad/s, the mean TSE are marginally different from the nominal system. Figure 9(f) shows that with the increased bandwidth of the α - β filter, more of the range measurement noise "passes" through the system. However, since this noise is very small ($\sigma_n = 1.0$ ft), the effects on the TSE are minimal.

The results of the simulation have shown that the DSAL system is most sensitive to estimated range rate quantization and filter bandwidth. An increase in the former and a decrease in the latter cause system oscillations. A decrease in range measurement sampling frequency (f) to 4 Hz causes no degradation of the system performance. Range quantization effects are felt at short ranges-to-go. An increase in this quantization results in a larger range rate TSE.

BANDWIDTH VARIATION
 NOMINAL SYSTEM , ---- BW=.2 , BW=10 RAD/S



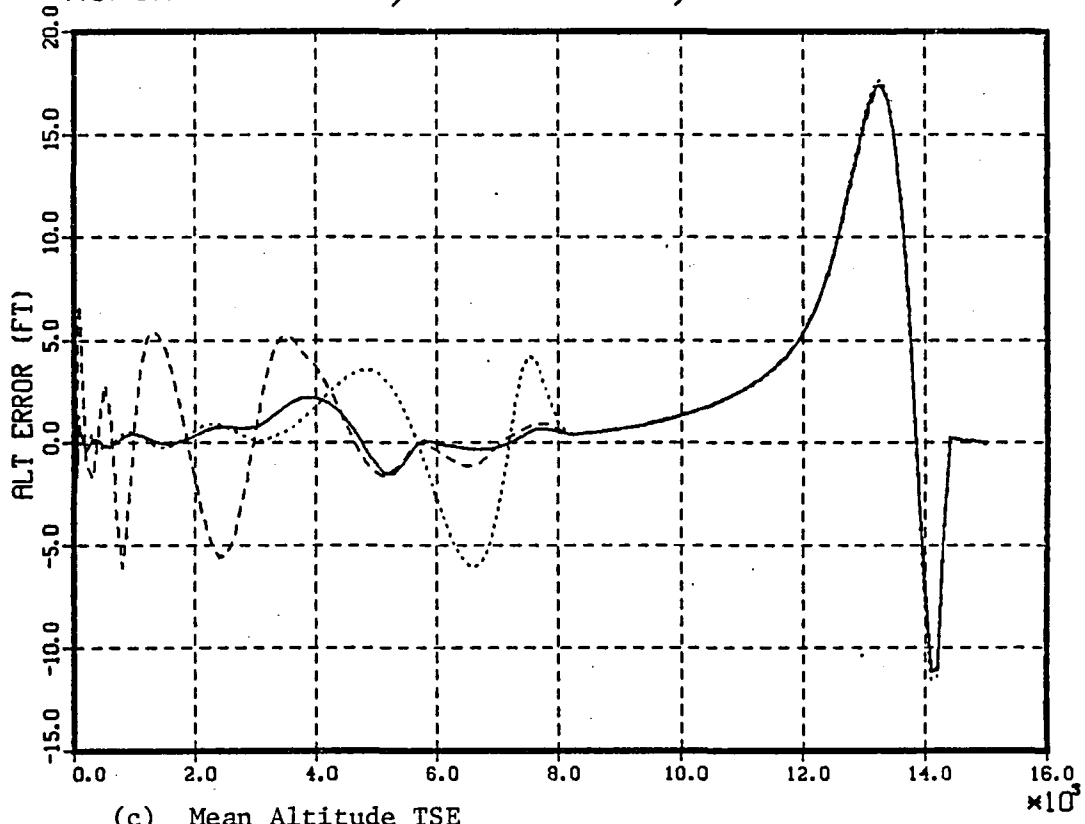
(a) Mean Localizer TSE



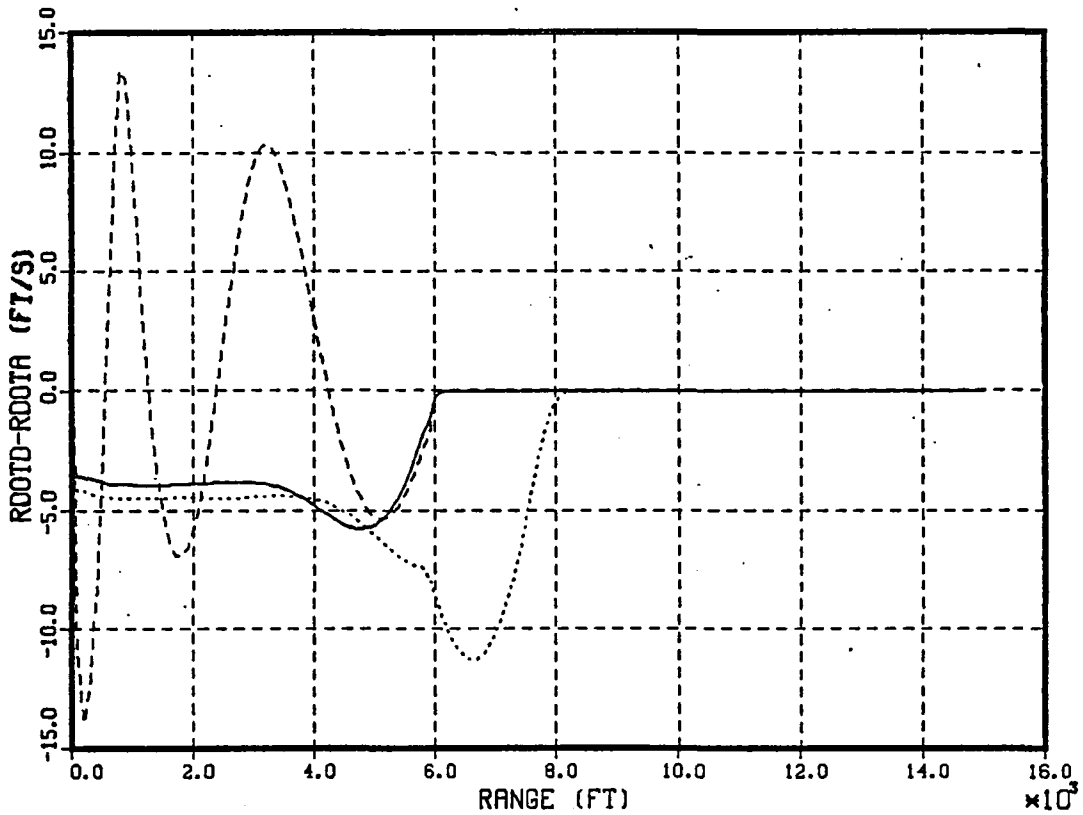
(b) Mean Glideslope TSE

Figure 9. Sensitivity Results as a Function of Bandwidth of α - β Filter

BANDWIDTH VARIATION
 NOMINAL SYSTEM, ---- BW=.2, BW=10 RAD/S



(c) Mean Altitude TSE



(d) Mean Range Rate TSE

Figure 9. Sensitivity Results as a Function of Bandwidth of α - β Filter

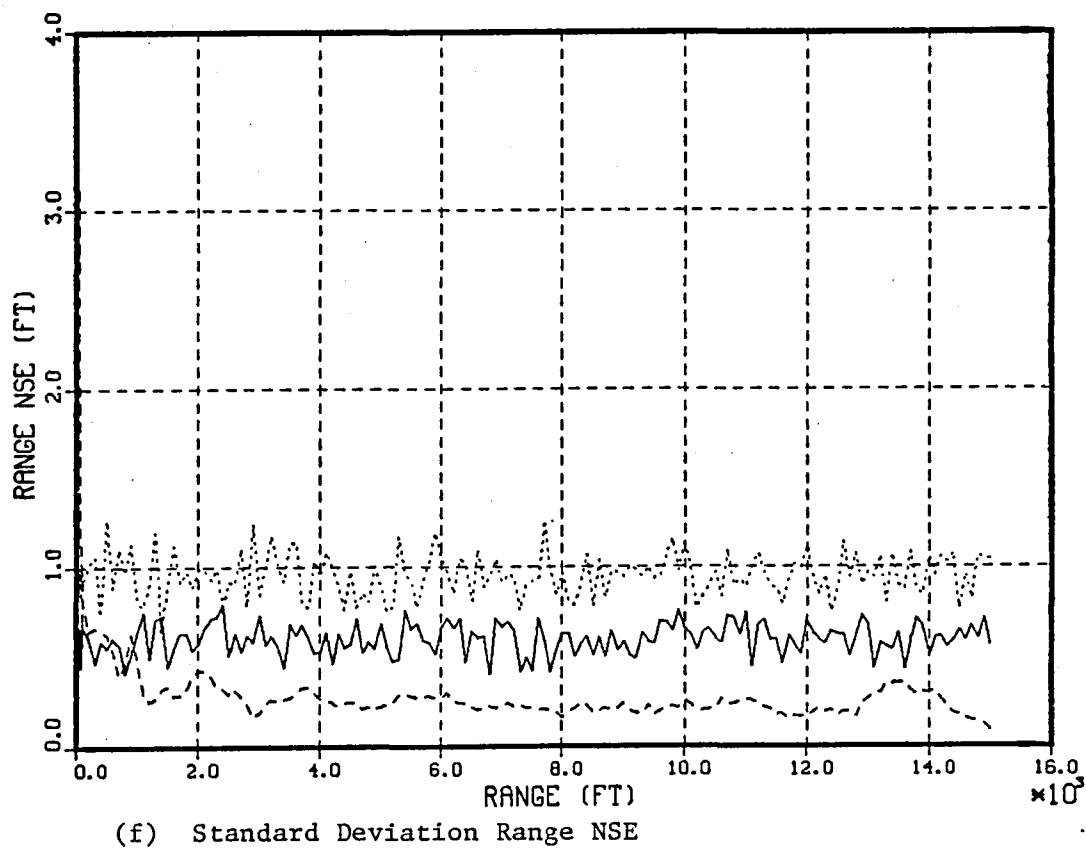
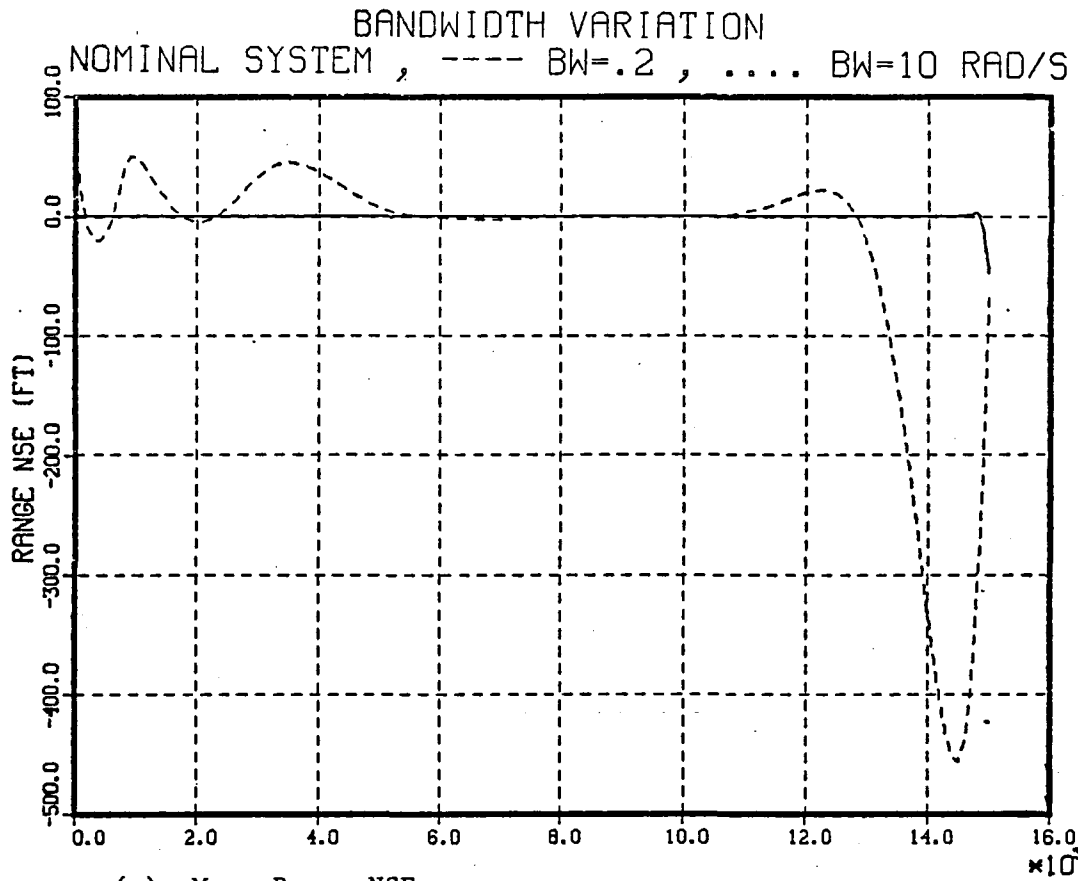


Figure 9. Sensitivity Results as a Function of Bandwidth of α - β Filter

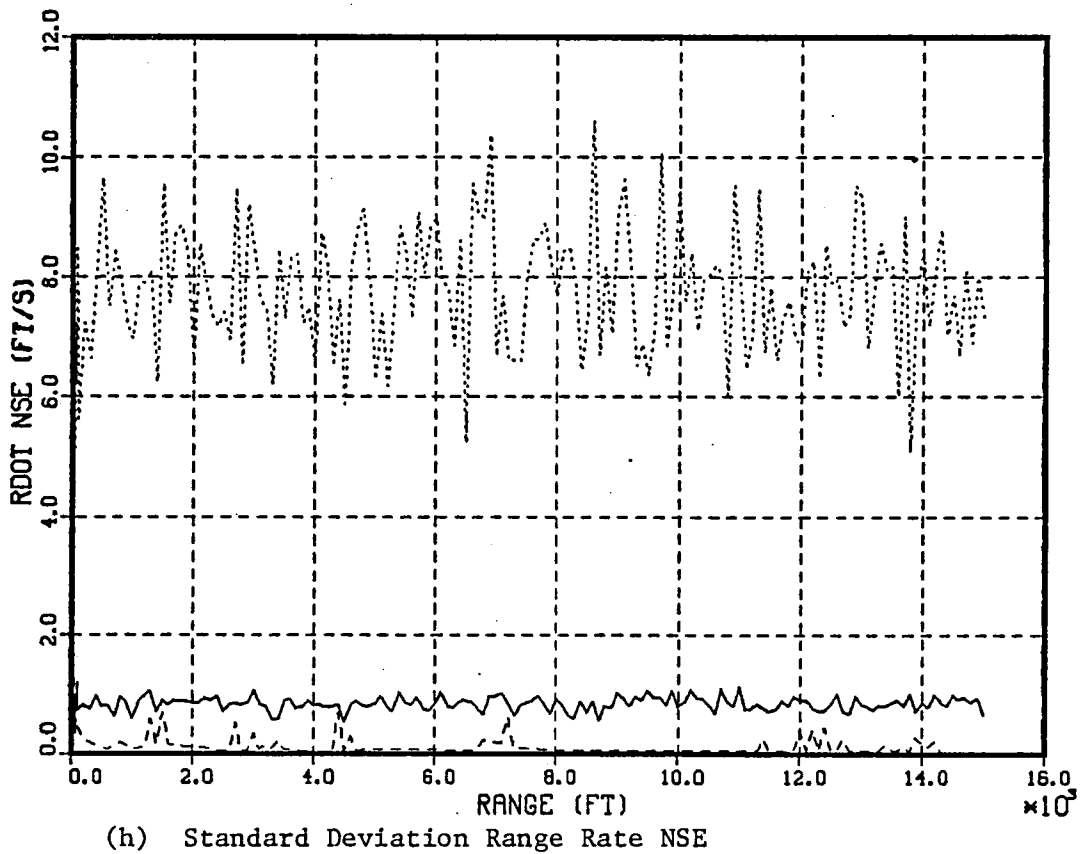
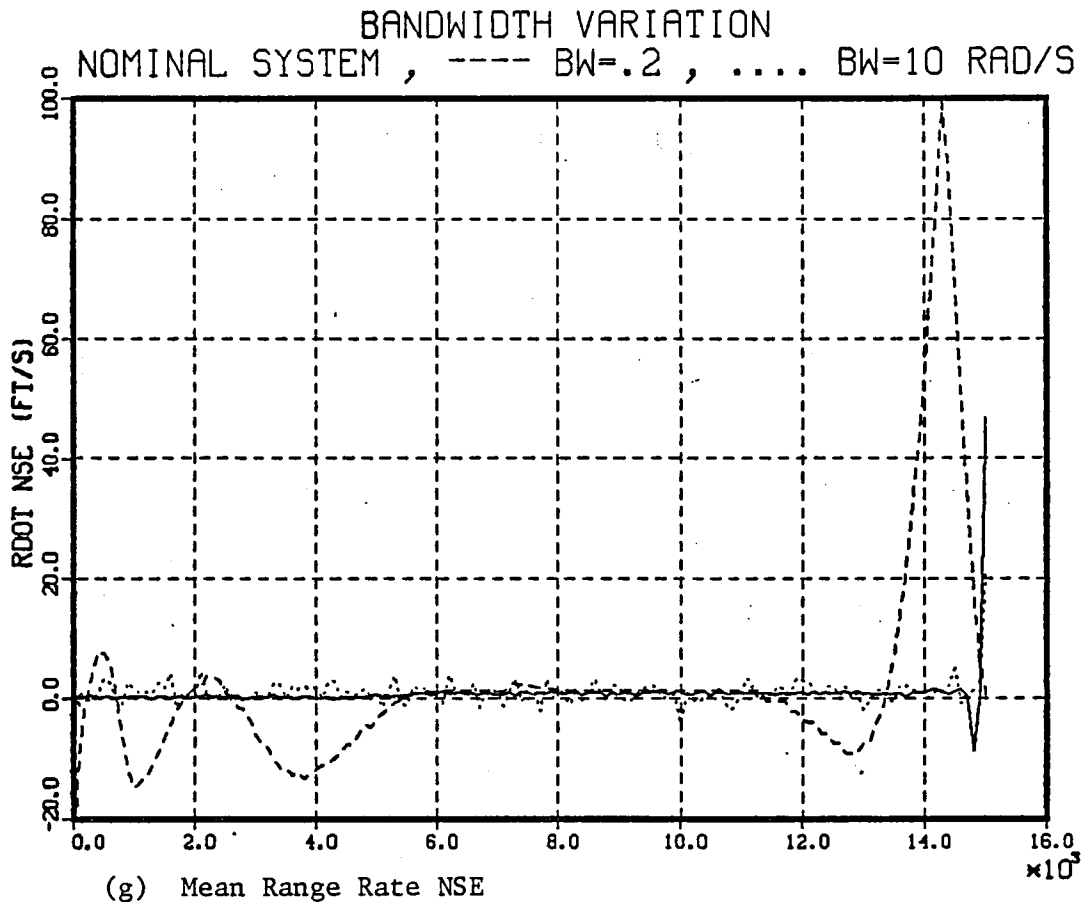


Figure 9. Sensitivity Results as a Function of Bandwidth of α - β Filter

Sensitivity to Ground-Based Navigation
(LGS) System Parameter

The ground-based segment of the navigation system has been modeled such that the range measurements are assumed to be corrupted by colored noise. The single parameter used in this study to characterize the noise properties of the range measurements is the standard deviation σ_n of the noise process.

Figures 10(a)-(c) show the effects of increasing the range noise σ_n from 1 to 30 ft. Note that a three fold increase in the range noise standard deviation from 10 to 30 ft, causes almost a ten fold increase in the standard deviation (σ) of the decision altitude TSE. Figures 10(a)-(c) show that increasing the range noise standard deviation causes an increase (in magnitude) of the total system errors. This effect is due to the non-linear nature of the overall system being simulated.

The ensemble statistics as a function of range-to-go when the noise level (σ_n) is varied are shown in Figures 11(a)-(h). Figures 11(c) and (d) show that with a σ_n of 30 ft, the mean altitude and range rate TSE are poorer than with $\sigma_n = 1$ or 10 ft. Note that Figure 11(d) shows that deceleration begins earlier when the noise level increases. This can be explained by considering Figure 11(g). The decision to initiate deceleration is made by comparing the commanded range rate and the estimated range rate. The wide excursions in the mean range rate NSE imply that over certain segments of the flight the estimated range rate is larger than the true range rate causing an earlier deceleration.

These simulation results show that: (a) the increases in the standard deviation of the range noise are felt in the mean of the TSE due to the non-linear nature of the system, and (b) the system performance degrades very rapidly as the range noise level is increased.

RANGE NOISE VARIATION

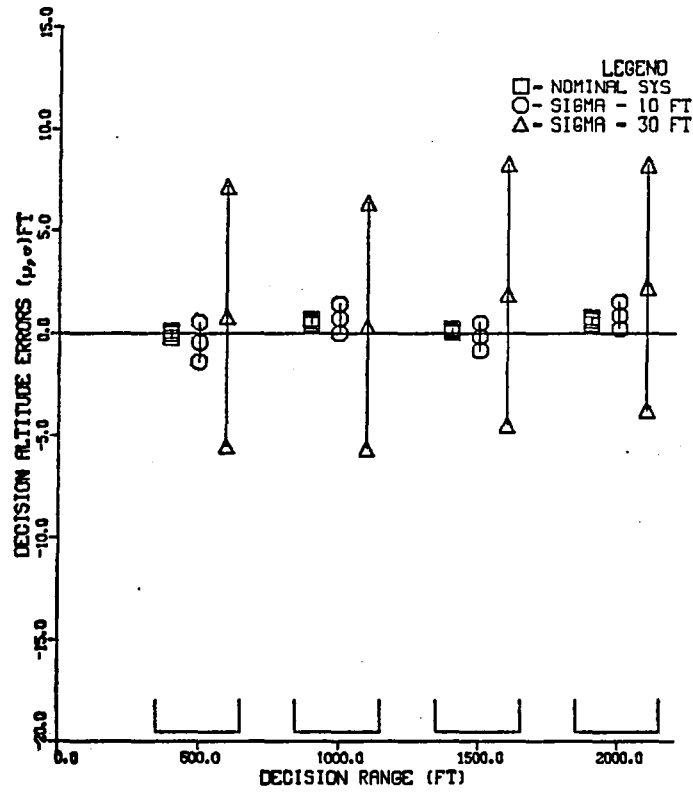


Figure 10(a). Sensitivity of Decision Altitude TSE to Ground-Based Navigation System Parameters

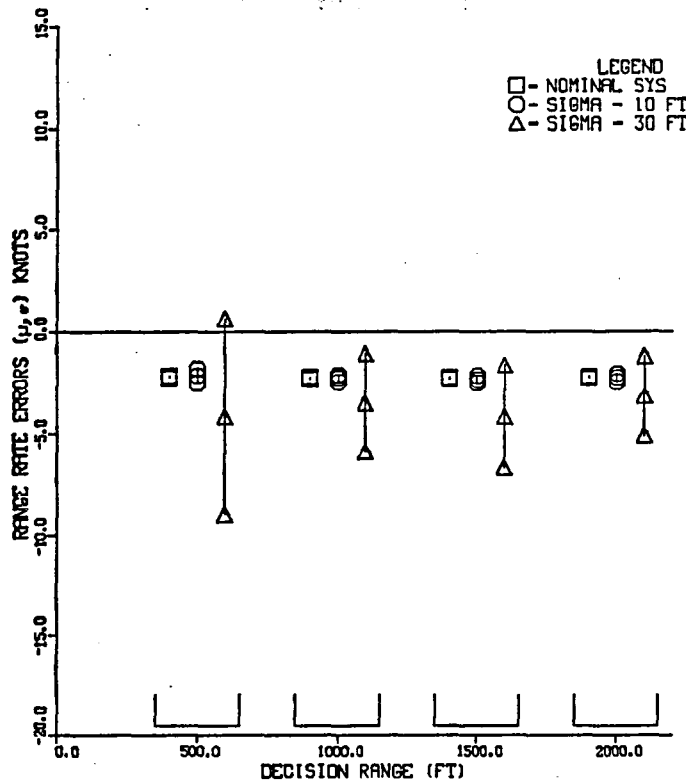


Figure 10(b). Sensitivity of Range Rate TSE to Ground-Based Navigation System Parameters

RANGE NOISE VARIATION

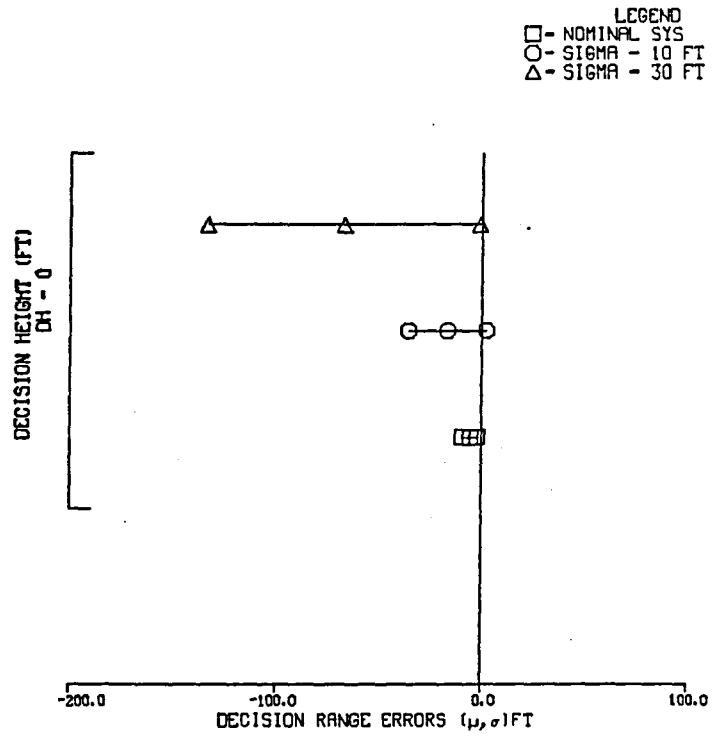


Figure 10(c). Sensitivity of Range TSE at Touchdown to Ground-Based Navigation System Parameters

RANGE NOISE VARIATION
 NOMINAL SYSTEM , ---- SIGMA=10 , SIGMA=30 FT

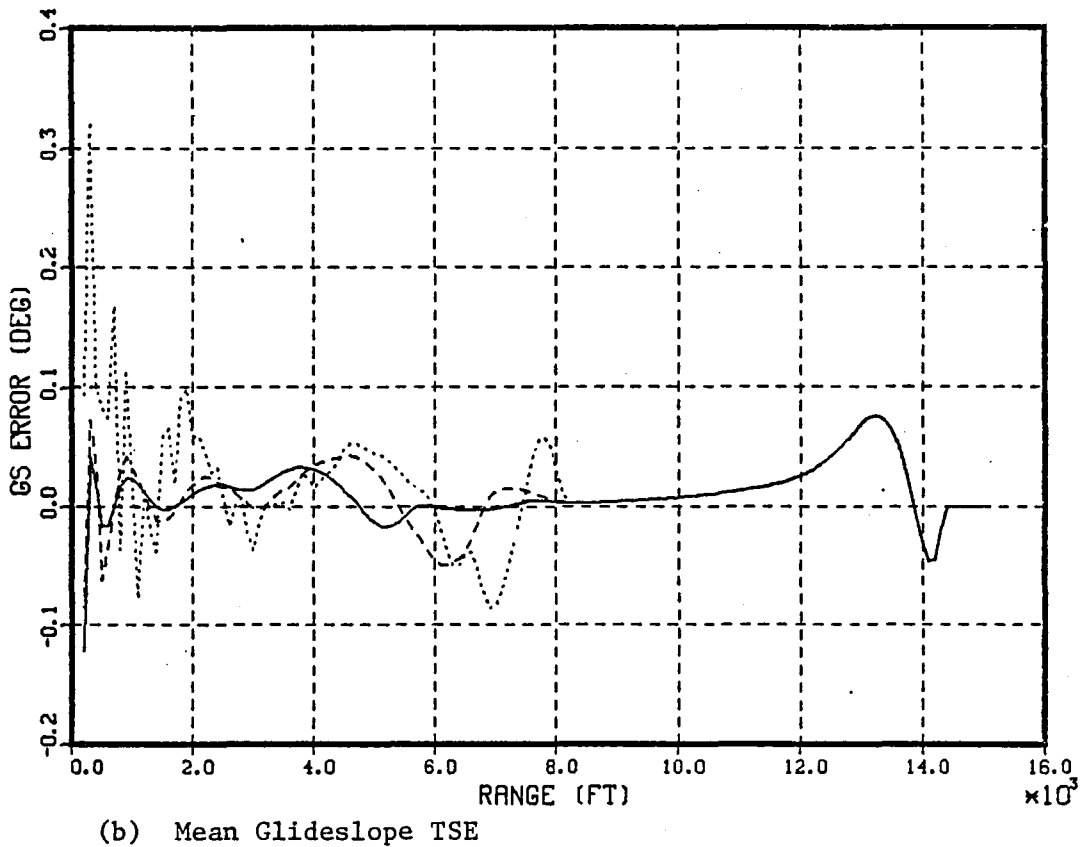
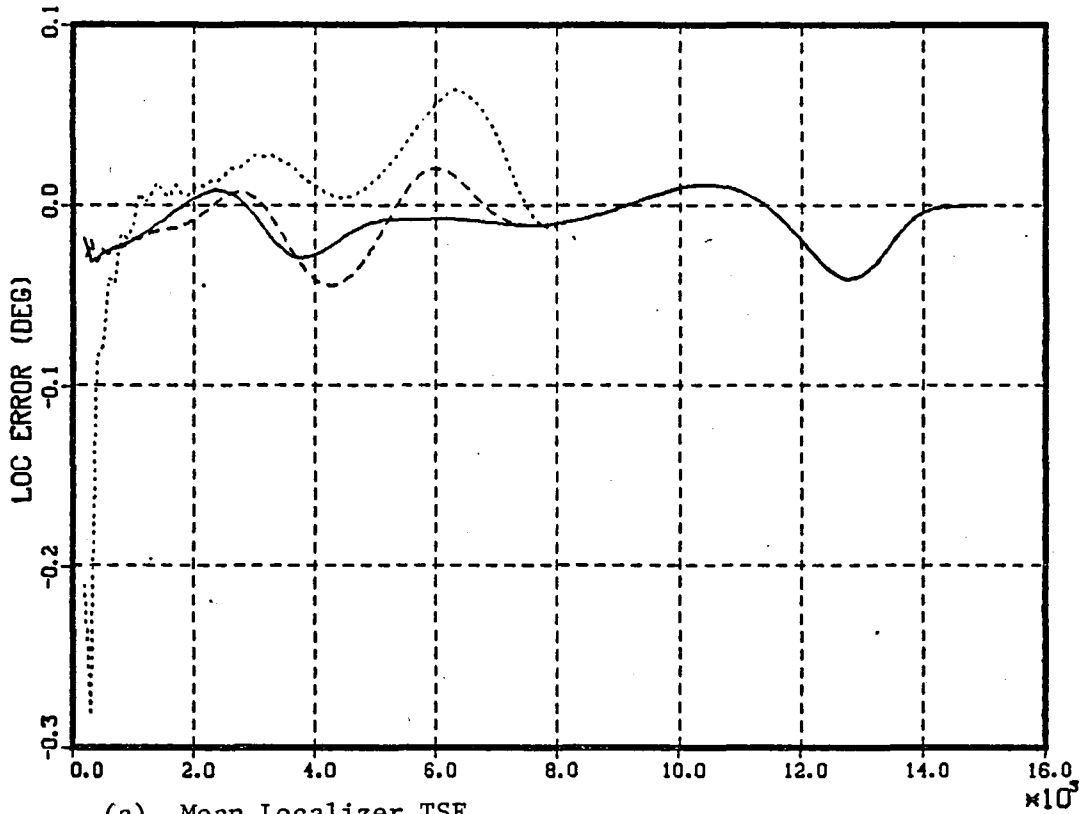


Figure 11. Sensitivity Results as a Function of Range Measurement Noise σ_n (ft)

RANGE NOISE VARIATION
 NOMINAL SYSTEM , ---- SIGMA=10 , SIGMA=30 FT

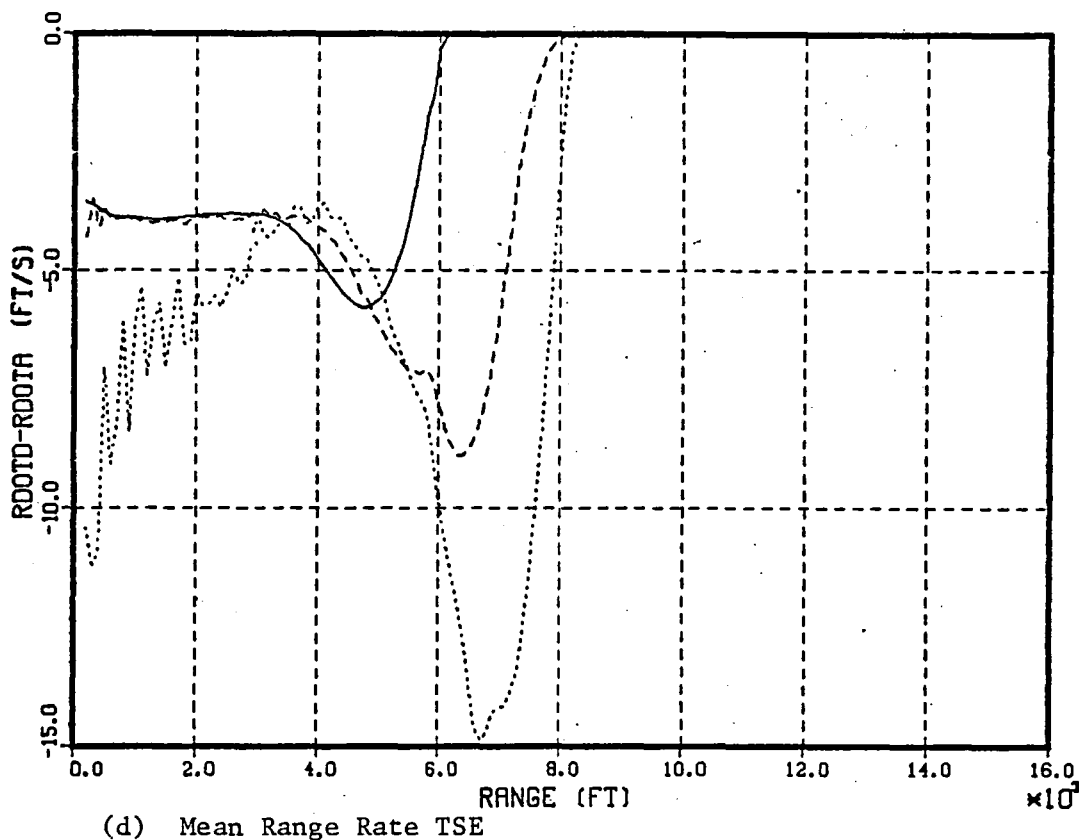
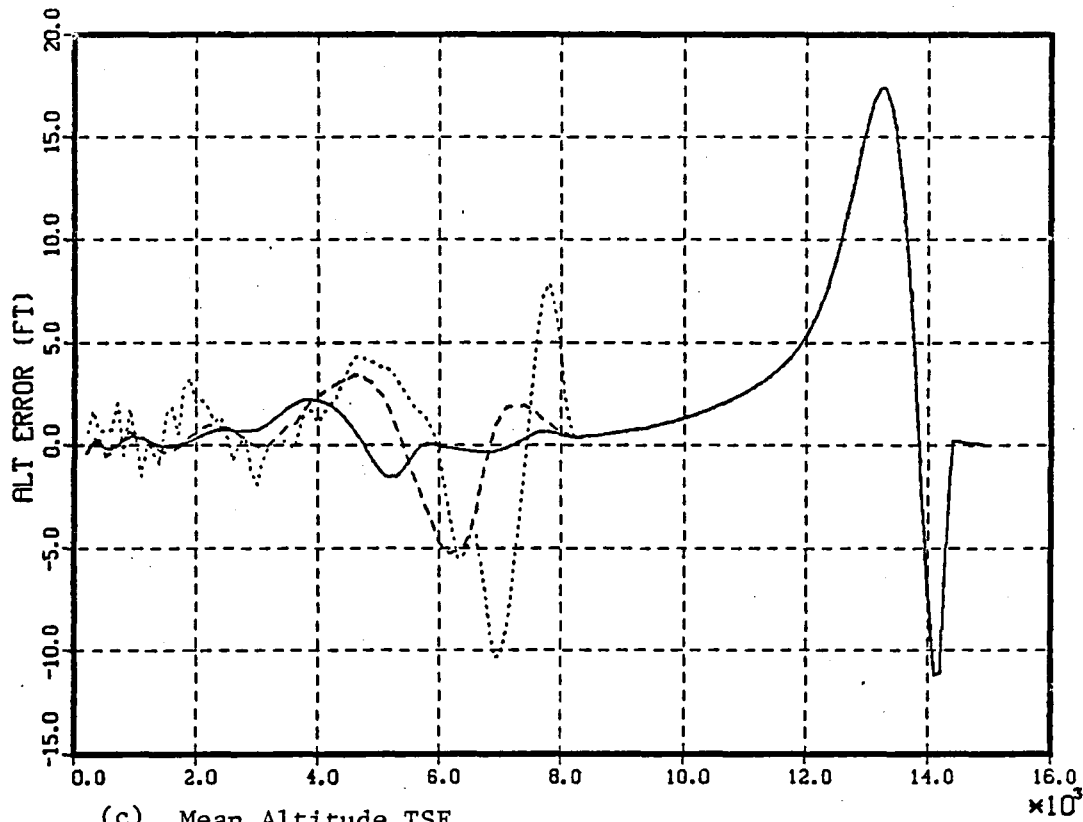
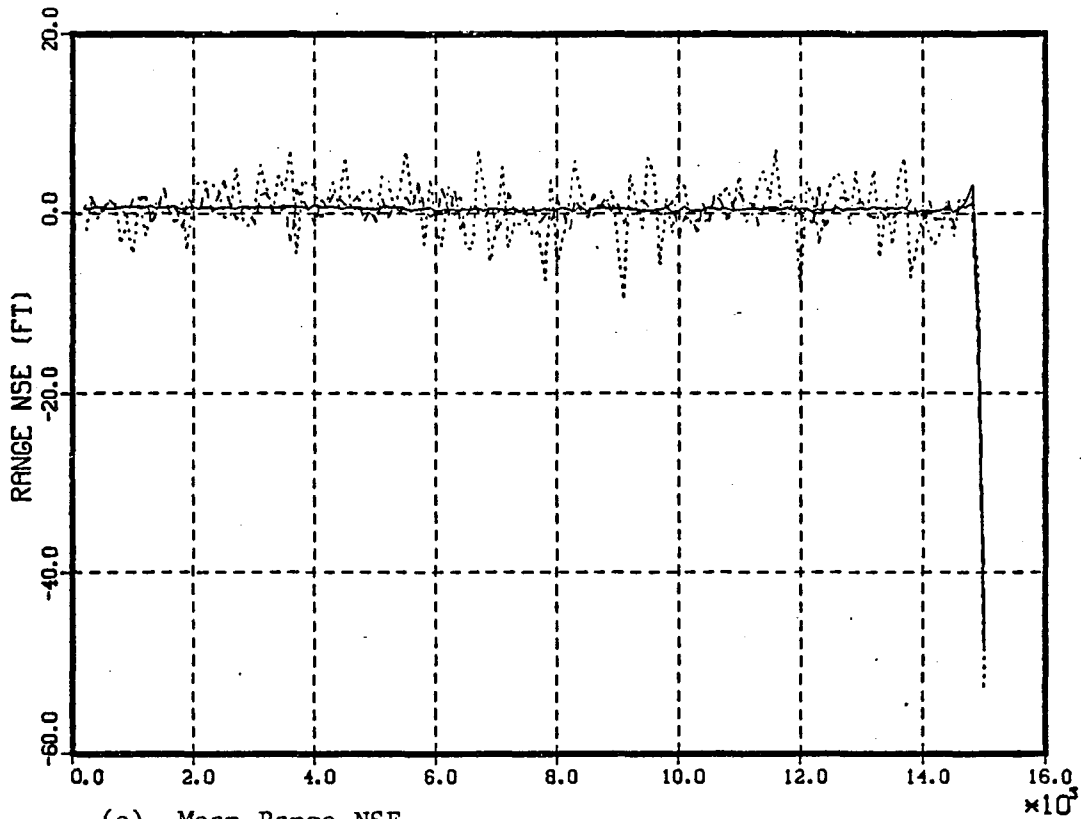
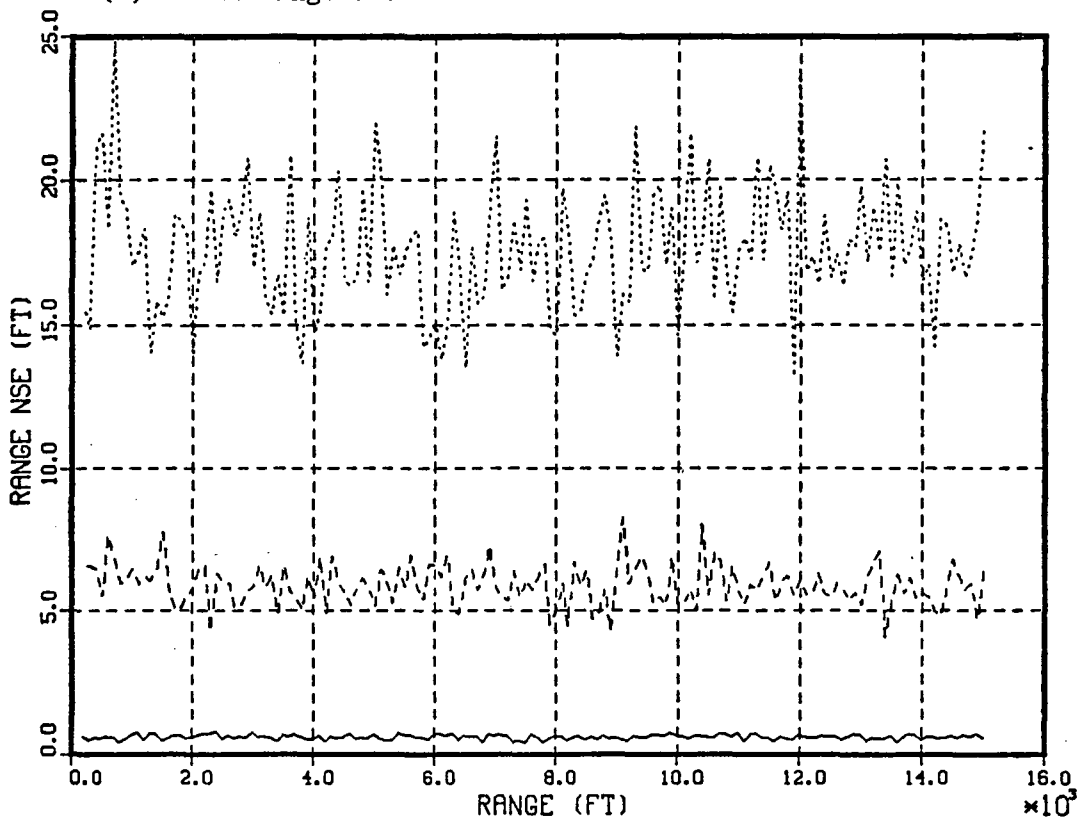


Figure 11. Sensitivity Results as a Function of Range Measurement Noise σ_n (ft)

RANGE NOISE VARIATION
 NOMINAL SYSTEM, ---- SIGMA=10, SIGMA=30 FT



(e) Mean Range NSE



(f) Standard Deviation Range NSE

Figure 11. Sensitivity Results as a Function of Range Measurement Noise σ_n (ft)

RANGE NOISE VARIATION
 NOMINAL SYSTEM , ---- SIGMA=10 , SIGMA=30 FT

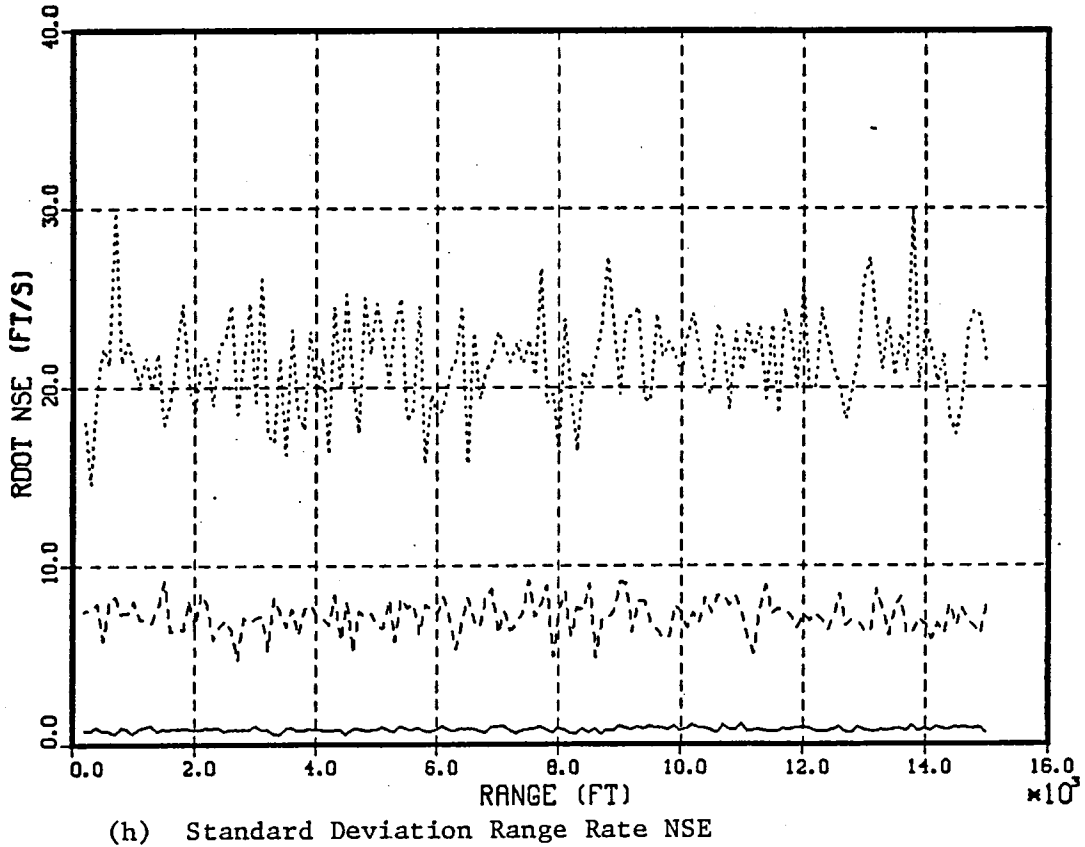
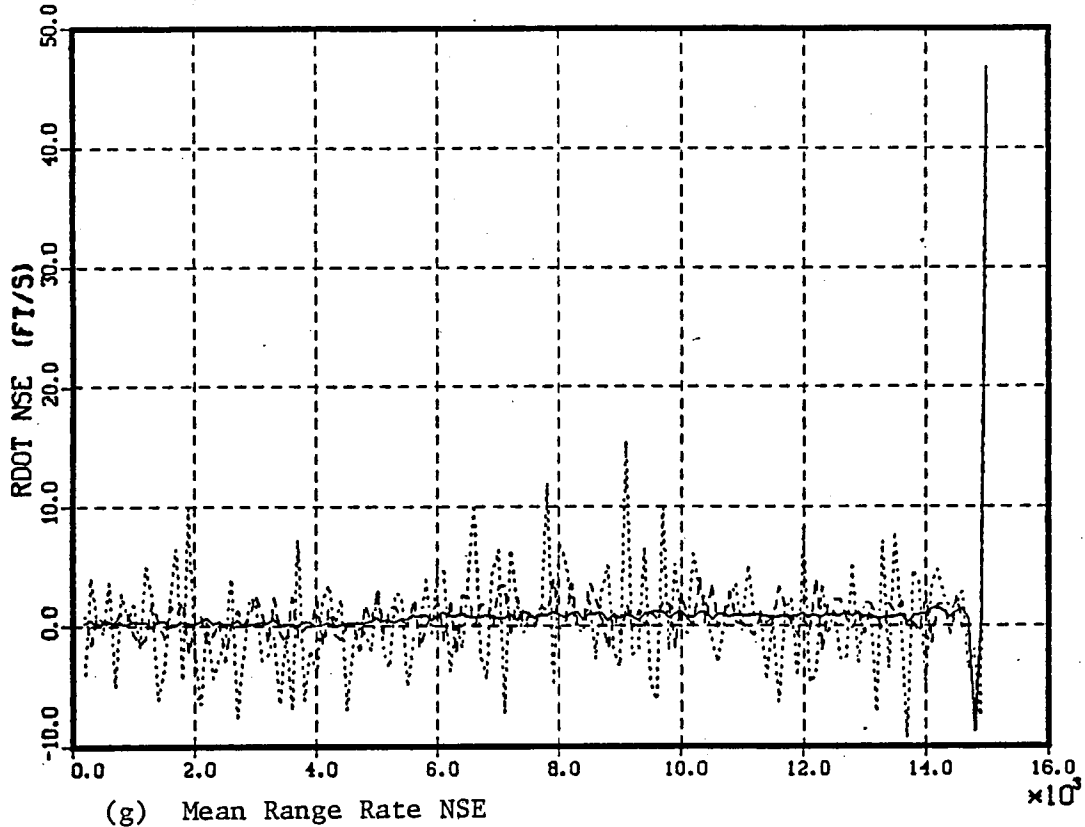


Figure 11. Sensitivity Results as a Function of Range Measurement Noise σ_n (ft)

The standard deviation of the range noise is one measure of the accuracy of the LGS and reflects on the price/performance tradeoff of the ground-based system. Since the impact of the range noise on the DSAL system performance is significant, it is important to study the system sensitivities to the on-board navigation parameters using a larger nominal range noise (σ_n).

Cases 1-8 of Table 2 were repeated using a nominal σ_n of 10 ft.

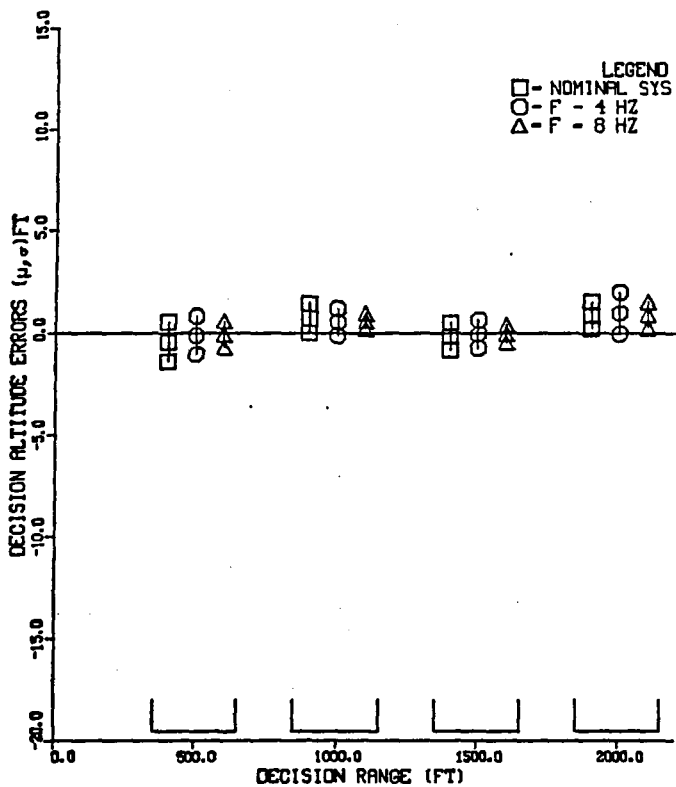
Figures 12(a)-(c) show the system performance sensitivity (measures 7-9, Table 1) as a function of on-board navigation parameters with $\sigma_n = 10$ ft. Comparing Figures 5(a) and 12(a), it can be seen that the system performance is not very sensitive to range measurement sampling frequency for both $\sigma_n = 1$ and 10 ft.

Although range quantization does not seem to have an effect on the decision altitude or range rate TSE (Figures 5(a),(b)) with a nominal $\sigma_n = 1$ ft, the effects on these performance measures are noticeable with $\sigma_n = 10$ ft and $q = 30$ ft (Figures 12(a),(b)). Note that the effects of the range measurement noise and range quantization on decision altitude TSE are not merely additive (Figure 12(a)). Further, the standard deviation of the decision altitude errors increases as the helicopter comes in to touchdown when the range quantization level is made larger (Figure 12(a)).

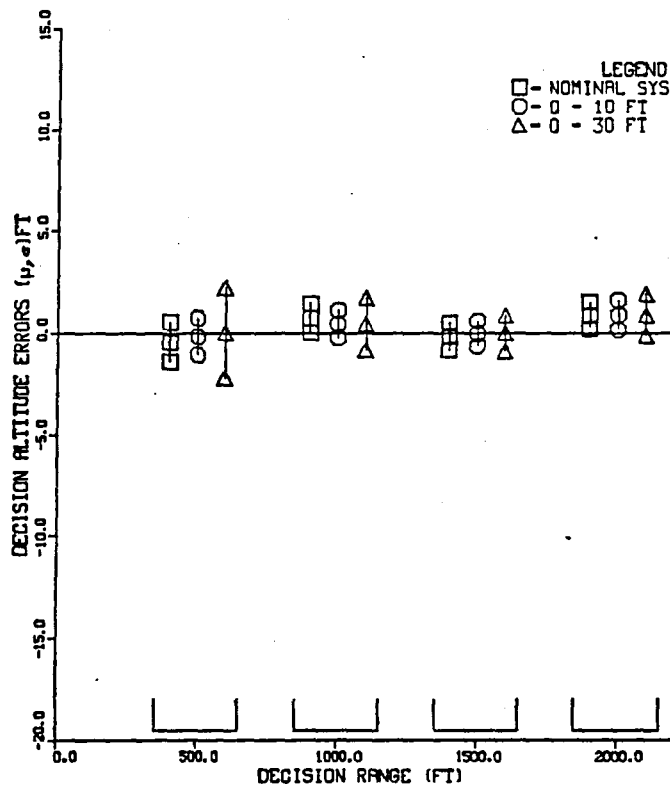
The effects of range rate quantization when $\sigma_n = 1$ or 10 ft are similar: both systems show oscillations when a range rate quantization (q_r) of 17 ft/s is used.

Figures 5(a),(b) and 12(a),(b) both show that decreasing the bandwidth of the α - β filter to .2 rad/s causes the helicopter system to oscillate. On the otherhand, increasing the bandwidth of the range/range rate filter to 10 rad/s when $\sigma_n = 10$ ft did not allow the DSAL simulation to terminate normally. This is because the larger filter bandwidth causes the range noise to "pass" through resulting in unacceptable range and range rate estimates.

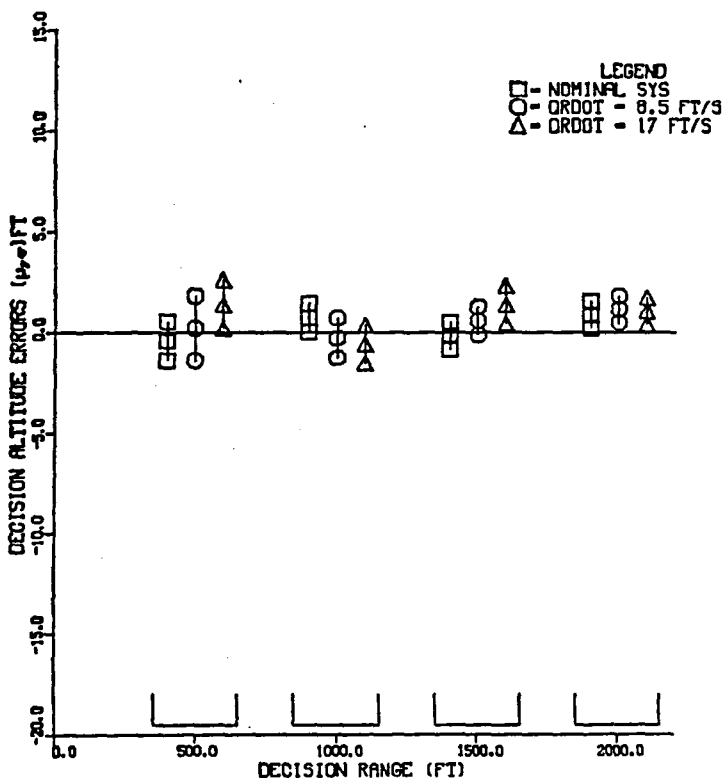
SAMPLING FREQUENCY VARIATION



RANGE QUANTIZATION VARIATION



RANGE RATE QUANTIZATION VARIATION



FILTER BANDWIDTH VARIATION

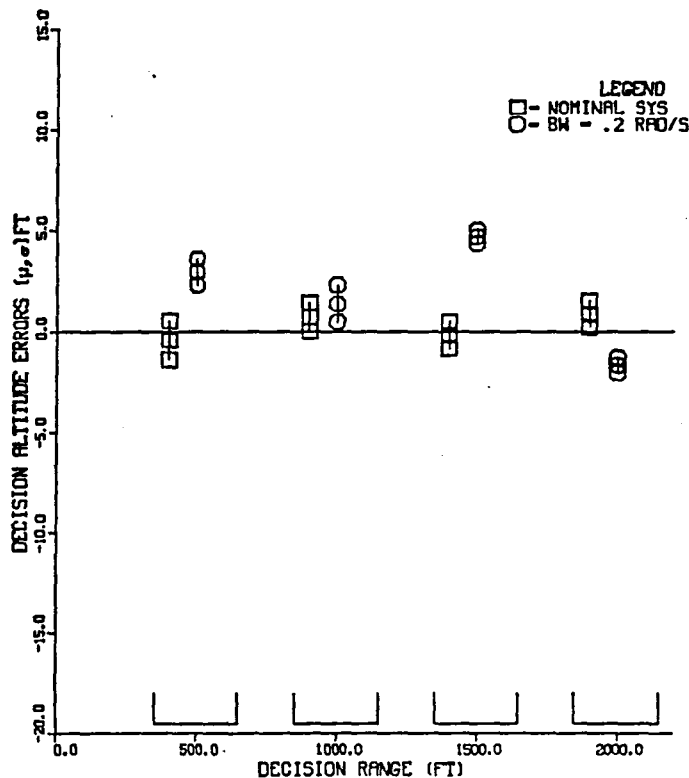
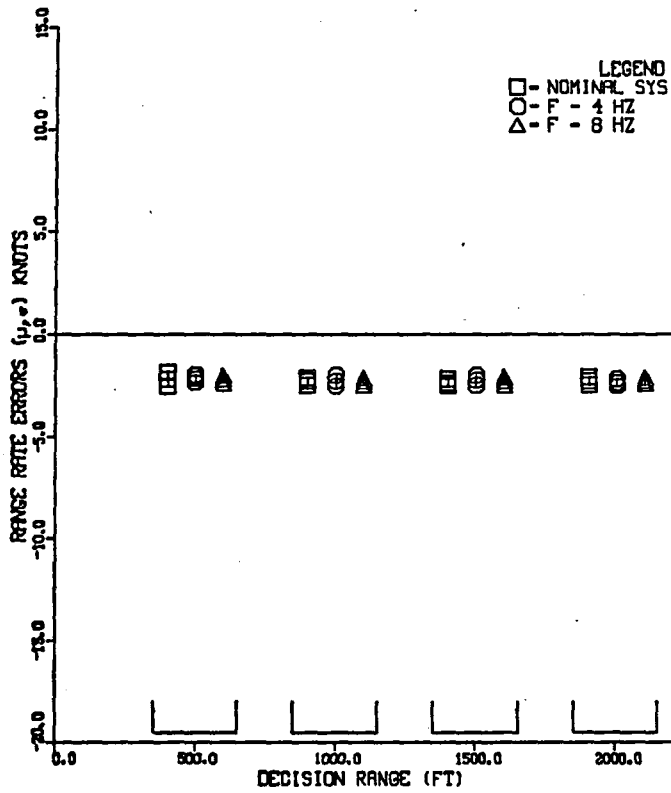
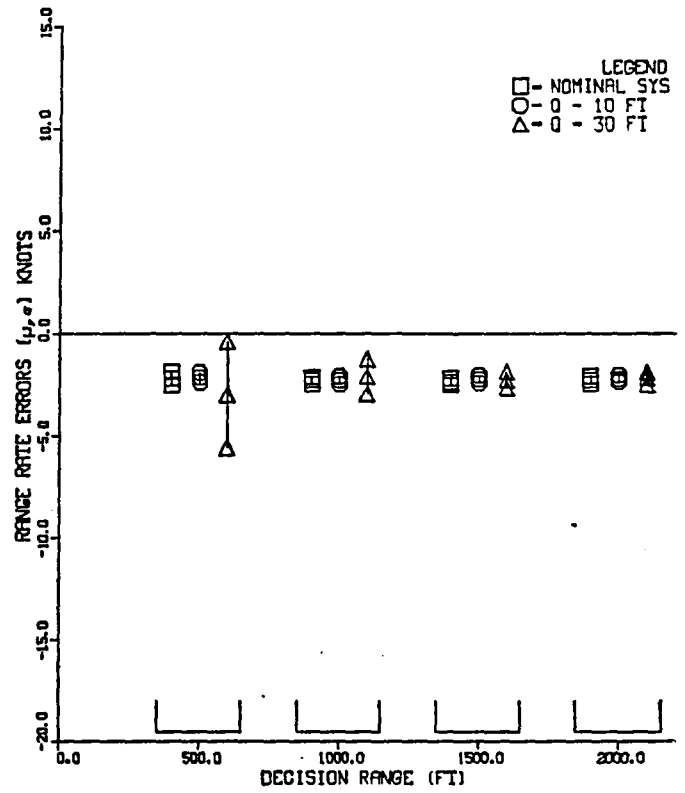


Figure 12(a). Sensitivity of Decision Altitude TSE to On-board Navigation Parameters (nominal $\sigma_n = 10$ ft)

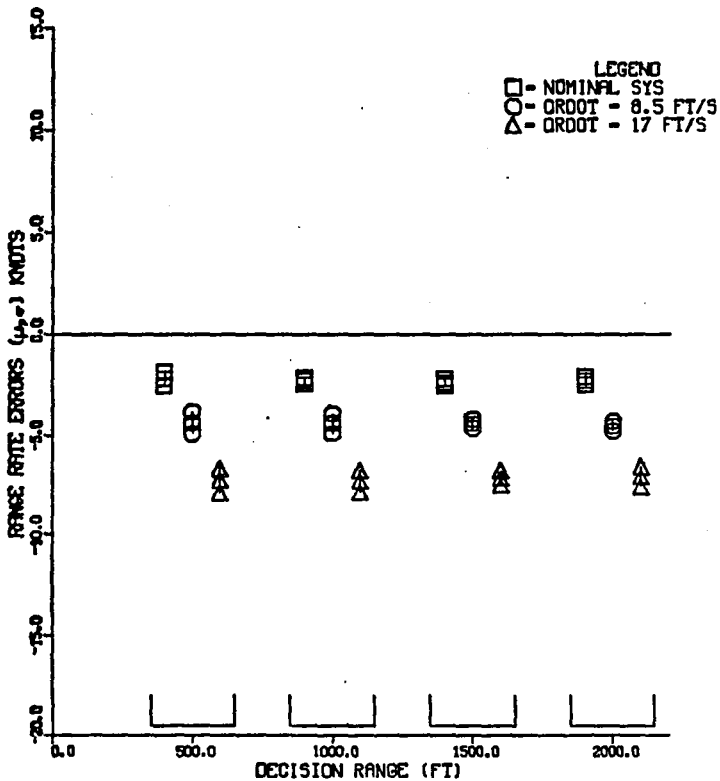
SAMPLING FREQUENCY VARIATION



RANGE QUANTIZATION VARIATION



RANGE RATE QUANTIZATION VARIATION



FILTER BANDWIDTH VARIATION

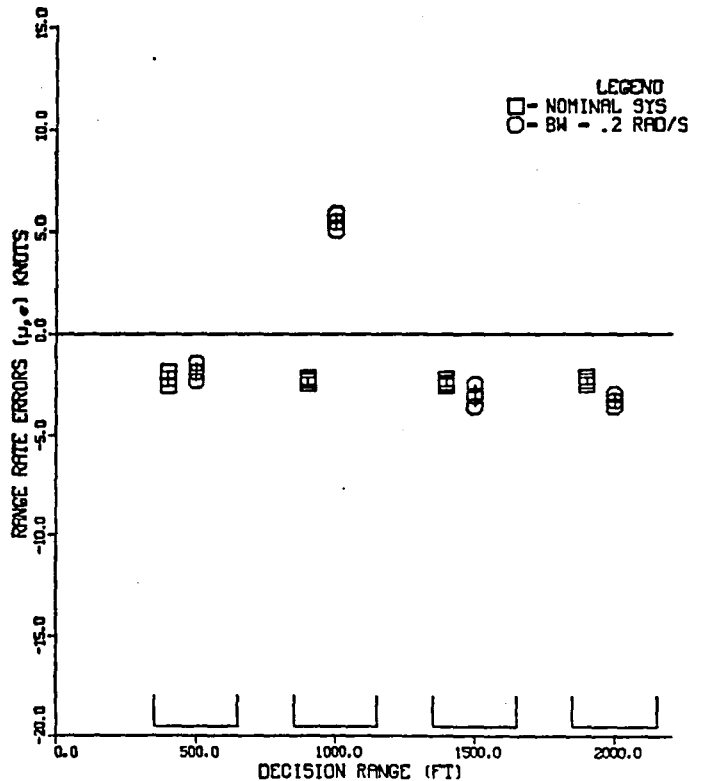
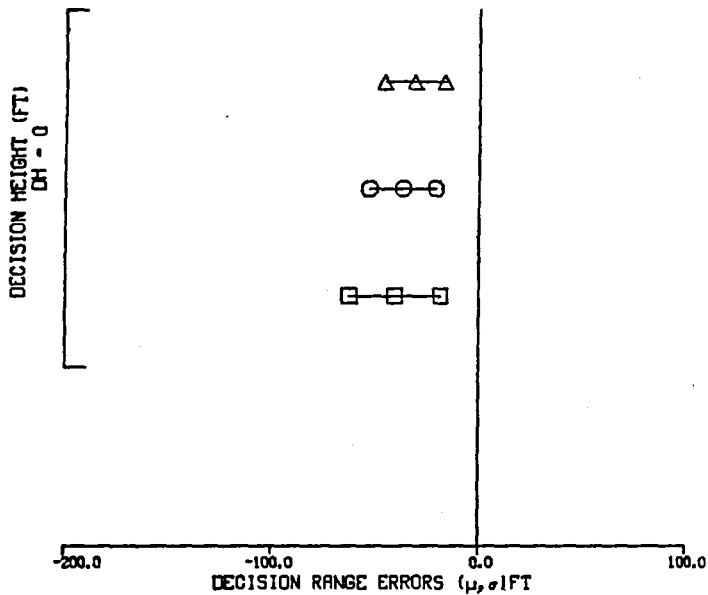


Figure 12(b). Sensitivity of Range Rate TSE to On-board Navigation Parameters (nominal $\sigma_n = 10$ ft)

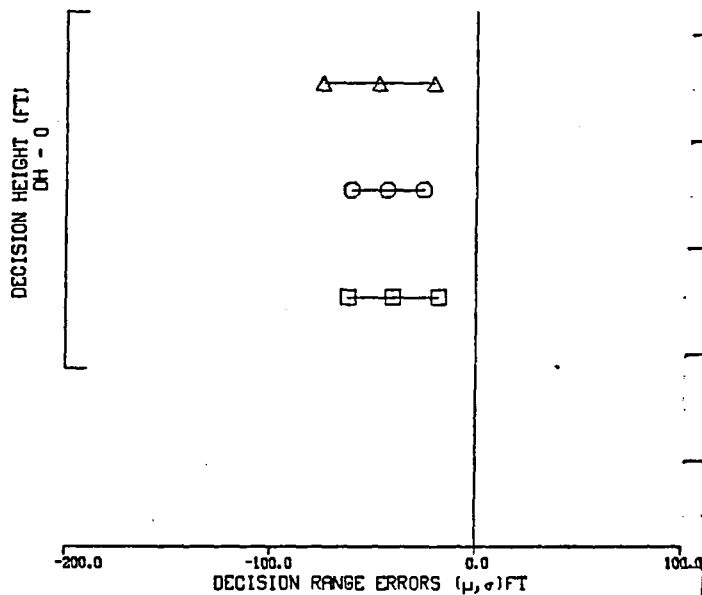
SAMPLING FREQUENCY VARIATION

LEGEND
 □ - NOMINAL SYS
 ○ - F = 4 HZ
 △ - F = 8 HZ



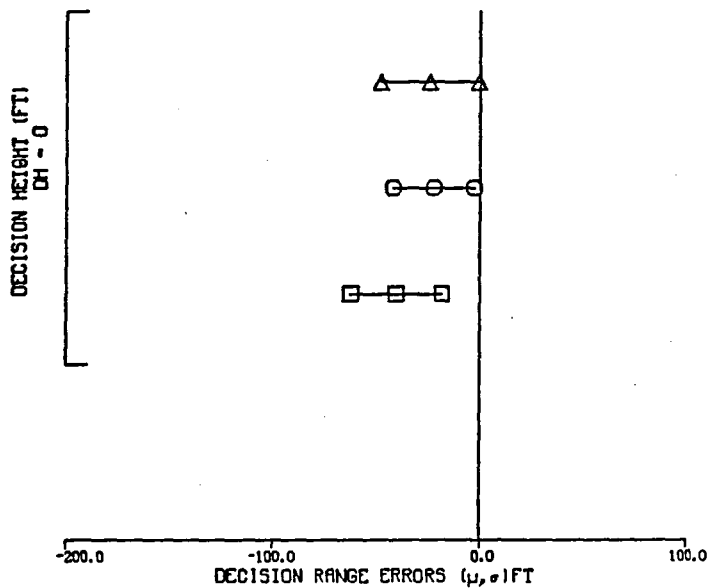
RANGE QUANTIZATION VARIATION

LEGEND
 □ - NOMINAL SYS
 ○ - Q = 10 FT
 △ - Q = 30 FT



RANGE RATE QUANTIZATION VARIATION

LEGEND
 □ - NOMINAL SYS
 ○ - ORDOT = 8.5 FT/S
 △ - ORDOT = 17 FT/S



FILTER BANDWIDTH VARIATION

LEGEND
 □ - NOMINAL SYS
 ○ - BW = .2 RAD

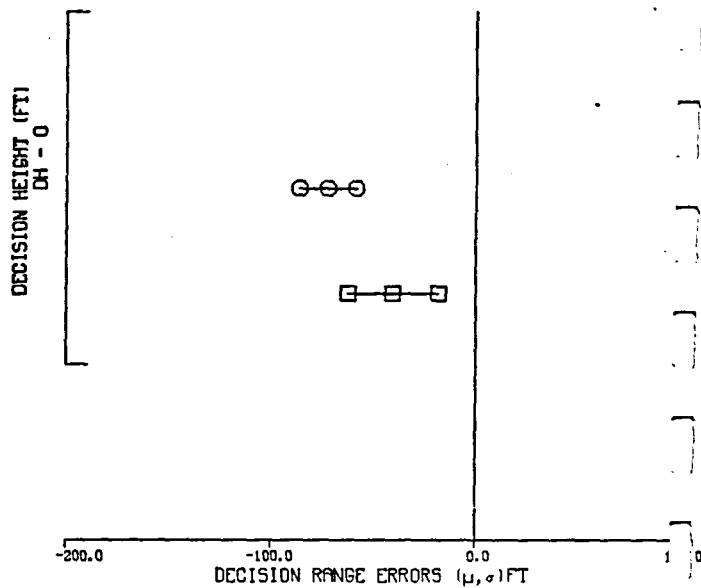


Figure 12(c). Sensitivity of Range TSE at Touchdown to On-board Navigation Parameters (nominal $\sigma_n = 10$ ft)

A comparison of Figures 5(c) and 12(c) indicates that increasing the range measurement noise increases the magnitude of the mean range touchdown error. This was observed in Figure 10(c) as well. Figure 5(c) shows that as the range rate quantization is increased, the magnitude of the mean touchdown error increases. However, if a σ_n of 10 ft is used, then this error decreases as the range rate quantization is increased (Figure 12(c)). This seems to indicate that the variations in the touchdown range TSE due to range measurement noise and range rate quantization are in opposite directions. This is not to say, that one can have a very large range measurement noise and compensate it by a very large range rate quantization. This is because the helicopter DSAL system oscillates as the range rate quantization increases.

CONCLUDING REMARKS

A closed loop computer simulation of the UH1H helicopter DSAL system was developed for investigating performance sensitivity to navigation model parameters. A navigation model consisting of on-board and ground-based (LGS) elements with five ($f, q, q_r, \omega_n, \sigma_n$) parameters was formulated. The first four parameters characterize the on-board system and the last one characterizes the LGS. These parameters were varied about a nominal set to study the sensitivity of the helicopter DSAL performance. Performance measures were defined in terms of the total system errors of the following flight path variables: localizer, glideslope, altitude, range rate, altitude and range rate at decision ranges and range at touchdown.

The following conclusions on system performance parameter sensitivity were drawn from simulation results:

1. On-Board Sampling Frequency (16, 8, 4 Hz).
System performance was not degraded by decreased sampling frequency.
2. On-Board Range Quantization (1, 10, 30 ft).
System performance was not degraded for increased range quantization, except only slightly when increased to 30 ft for the nominal case with ground-based range noise equal to 10 ft.
3. On-Board Range Rate Quantization (1, 5, 10 kts).
Increased range rate quantization caused an almost proportional increase in negative bias for range rate error. Increased range rate quantization also caused system oscillations to increase.
4. On-Board Filter Bandwidth (0.2, 2.0, 10.0 rad/sec).
A filter bandwidth of 0.2 rad/sec was too low and caused an undesirable increase in glideslope tracking oscillations. A filter bandwidth of 10.0 rad/sec caused the system to go unstable when ground-based range noise was increased from 1 to 10 feet.
5. Ground-Based Range Noise (1, 10, 30 ft).
System performance was significantly degraded when ground-based range noise was increased from 10 to 30 feet. When ground-based range noise was increased to 30 feet, along-track range error at touchdown (-70 ± 65 ft) was significantly greater than in all other parameter sensitivity cases tested.

1 2 3 4 5 6 7 8 9 10 11 12 13 14 15 16 17 18 19 20 21 22 23 24 25 26 27 28 29 30 31 32 33 34 35 36 37 38 39 40 41 42 43 44 45 46 47 48 49 50 51 52 53 54 55 56 57 58 59 60 61 62 63 64 65 66 67 68 69 70 71 72 73 74 75 76 77 78 79 80 81 82 83 84 85 86 87 88 89 90 91 92 93 94 95 96 97 98 99 100

REFERENCES

1. Talbot, P.D. and Corliss, L.D., "A Mathematical Force and Moment Model of the UH1H Helicopter for Flight Dynamics Simulations," NASA TM-73, 254, Nov., 1977.
2. Benedict, T.R. and Bordner, C.W., "Synthesis of an Optional Set of Radar Track-while-Scan Smoothing Equations," I.R.E. Transaction on Automatic Control, 1962.
3. Demko, P.S. and Boschma, J.H., "Advances in Decelerating Steep Approach and Landing for Helicopter Instrument Approaches," 35th Annual National Forum of the American Helicopter Society, Washington D.C., May 1979.
4. Phatak, A.V., et al, "A Piloted Simulator Investigation of Helicopter Precision Decelerating Approaches to Hover to Determine Single Pilot IFR (SPIFR) Requirements," 1979 AIAA Guidance and Control Conference, Boulder, Co., AIAA Paper No. 79-1886, Aug. 1979.
5. Franklin, G.F. and Powell, J.D., "Digital Control of Dynamic System," Addison-Wesley, 1980.
6. Jury, E.I.: "Sampled Data Control Systems," John Wiley, 1958.

APPENDIX A

DSAL AUTOPILOT/FLIGHT-CONTROL SYSTEM

This appendix describes the four-axis stability augmentation system (SAS) and autopilot used in the simulation of the overall closed-loop DSAL system.

Collective Axis

The autopilot flight path coupler in the collective axis operates in the altitude hold mode (ALT) or in the approach mode (APP) (Figure A.1).

Altitude hold is accomplished by synchronizing to the aircraft's altitude at the time of engagement and then applying the error signal as a command to the collective axis. The error signal is augmented by the error rate which is obtained by differentiation (with a lag) of the error. This error rate is complemented by attitude (θ) stabilized vertical acceleration (a_z),

In the approach mode (APP), the filtered range (r) and angular glideslope deviation are multiplied to give vertical deviation about the desired glideslope. This error signal is augmented by a computed error rate (as in the altitude hold mode). The error plus the error rate signals then go through an integrator to provide a proportional plus integral plus derivative (PID) controller. The collective stick position is fed forward through a 1.5 second washout filter to the PID signal. The above summed signal is then applied to the collective axis autopilot (Figure A.2). The collective axis autopilot has no SAS and therefore the flight path coupler command goes straight through the series and parallel servo to generate the collective axis command.

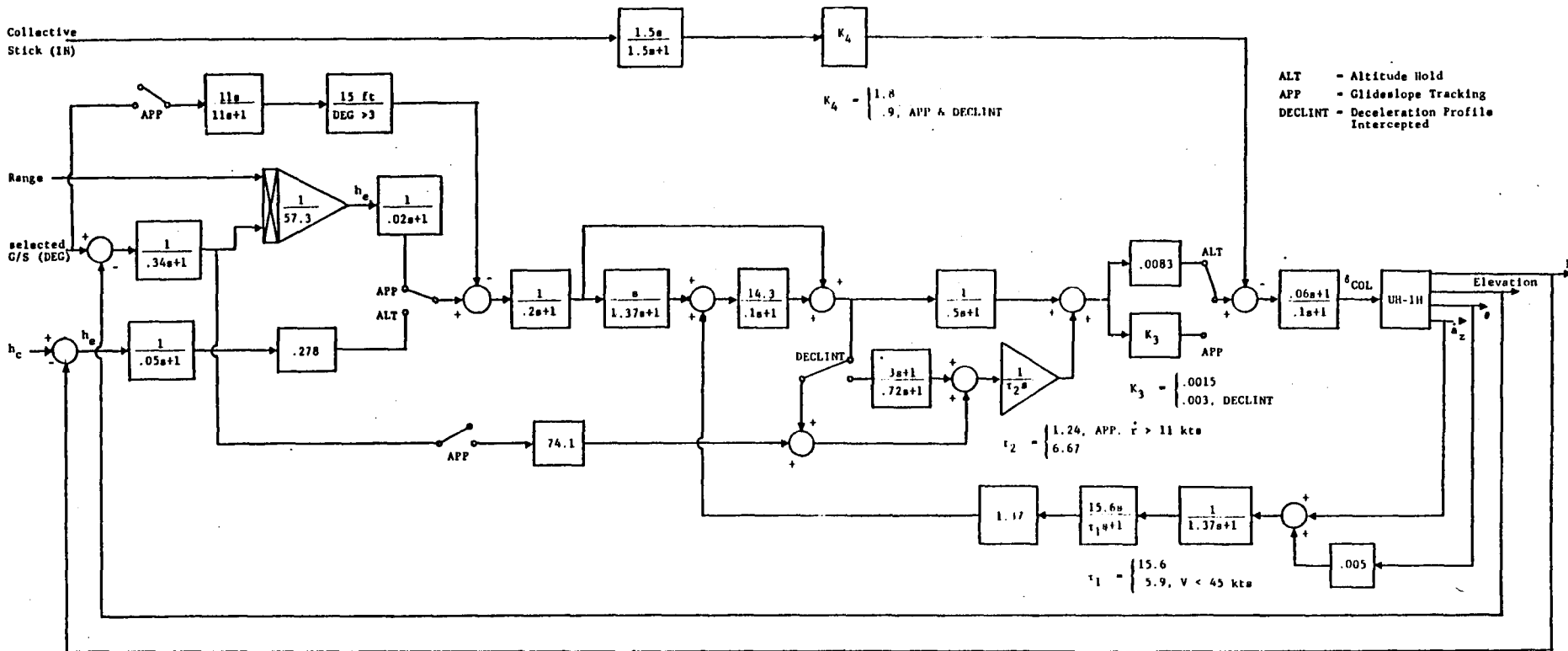


Figure A.1. Autopilot Flight Path Coupler - Collective Axis

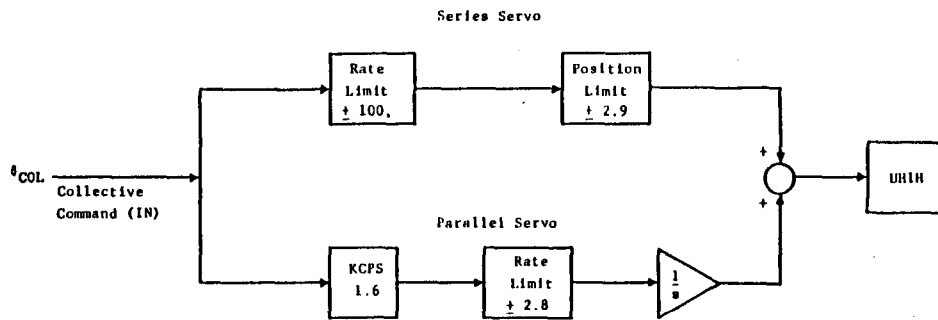


Figure A.2. Autopilot Collective Axis

NOTE: The switches are interpreted as closed when moved towards the appropriate symbol defining the switch.

Pitch Axis

The pitch axis uses a relatively simple control law to control airspeed or range rate (Figures A.3, A.4). It operates in one of two modes: speed hold (SPD) or deceleration (DECL). In the speed hold mode, the synchronizing speed is compared with the airspeed. The airspeed being rather noisy is filtered by a .1 second lag first order filter. The filtered airspeed is complemented by attitude (θ) stabilized longitudinal acceleration (a_x). The error signal is then limited and added to a washed out collective stick position signal. The total signal is then multiplied by a gain of .57 deg/ft/sec to give the pitch command (θ_c). At a range of 8300 feet or less, the DECL mode goes from ARMED to ON and the estimated range rate is fed back instead of airspeed. However, the actual deceleration does not begin until the deceleration profile is intercepted (approximately at 5285 feet for a cruise speed of 60 knots and a deceleration of .03G). The deceleration profile generator computes the commanded range rate as a function of estimated range. (A constant velocity offset is subtracted from the commanded range rate to reduce the range rate error noticed in the simulation). The commanded range rate is continuously compared to the aircraft's speed. In the speed hold mode the resulting error signal is limited to zero so that no speed up command is generated. When the deceleration profile has been intercepted (DECLINT), the error signal is limited to ± 5 ft/sec. As in the speed hold mode, the error signal is added to washed out collective stick position signal. The total signal then goes through a gain of .57 deg/ft/sec to give the pitch command θ_c which then acts as an input to the pitch axis SAS (Figure A.4).

The pitch axis SAS is very similar to the roll axis, described in the following section.

Roll Axis

Figures A.5, A.6 show the roll control system. The roll axis commands the aircraft towards the localizer. The lateral displacement is computed by multiplying the filtered range (r) and angular localizer deviation (α_e).

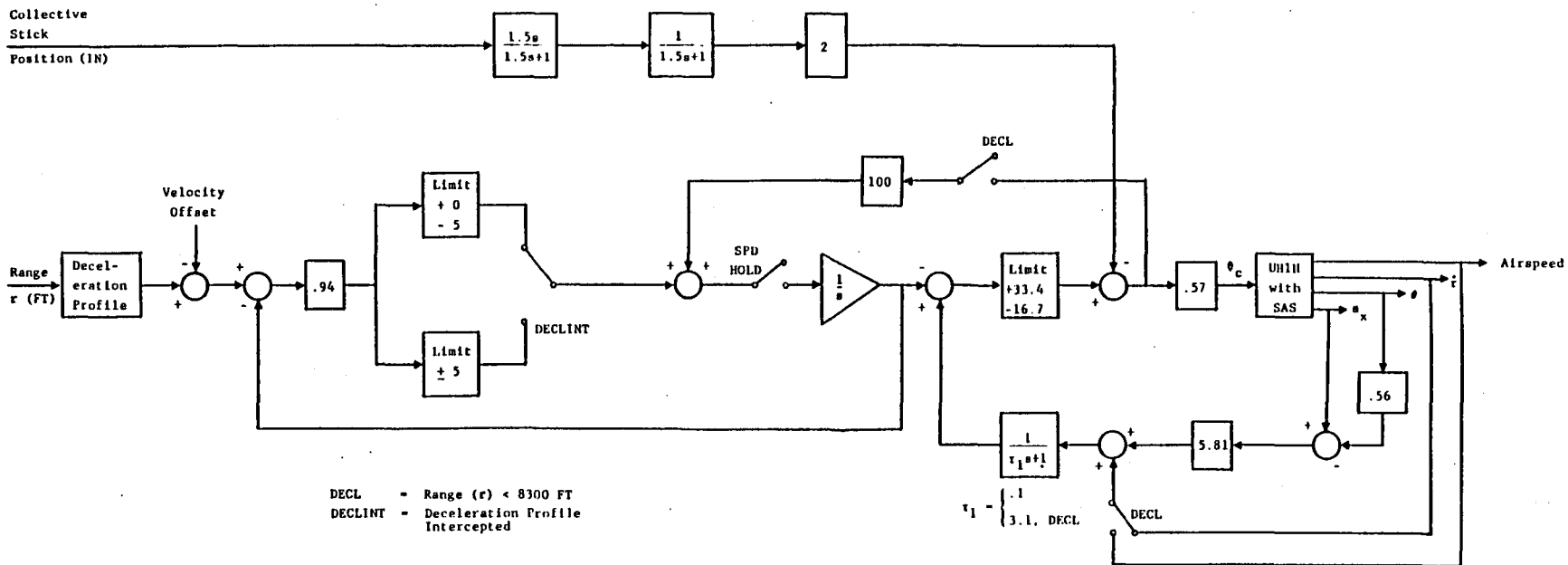


Figure A.3. Autopilot Flight Path Coupler - Pitch Axis

NOTE: The switches are interpreted as closed when moved towards the appropriate symbol defining the switch.

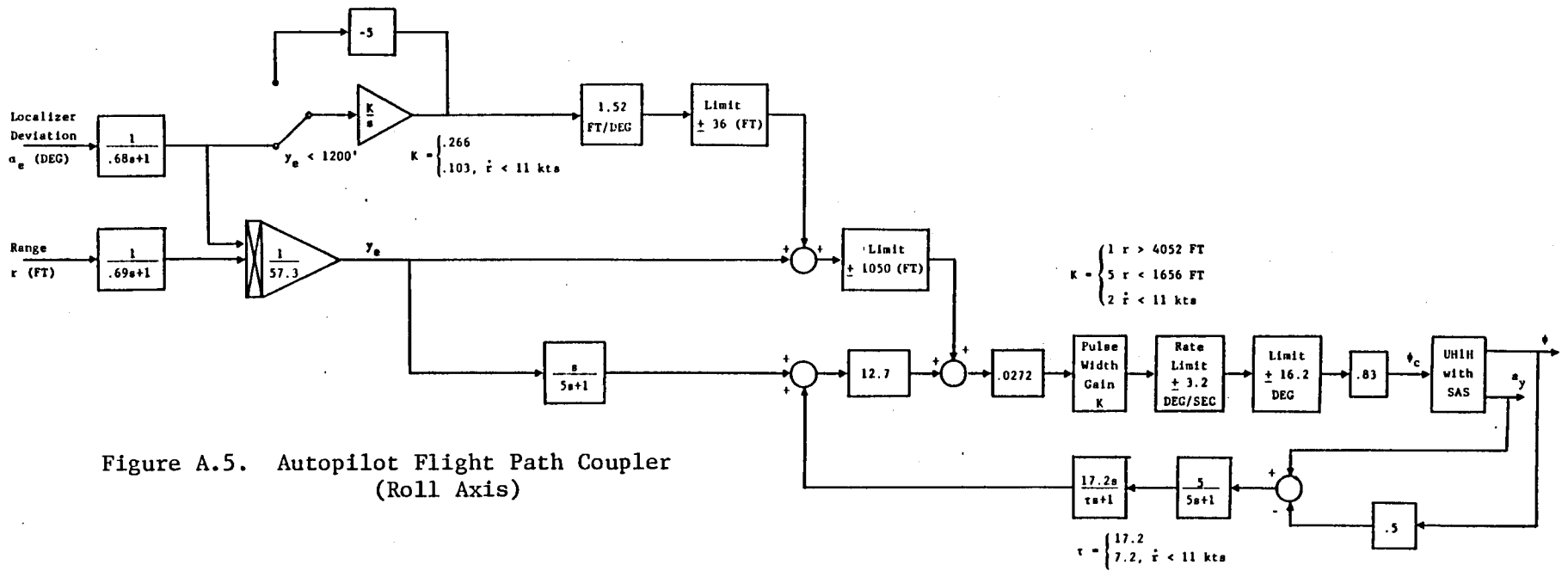


Figure A.5. Autopilot Flight Path Coupler (Roll Axis)

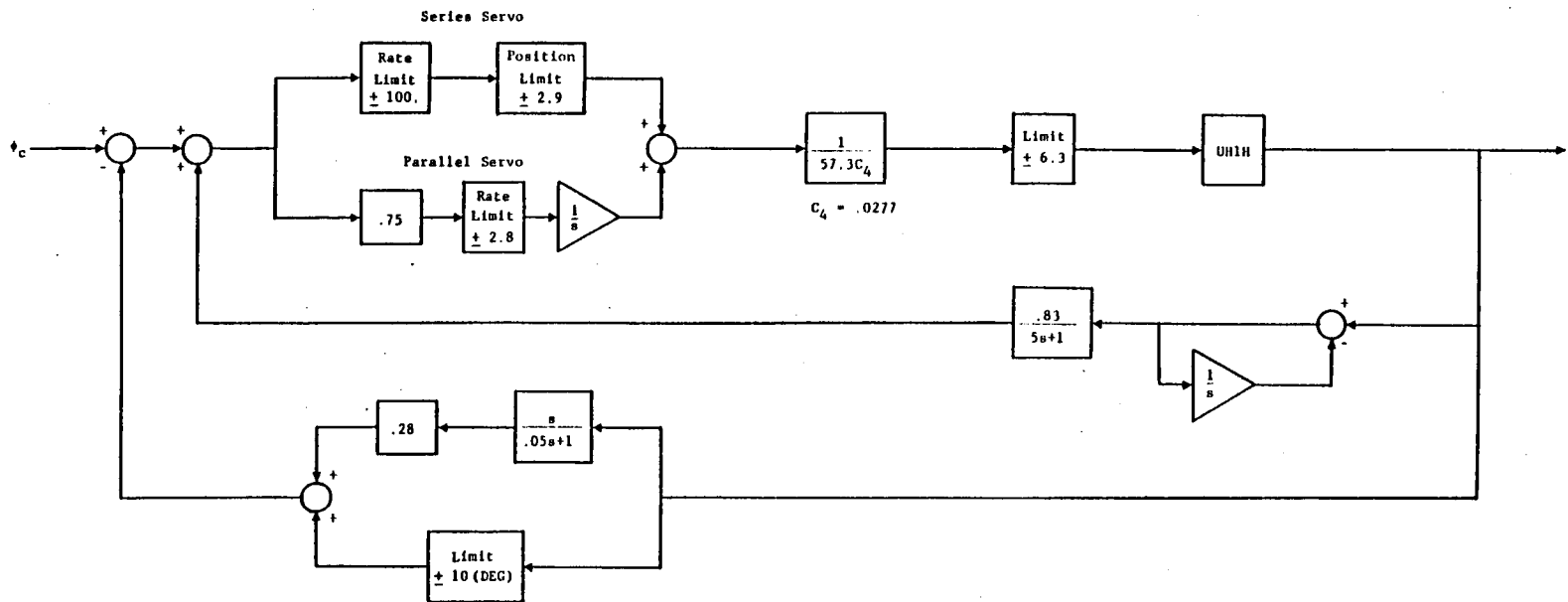


Figure A.6. SAS - Roll Axis

The filtered range (r) is obtained by onboard processing of the DME signal from the ground based navigation system. This filtering of the range signal is described under Navigation Systems. The lateral displacement rate is derived from the computed displacement. The rate has a 5 second lag built in it because of the noise in the computed lateral displacement. This is complemented with attitude (ϕ) stabilized lateral acceleration (a_y). The lateral displacement and the lateral rate (complemented as above), are added to the integral of the localizer angle to form a proportional plus integral plus derivative (PID) type controller. The above signal is then multiplied by a gain and limited to form the roll command (ϕ_c). The roll command is then fed into the stability augmentation system (Figure A.6). Roll attitude and roll rate are fed back to produce a lateral cyclic command through a series and a parallel servo. The roll rate is obtained by differentiating the roll angle assuming no rate gyros are available.

Yaw Axis

Figure A.7 shows the stability and control augmentation system (SCAS) for the yaw axis at high speeds (turn coordination mode). Since the aircraft tends to yaw when the collective is dropped or raised, the collective stick position (radians) acts as the primary input to the system. The turn coordination mode requires lateral acceleration, yaw and roll rate feedbacks as shown. The pedal command is generated by passing the yaw signal through a series and parallel servo. In the heading hold mode, the commanded heading angle (ψ_c) acts as an input in addition to the collective stick position. This mode requires only the yaw angle and yaw rate feedback (Figure A.8).

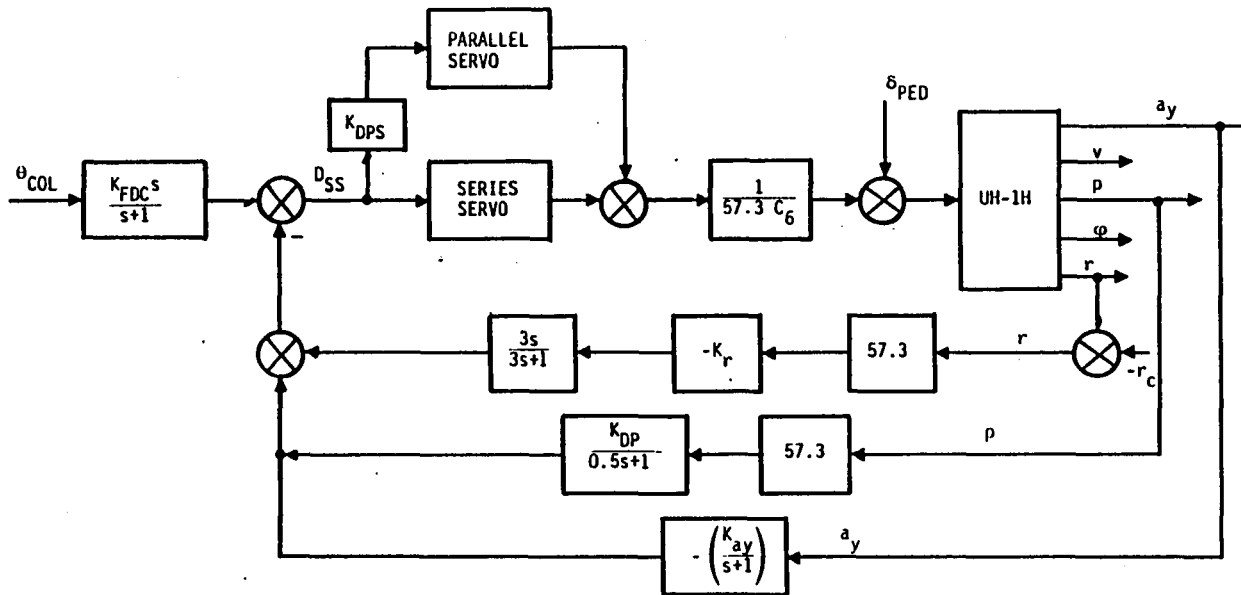


Figure A.7. SCAS: Turn Coordination Mode

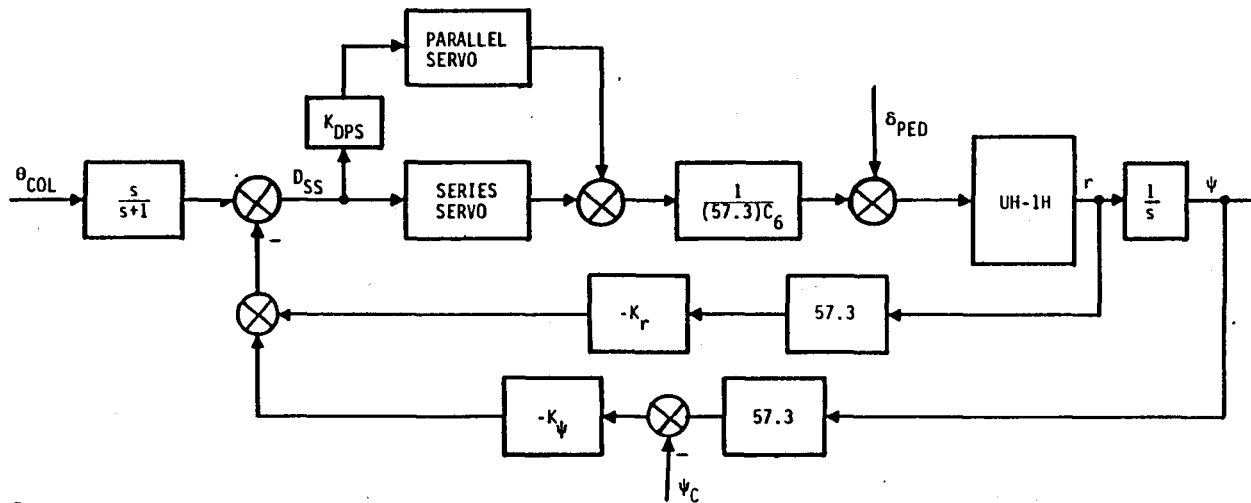


Figure A.8. SCAS: Heading Hold Mode

Yaw Axis

APPENDIX B

RANGE AND RANGE RATE FILTERS

α - β Range/Range Rate Filters

The range/range rate filters investigated in this study is the classical second order α - β filter [2]. Figure B.1 shows the analog representation of this filter. In this filter r_m is the range measurement, \hat{x}_1 and \hat{x}_2 are the estimates of the range and range rate respectively. The state space representation of the filter is:

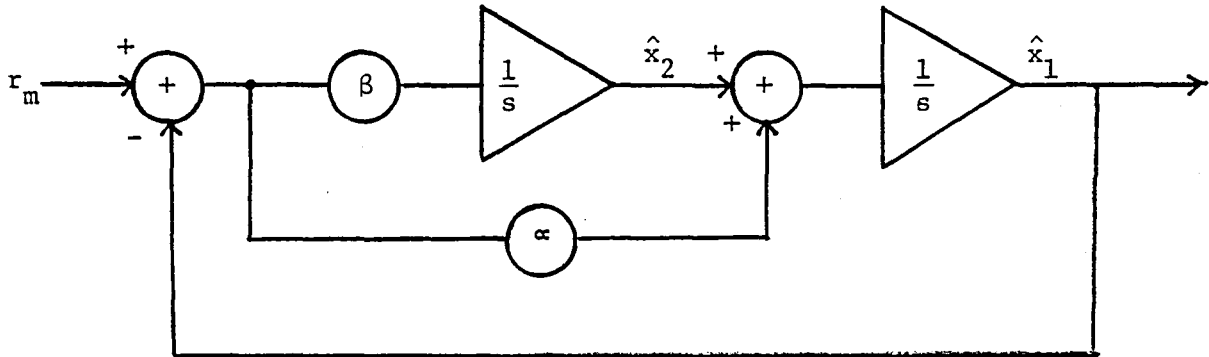


Figure B.1. Analog Representation of the α - β Filter

$$\begin{bmatrix} \hat{x}_1 \\ \hat{x}_2 \end{bmatrix} = \begin{bmatrix} -\alpha & 1 \\ -\beta & 0 \end{bmatrix} \begin{bmatrix} \hat{x}_1 \\ \hat{x}_2 \end{bmatrix} + \begin{bmatrix} \alpha \\ \beta \end{bmatrix} r_m \quad \text{B.1}$$

The transfer functions \hat{x}_1/r_m , \hat{x}_2/r_m are:

$$\frac{\hat{x}_1(s)}{r_m(s)} = \frac{s\alpha + \beta}{s^2 + \alpha s + \beta} \quad \text{B.2}$$

$$\frac{\hat{x}_2(s)}{r_m(s)} = \frac{s}{s^2 + \alpha s + \beta} \quad \text{B.3}$$

Equations B.2 and B.3 show that the filter bandwidth and damping ratio are related by:

$$\omega_n = \sqrt{\beta} \quad \text{B.4}$$

$$\zeta = \frac{\alpha}{2 \omega_n} \quad \text{B.5}$$

Discretizing B.1 by a simple Euler explicit scheme gives the following discrete equations for \hat{x}_1 and \hat{x}_2 :

$$\begin{bmatrix} \hat{x}_1(n+1) \\ \hat{x}_2(n+1) \end{bmatrix} = \begin{bmatrix} 1 - \alpha\Delta T & \Delta T \\ -\beta\Delta T & 1 \end{bmatrix} \begin{bmatrix} \hat{x}_1(n) \\ \hat{x}_2(n) \end{bmatrix} + \begin{bmatrix} \alpha\Delta T \\ \beta\Delta T \end{bmatrix} r_m(n+1) \quad \text{B.6}$$

where ΔT is the measurement update period. This scheme requires:

$$|\alpha\Delta T| \ll 1 \quad \text{B.7}$$

for the discrete solution to be accurate. Consequently, the measurement update period has to be sufficiently small to obtain accurate estimates of range and range rate.

Since the α - β filter is based on a kinematic model where the acceleration is assumed zero, the filter can be implemented in a different way in which the measurement update period need not be small. The kinematic model can be written as:

$$\dot{\underline{x}} = \begin{bmatrix} \dot{x}_1 \\ \dot{x}_2 \end{bmatrix} = \begin{bmatrix} 0 & 1 \\ 0 & 0 \end{bmatrix} \begin{bmatrix} x_1 \\ x_2 \end{bmatrix} = \underline{A} \underline{x} \quad \text{B.8}$$

$$r_m = [1 \quad 0] \begin{bmatrix} x_1 \\ x_2 \end{bmatrix} = \underline{h}^T \underline{x} \quad \text{B.9}$$

where x_1 and x_2 are the range and range rate of the helicopter. Using a Kalman filter representation for the model described by B.8, B.9 gives the following procedure for estimating x_1 and x_2 :

$$\hat{\underline{x}}(n) = \bar{\underline{x}}(n) + K(r_m(n) - \underline{h}^T \bar{\underline{x}}(n)) \quad \text{B.10}$$

$$\bar{\underline{x}}(n+1) = \Phi \hat{\underline{x}}(n) \quad \text{B.11}$$

$$\Phi = \begin{bmatrix} 1 & \Delta T \\ 0 & 1 \end{bmatrix} \quad \text{B.12}$$

$$K = \begin{bmatrix} \alpha \cdot \Delta T \\ \beta \cdot \Delta T \end{bmatrix} \quad \text{B.13}$$

B.10 is termed the measurement update equation and B.11 is the time update equation. In between measurements the range (\hat{x}_1) and range rate (\hat{x}_2) estimates are propagated by use of equation B.11 and when a new measurement is available, the innovation is added to the propagated estimates as shown in equation B.10.

The steady-state performance of the filter represented by equations B.10 through B.13 is best studied in the Z transform domain. Equations B.10 through B.13 can be written as:

$$\hat{x}_1(n+1) = \hat{x}_1(n) + \Delta T \cdot \hat{x}_2(n) + \alpha \cdot \Delta T (r_m(n+1) - \hat{x}_1(n) - \Delta T \cdot \hat{x}_2(n)) \quad \text{B.14}$$

$$\hat{x}_2(n+1) = \hat{x}_2(n) + \beta \cdot \Delta T (r_m(n+1) - \hat{x}_1(n) - \Delta T \cdot \hat{x}_2(n)) \quad \text{B.15}$$

Taking Z transforms of B.14 and B.15 gives:

$$\frac{\hat{x}_1(z)}{r_m(z)} = \frac{z [(z-1)\alpha' + \beta' \Delta T]}{(z-1)^2 + (\alpha' + \beta' \Delta T)(z-1) + \beta' \Delta T} \quad \text{B.16}$$

where $\alpha' = \alpha \cdot \Delta T$

$\beta' = \beta \cdot \Delta T$

If the error $e(t)$ is defined as:

$$e(t) = r_m(t) - \hat{x}_1(t)$$

then the transfer function $e(z)/r_m(z)$ can be obtained from B.16:

$$\frac{e(z)}{r_m(z)} = \frac{(z-1)^2 (1-\alpha')}{\Delta(z)} \quad \text{B.17}$$

where

$$\Delta(z) = (z-1)^2 + (\alpha' + \beta' \Delta T) (z-1) + \beta' \Delta T \quad \text{B.18}$$

Using the final value theorem [6], the following equations show the steady-state behavior of the error $e(t)$:

$$\begin{aligned} \text{For a step } r_m(t), \quad \lim_{t \rightarrow \infty} e(t) &= \lim_{z \rightarrow 1} (z-1) e(z) \\ &= \lim_{z \rightarrow 1} (z-1) \cdot \left[\frac{(z-1)^2 (1-\alpha')}{\Delta(z)} \right] \cdot \frac{z}{(z-1)} = 0 \end{aligned} \quad \text{B.19}$$

$$\begin{aligned} \text{For a ramp } r_m(t), \quad \lim_{t \rightarrow \infty} e(t) &= \lim_{z \rightarrow 1} (z-1) \cdot \left[\frac{(z-1)^2 (1-\alpha')}{\Delta(z)} \right] \cdot \frac{\Delta T z}{(z-1)^2} = 0 \end{aligned} \quad \text{B.20}$$

$$\begin{aligned} \text{For a parabolic } r_m(t), \quad \lim_{t \rightarrow \infty} e(t) &= \lim_{z \rightarrow 1} (z-1) \cdot \left[\frac{(z-1)^2 (1-\alpha')}{\Delta(z)} \right] \cdot \frac{(\Delta T)^2 z(z+1)}{z(z-1)^3} \\ &= \frac{(1-\alpha')}{\beta'} \cdot \Delta T \end{aligned} \quad \text{B.21}$$

For the DSAL law used in this study, the range is a parabolic function of time. Consequently the α - β filter will show a steady state error in the range estimate as shown by equation B.21.

Equations B.14 and B.15 can also be used to derive the transfer function $x_2(z)/v(z)$ where $v(z)$ is the Z transform of the velocity function $v(t)$:

$$\frac{\hat{x}_2(z)}{v(z)} = \frac{\beta' z \cdot \Delta T}{\Delta(z)} \quad \text{B.22}$$

$$\frac{e_v(z)}{v(z)} = \frac{(z-1) ((z-1) + \alpha')}{\Delta(z)} \quad \text{B.23}$$

For a step velocity input the steady-state error $e_v(t)$ can also be obtained by using the final value theorem:

$$\begin{aligned} \lim_{t \rightarrow \infty} e_v(t) &= \lim_{z \rightarrow 1} (z-1) (z-1) \frac{((z-1) + \alpha')}{\Delta(z)} \cdot \frac{z}{(z-1)} \\ &= 0 \end{aligned}$$

B.24

For a ramp input velocity, the steady state error is:

$$\begin{aligned} \lim_{t \rightarrow \infty} e_v(t) &= \lim_{z \rightarrow 1} (z-1) (z-1) \frac{((z-1) + \alpha')}{\Delta(z)} \cdot \frac{\Delta T}{(z-1)^2} \\ &= \frac{\alpha'}{\beta} \end{aligned}$$

B.25

The parameters α and β are related to damping and bandwidth of the analog filter via equations B.4 and B.5. However, since the filter is implemented digitally, the mapping of α and β into ζ and ω has to be derived using equation B.16. Since $z = e^{s\Delta T}$, substituting B.26 for z in B.16 gives B.27 below.

$$z = 1 + s\Delta T \quad \text{B.26}$$

$$\frac{x_1(s)}{r_m(s)} = \frac{(1 + s\Delta T)(\alpha s + \beta)}{s^2 + (\alpha + \beta\Delta T)s + \beta} \quad \text{B.27}$$

Assuming that $1 + s\Delta T = 1$, B.27 can be reduced to:

$$\frac{x_1(s)}{r_m(s)} = \frac{(\alpha s + \beta)}{s^2 + (\alpha + \beta\Delta T)s + \beta} \quad \text{B.28}$$

Equation B.28 shows that the bandwidth (ω_n) and damping (ζ) are related to α and β via B.29 and B.30:

$$\beta = \omega_n^2 \quad \text{B.29}$$

$$\alpha = 2\zeta\omega_n - \beta\Delta T \quad \text{B.30}$$

It can be seen that B.29 is identical with B.4 whereas B.30 is equal to B.5 only if

$$\Delta T \ll \frac{2\zeta}{\omega_n} .$$

B.31

1. Report No. NASA CR- 166412	2. Government Accession No.	3. Recipient's Catalog No.	
4. Title and Subtitle SENSITIVITY ANALYSIS OF HELICOPTER IMC DECELERATING STEEP APPROACH AND LANDING PERFORMANCE TO NAVIGATION SYSTEM PARAMETERS		5. Report Date September 1982	
		6. Performing Organization Code	
7. Author(s) Mehebbub S. Karmali and Anil V. Phatak		8. Performing Organization Report No. AMA Report No. 82-18	
		10. Work Unit No. T3771Y	
9. Performing Organization Name and Address Analytical Mechanics Associates, Inc. 2483 Old Middlefield Way Mountain View, CA 94043		11. Contract or Grant No. NAS2-10670*	
		13. Type of Report and Period Covered Contractor Report	
12. Sponsoring Agency Name and Address National Aeronautics and Space Administration Washington, D.C. 20546		14. Sponsoring Agency Code RTOP # 532-01-11	
		15. Supplementary Notes Point of Contact: Technical Monitors, J.S. Bull and L.L. Peach, M/S 210-9 Ames Research Center, Moffett Field, CA 94035 (415) 964-5425/5469 or FTS 448-5425/5469	
16. Abstract Results of a study to investigate, by means of a computer simulation, the performance sensitivity of helicopter IMC DSAL operations as a function of navigation system parameters are presented. A mathematical model representing generically a navigation system is formulated. The scenario simulated consists of a straight in helicopter approach to landing along a 6° glideslope. The deceleration magnitude chosen is .03g. The navigation model parameters are varied and the statistics of the total system errors (TSE) computed. These statistics are used to determine the critical navigation system parameters that affect the performance of the closed-loop navigation, guidance and control system of a UH-1H helicopter. * This study was jointly funded with the U.S. Army Avionics Research and Development Activity at Ft. Monmouth, New Jersey.			
17. Key Words (Suggested by Author(s)) Navigation System Parameters Sensitivity Analysis Helicopter IMC DSAL Approaches Total System Errors		18. Distribution Statement Unclassified - Unlimited STAR Catagory 45	
19. Security Classif. (of this report) Unclassified	20. Security Classif. (of this page) Unclassified	21. No. of Pages 31	22. Price*

End of Document